

1 List of changes

2	Replaced: Static	21
3	Replaced: Dynamic	21
4	Replaced: Parameter	22
5	Replaced: Limiting	22
6	Replaced: Constructing	22
7	Replaced: Producing	22
8	Replaced: Adding	22
9	Replaced: Calculating	22
10	Replaced: Including Limiting Co...	23
11	Replaced: Intermediate	23
12	Replaced: Dynamic	23
13	Replaced: Static	24
14	Replaced: Static	28
15	Replaced: the more conventional...	39
16	Added: of operation	41
17	Replaced: dynamic	41
18	Replaced: static	41
19	Replaced: static	41
20	Replaced: dynamic	41
21	Replaced: Dynamic	41
22	Added: (see Table 3.1)	41
23	Replaced: Static	41

24	Added: The overall structure	42
25	Replaced: many hours	42
26	Added: density	42
27	Added: – see Fig. 2-1	42
28	Replaced: Is it stretched out like	42
29	Replaced: cross-sections	43
30	Replaced: result from a slice acr	43
31	Added: Their exact usage wit	43
32	Replaced: essentially parabolas	44
33	Added: density	44
34	Replaced: profiles	45
35	Deleted: profiles	45
36	Added: just	45
37	Added: Although not self-	45
38	Added: The reason \bar{n} is referr	46
39	Added: A final point to make	46
40	Added: Density	46
41	Added: density	46
42	Added: These are derived in A	47
43	Replaced: The steady current wi	47
44	Replaced: a density limit that a	48
45	Replaced: disrupt.	48
46	Added: These conclusions can	48
47	Added: and	48

48	Added:	48
49	Deleted: and π has its usual m	48
50	Replaced: it accurately predicts	49
51	Deleted: (i.e. the ones we use)	50
52	Replaced: dynamic	50
53	Replaced: static	50
54	Replaced: static	50
55	Replaced: in equilibrium	50
56	Replaced: Its underlying behavi	50
57	Replaced: Utilizing the surface i	50
58	Deleted: Here, Q is an arbitrar	50
59	Deleted: This allows the boots	51
60	Added: The second definition	51
61	Deleted: For a more formal loo	51
62	Added: The instructions to do	51
63	Deleted: Getting back on track	51
64	Deleted: Recognizing that the l	51
65	Deleted: In standardized units,	51
66	Added: Finally, summarizing	52
67	Replaced: static	52
68	Deleted: The next segue on our	52
69	Deleted: The natural place to s	52
70	Deleted: What this reaction de	53
71	Deleted: The final point to ma	53

72	Added: The next segue on our	53
73	Replaced: Summarized, though,	53
74	Replaced: the following volume i	53
75	Added: The E_F quantity is th	53
76	Added: then	53
77	Added: (f_D). This dilution fa	53
78	Replaced: dynamic	54
79	Deleted: As mentioned before,	55
80	Replaced: this chapter's	55
81	Replaced: static	55
82	Replaced: static	56
83	Replaced: static	56
84	Replaced: The	56
85	Replaced: chapter	56
86	Added: Further, each temper	57
87	Replaced: limiting	58
88	Replaced: static	59
89	Replaced: dynamic	59
90	Replaced: dynamic	59
91	Deleted: then	59
92	Replaced: redirect focus	59
93	Replaced: the underlying solvers	59
94	Added: The end result of this	59
95	Added: Actual methodologies	59

96	Replaced: Static	60
97	Replaced: static	60
98	Replaced: couple dozen	60
99	Replaced: static	60
100	Replaced: Appendix A	60
101	Replaced: static	60
102	Replaced: immutable	60
103	Replaced: static	60
104	Replaced: Dynamic	60
105	Replaced: Dynamic	60
106	Replaced: equations are	60
107	Replaced: them	60
108	Replaced: collapsing	60
109	Replaced: reduced	61
110	Replaced: nonlinear	61
111	Replaced: framework	61
112	Replaced: black-box	61
113	Replaced: is the most straightfo...	61
114	Added: where	61
115	Replaced: corresponds	61
116	Added: with its own field stre...	61
117	Replaced: The constant value, here,	61
118	Added: keV	61
119	Added: keV	61

120	Added: keV	61
121	Replaced: The Greenwald densit	61
122	Deleted: Therefore, any reacto	62
123	Replaced: unique	63
124	Replaced: uses	63
125	Added: the	63
126	Replaced: inherent to every	63
127	Replaced: device incapable of pr	63
128	Replaced: unique	64
129	Replaced: The model therefore u	64
130	Deleted: laundry	64
131	Replaced: limiting	64
132	Replaced: These	64
133	Replaced: represent	64
134	Replaced: device incapable of pr	64
135	Replaced: Within a tokamak, it	64
136	Added: from fusion reactions	64
137	Deleted: Here, the resistance of	65
138	Replaced: This	65
139	Added: ³	65
140	Replaced: This	66
141	Added: Within most designs,	66
142	Added: effects of	66
143	Replaced: are emitted from the	66

144	Replaced: electrons collide with	66
145	Replaced: This term can be	66
146	Added: ³	66
147	Replaced: Where	67
148	Replaced: reducing	67
149	Replaced: each ion	67
150	Replaced: single representative	67
151	Replaced: one of the most diffic	67
152	Replaced: moves about randomly	67
153	Replaced: is a critical	68
154	Replaced: nonlinear behaviors	68
155	Replaced: quick-running code	68
156	Replaced: can be found using th	68
157	Replaced: undergo an e-folding	68
158	Replaced: device	68
159	Replaced: After several substitu	69
160	Replaced: Parameter	69
161	Replaced: arriving at a formula for	69
162	Replaced: using	69
163	Replaced: balance,	69
164	Replaced: Parameter	69
165	Replaced: Parameter	69
166	Replaced: tokamak ever	69
167	Replaced: reactor.	69

168	Replaced: Parameter	69
169	Replaced: Parameter	70
170	Replaced: As shown in Fig. 3-2, this	70
171	Replaced: well known to	70
172	Replaced: As expected, this sha	71
173	Replaced: Parameter	71
174	Replaced: Parameter	72
175	Replaced: motivated by the goal	72
176	Replaced: convoluted	72
177	Replaced: difficult to obtain	72
178	Replaced: reduce	72
179	Replaced: nonlinear behaviors	72
180	Replaced: regressional fit	72
181	Replaced: fits of this kind	72
182	Deleted: However, many have a	72
183	Replaced: enhancement factor o	73
184	Replaced: Next,	73
185	Replaced: However, similar scali	73
186	Replaced: written	73
187	Deleted: Although not actually	73
188	Replaced: Parameter	73
189	Replaced: After a few lines of al	73
190	Replaced: a formula	73
191	Deleted: Again, if the alternate	74

192	Replaced: limiting constraints.	74
193	Replaced: Parameter	74
194	Deleted: Before moving onto t...	74
195	Replaced: Parameter	74
196	Deleted: As is readily apparent...	74
197	Replaced: Limiting	75
198	Replaced: static	75
199	Added: Our analysis is always...	75
200	Replaced: limiting	75
201	Replaced: not completely unique...	75
202	Replaced: limiting	75
203	Replaced: limiting	75
204	Replaced: static	75
205	Deleted: physics-based	76
206	Replaced: Limit derived using st...	76
207	Replaced: static	76
208	Replaced: *	77
209	Replaced: *	77
210	Deleted: is subscripted by 95, a...	77
211	Added: ⁷	77
212	Deleted: Next, the f_q variable...	77
213	Replaced: *	77
214	Replaced: limiting	77
215	Replaced: limiting	77

216	Replaced: limiting	77
217	Replaced: begin	77
218	Replaced: limiting	77
219	Added: For clarity, the wall lo...	77
220	Replaced: collide with the tokam...	78
221	Replaced: simple	78
222	Replaced: *	78
223	Replaced: static	78
224	Replaced: limiting	78
225	Replaced: limiting	78
226	Replaced: constraint set by econ...	78
227	Added: Note that this 4000 M...	78
228	Replaced: static	79
229	Deleted: The constant in front...	79
230	Added: And the constant in f...	79
231	Replaced: limiting	79
232	Replaced: fundamentally an uns...	79
233	Replaced: modern	79
234	Added: ⁸	79
235	Replaced: Fusion plasmas	80
236	Replaced: relation	80
237	Replaced: – which makes 15 keV...	80
238	Replaced: slightly	80
239	Replaced: heat damage to	80

240	Added: -per-square-meter	80
241	Replaced: ⁸	80
242	Replaced: As such, this model t...	80
243	Replaced: completeness	80
244	Replaced: limiting	80
245	Added: This is the heat load...	80
246	Replaced: limiting	81
247	Replaced: Stepping back, this	81
248	Replaced: moved onto	81
249	Deleted: moving onto	81
250	Replaced: allow modeling	81
251	Added: though,	81
252	Replaced: described	81
253	Replaced: a simple relation assu...	81
254	Replaced: limiting	82
255	Replaced: not completely unique	82
256	Deleted: The next step now is...	82
257	Added: The next step now is...	82
258	Added: reactor design	83
259	Added: This generalized plas...	83
260	Replaced: This is described by t...	84
261	Added: During this time, a pl...	87
262	Added: The exact definitions f...	87
263	Added: – usually measured in...	88

264	Added: microhenry-scale	88
265	Replaced: static	93
266	Replaced: Constructing	94
267	Added: – as dictated by cycli	94
268	Added: flattop	94
269	Replaced: expected	94
270	Added: This analysis of cours	95
271	Replaced: Producing	95
272	Added: the	96
273	Added: code	96
274	Replaced: Adding	96
275	Replaced: as much as a 50% im	96
276	Replaced: drifting radially	97
277	Added: (valid for a circular pl	97
278	Replaced: After a few lines of al	97
279	Replaced: spiraled	98
280	Replaced: Calculating	99
281	Deleted: strongly	100
282	Added: mainly	100
283	Deleted: a little	100
284	Deleted: Here, the constant ter	100
285	Replaced: Here, P_W	100
286	Replaced: Section 3.4.3	100
287	Replaced: a previous model	100

288	Replaced: dynamic	101
289	Replaced: static	101
290	Replaced: static	101
291	Replaced: dynamic	101
292	Replaced: 600	102
293	Replaced: 100	102
294	Replaced: static	103
295	Replaced: dynamic	104
296	Replaced: dynamic	105
297	Replaced: resolve a similar problem	106
298	Added: A simple algebra will...	109
299	Replaced: In essence,	109
300	Replaced: reasonably	109
301	Replaced: proved to be	110
302	Replaced: complicated.	110
303	Replaced: shown,	110
304	Deleted: – the stability require...	110
305	Replaced: the more difficult of t...	110
306	Replaced: current balance	110
307	Replaced: equation	110
308	Replaced: is substituted	110
309	Replaced: do a final	110
310	Added: wall loading term in	110
311	Replaced: quantifies its net elect...	110

312	Added: partially	111
313	Deleted: user-supplied	111
314	Replaced: varieties:	111
315	Replaced: intermediate	111
316	Replaced: dynamic	111
317	Replaced: dynamic (D)	111
318	Replaced: intermediate (I)	111
319	Replaced: *	111
320	Replaced: Including Limiting Co...	112
321	Replaced: composed of the limit...	112
322	Replaced: *	112
323	Replaced: current,	112
324	Replaced: dynamic	112
325	Replaced: intermediate	112
326	Added: -per-square-meter	112
327	Replaced: machine. ⁸	112
328	Replaced: dynamic	113
329	Replaced: static	113
330	Replaced: Intermediate	113
331	Replaced: intermediate	113
332	Replaced: This	113
333	Replaced: The first of which is to...	113
334	Replaced: Dynamic	115
335	Replaced: dynamic	115

336	Replaced: difficulty for the algeb...	115
337	Added: Overcoming this diffic...	115
338	Added: for	115
339	Replaced: reduces	116
340	Replaced: These	116
341	Deleted: we will encounter	116
342	Replaced: scans that	116
343	Replaced: against other	117
344	Replaced: These are created using	117
345	Replaced: The	117
346	Replaced: will then be used to c...	117
347	Replaced: static	117
348	Added: – one at a time.	117
349	Replaced: static	117
350	Replaced: matchers	117
351	Replaced: type	117
352	Replaced: dynamic	125
353	Replaced: limiting	126
354	Replaced: static	128
355	Replaced: dynamic	133
356	Replaced: static	133
357	Replaced: less expensive LTS m...	137
358	Replaced: static	140
359	Replaced: Static	155

360	Replaced: Static	155
361	Replaced: *	155
362	Replaced: static	160
363	Replaced: static	161
364	Replaced: dynamic	162
365	Replaced: static	162
366	Replaced: dynamic	162
367	Replaced: static	162
368	Replaced: dynamic	162

A Levelized Comparison of Pulsed and Steady-State Tokamaks

by

Daniel Joseph Segal

B.S. Engineering Physics, University of Wisconsin (2014)

Submitted to the Department of Nuclear Science and Engineering
in partial fulfillment of the requirements for the degree of

Master of Science in Nuclear Science and Engineering

at the

MASSACHUSETTS INSTITUTE OF TECHNOLOGY

February 2018

© Massachusetts Institute of Technology 2018. All rights reserved.

Author

Department of Nuclear Science and Engineering

November 11, 2018

Certified by

Jeffrey P. Freidberg

KEPCO Professor Emeritus

Thesis Supervisor

Certified by

Anne E. White

Cecil and Ida Green Associate Professor

Thesis Reader

Accepted by

Ju Li

Battelle Energy Alliance Professor

Chair, Department Committee on Graduate Students

369 **A Levelized Comparison of**
370 **Pulsed and Steady-State Tokamaks**

371 by

372 Daniel Joseph Segal

373 Submitted to the Department of Nuclear Science and Engineering
374 on November 11, 2018, in partial fulfillment of the
375 requirements for the degree of
376 Master of Science in Nuclear Science and Engineering

377 **Abstract**

378 The goal of fusion energy research is to build a profitable reactor. This thesis develops
379 a cost estimate model for fusion reactors from a physicist's perspective. It then applies
380 it to the two main modes of operation for a tokamak reactor: pulsed and steady-state.
381 In the end, an apples-to-apples comparison is developed, which is used to explain:
382 the relative advantages of pulsed and steady-state operation, as well as, the design
383 parameters that provide the most leverage in lowering machine costs. The most
384 notable of these is the magnetic field strength – which should be doubled by ongoing
385 research efforts at MIT using high-temperature superconducting (HTS) tape.

Thesis Supervisor: Jeffrey P. Freidberg
Title: Professor of Nuclear Science and Engineering (Emeritus)

Contents

387	1	Introducing Fusion Reactors	31
388	1.1	Treating Fusion as a Science	31
389	1.2	Treating Fusion as a Business	34
390	1.3	Pricing a Fusion Reactor	36
391	1.4	Modeling a Fusion Reactor	38
392	2	Designing a Steady-State Tokamak	41
393	2.1	Defining Plasma Parameters	42
394	2.1.1	Understanding Tokamak Geometry	42
395	2.1.2	Prescribing Plasma Profiles	44
396	2.2	Solving the Steady Current	47
397	2.2.1	Enforcing the Greenwald Density Limit	48
398	2.2.2	Declaring the Bootstrap Current	50
399	2.2.3	Deriving the Fusion Power	52
400	2.2.4	Using Current Drive	55
401	2.2.5	Completing the Steady Current	56
402	2.3	Handling Current Drive Self-Consistently	57
403	3	Formalizing the Systems Model	59
404	3.1	Explaining StaticFixed Variables	60
405	3.2	Connecting DynamicFloating Variables	60
406	3.3	Enforcing Power Balance	64
407	3.3.1	Collecting Power Sources	65
408	3.3.2	Approximating Radiation Losses	66

409	3.3.3	Estimating Heat Conduction Losses	67
410	3.3.4	Writing the Lawson Parameter Criterion	69
411	3.3.5	Finalizing the Primary Constraint	72
412	3.4	Collecting Limiting Secondary Constraints	75
413	3.4.1	Introducing the Beta Limit	75
414	3.4.2	Giving the Kink Safety Factor	76
415	3.4.3	Working under the Wall Loading Limit	77
416	3.4.4	Setting a Maximum Power Cap	78
417	3.4.5	Listing the Heat Loading Limit	80
418	3.5	Summarizing the Fusion Systems Model	81
419	4	Designing a Pulsed Tokamak	83
420	4.1	Modeling Plasmas as Circuits	84
421	4.1.1	Drawing the Circuit Diagram	84
422	4.1.2	Plotting Pulse Profiles	86
423	4.1.3	Specifying Circuit Variables	90
424	4.1.4	Constructing Reasoning the Pulse Length	94
425	4.2	Producing Salvaging Flux Balance	95
426	4.2.1	Rearranging the Circuit Equation	95
427	4.2.2	Adding Importing Poloidal Field Coils	96
428	4.3	Improving Tokamak Geometry	98
429	4.3.1	Defining Central Solenoid Dimensions	98
430	4.3.2	Calculating Measuring Component Thicknesses	99
431	4.3.3	Revisiting Central Solenoid Dimensions	102
432	4.4	Piecing Together the Generalized Current	103
433	4.5	Simplifying the Generalized Current	105
434	4.5.1	Recovering the Steady Current	105
435	4.5.2	Extracting the Pulsed Current	106
436	4.5.3	Rationalizing the Generalized Current	107
437	5	Completing the Systems Model	109

438	5.1	Describing a Simple Algebra	109
439	5.2	Generalizing Previous Equations	111
440	5.2.1	Including Limiting Constraints Rehashing the Limits	112
441	5.2.2	Minimizing Intermediate Derived Quantities	113
442	5.2.3	Pinning Dynamic Floating Variables	115
443	5.2.4	Detailing the Equation Solver	115
444	5.3	Wrapping up the Logic	116
445	6	Presenting the Code Results	119
446	6.1	Validating Code with other Models	120
447	6.1.1	Comparing with the PSFC Arc Reactor	121
448	6.1.2	Contrasting with the Aries Act Studies	122
449	6.1.3	Benchmarking with the Process DEMO Designs	125
450	6.2	Developing Prototype Reactors	128
451	6.2.1	Navigating around Charybdis	131
452	6.2.2	Pinning down Proteus	132
453	6.3	Learning from the Data	133
454	6.3.1	Picking a Design Point	133
455	6.3.2	Utilizing High Field Magnets	137
456	6.3.3	Looking at Design Alternatives	140
457	7	Planning Future Work	147
458	7.1	Incorporating Stellarator Technology – Ladon	147
459	7.2	Making a Hybrid Reactor – Janus	148
460	7.3	Bridging Confinement Scalings – Daedalus	149
461	7.4	Addressing Model Shortcomings	150
462	7.4.1	Integrating Pedestal Temperature Profiles	150
463	7.4.2	Expanding the Radiation Loss Term	151
464	7.4.3	Taking Flux Sources Seriously	151
465	8	Concluding Reactor Discussion	153

466	A Presenting StaticFixed Variables	155
467	B Simulating with Fussy.jl	157
468	B.1 Getting the Code to Work	157
469	B.2 Sorting out the Codebase	158
470	B.2.1 Typing out Structures	159
471	B.2.2 Referencing Input Decks and Solutions	161
472	B.2.3 Acknowledging Utility Functions	161
473	B.2.4 Mentioning Base Level Files	161
474	B.3 Delving into Reactor Methods	162
475	B.4 Demonstrating Code Usage	163
476	B.4.1 Initializing the Workspace	164
477	B.4.2 Running a Study	164
478	B.4.3 Extracting Results	165
479	B.4.4 Plotting Curves	166
480	C Discussing Fusion Power	171
481	C.1 Fusion Power – P_F	171
482	C.2 Reactivity – (σv)	173
483	D Selecting Plasma Profiles	177
484	D.1 Density – n	177
485	D.2 Temperature – T	179
486	D.3 Pressure – p	181
487	D.4 Bootstrap Current – f_{BS}	181
488	D.5 Volume Averaged Powers	183
489	E Determining Plasma Flux Surfaces	185
490	E.1 Flux Surface Coordinates	185
491	E.2 Cross-sectional Area and Volume	187
492	E.3 Surface and Volume Integrals	188

493	F Expanding on the Bootstrap Current	191
494	F.1 Summarized Results	191
495	F.2 Detailed Analysis	192

496 List of Figures

497	1-1	Cut-Away of Tokamak Reactor	32
498	1-2	Comparison of Pulsed and Steady-State Current	33
499	1-3	Fusion Never Funding Timeline	34
500	1-4	H-Mode Confinement Time Scaling	35
501	1-5	Steady State Magnet Components	40
502	1-6	Pulsed Magnet Components	40
503	2-1	Geometry of a Tokamak	43
504	2-2	Geometric Parameters	44
505	2-3	Radial Plasma Profiles	45
506	2-4	Greenwald Density Limit	49
507	3-1	Current Balance in a Tokamak	63
508	3-2	Power Balance in a Reactor	70
509	4-1	A Simple Plasma Transformer Description	85
510	4-2	Time Evolution of Circuit Profiles	86
511	4-3	Dimensions of Tokamak Cross-Section	99
512	5-1	Minimize Cost Step II/III – Optimize Reactor	114
513	6-1	Arc Model Comparison	121
514	6-2	Act Studies Cost Dependence on the H Factor	122
515	6-3	Aries Act I Model Comparison	123
516	6-4	Aries Act II Model Comparison	124
517	6-5	Demo Steady Model Comparison	126
518	6-6	Demo Pulsed Model Comparison	127

519	6-7	How to Build a Fusion Reactor	130
520	6-8	Steady State Prototype Comparison	131
521	6-9	Pulsed Prototype Comparison	132
522	6-10	Limit Regimes as function of B_0	134
523	6-11	Steady State Cost Curves	135
524	6-12	Pulsed Cost Curves	136
525	6-13	Pulsed B_{CS} Sensitivity	138
526	6-14	Pulsed Monte Carlo Sampling	139
527	6-15	Bootstrap Current Monte Carlo Sampling	141
528	6-16	Internal Inductance Sensitivities	142
529	6-17	Pulsed H Sensitivities	144
530	6-18	Steady State Current Drive Efficiency	145
531	6-19	Current Drive Efficiency vs Launch Angle	146
532	7-1	Cut-Away of Stellarator Reactor	148
533	7-2	Current Balance in a Tokamak	149
534	B-1	A Blank Plot	167
535	B-2	An Empty Plot	168
536	B-3	An Unscaled Plot	169
537	B-4	A Scaled Plot	169
538	C-1	Comparing Nuclear Fusion and Fission	172
539	C-2	The D-T Fusion Reaction	173
540	D-1	Radial Plasma Profiles	177
541	E-1	Cut-Away of Tokamak Reactor	185
542	E-2	Dimensions of Tokamak Cross-Section	187

543 List of Tables

544	3.1	Dynamic Variables	60
545	4.1	Piecewise Linear Scheme for Pulsed Operation	87
546	4.2	Example TF Coils and Central Solenoid Critical Values	102
547	5.1	Main Equation Bank	111
548	6.1	Arc Variables	121
549	6.2	Act I Variables	123
550	6.3	Act II Variables	124
551	6.4	Demo Steady Variables	127
552	6.5	Demo Pulsed Variables	128
553	6.6	Charybdis Variables	131
554	6.7	Proteus Variables	132
555	A.1	List of Static Fixed Variables	155

List of Equations

557	1.1	Magnetic Energy – W_M	37
558	1.2	Cost per Watt – C_W	38
559	2.1	Minor Radius – a	43
560	2.2	Density Profile – n	45
561	2.4	Temperature Profile – T	46
562	2.5	Current Profile – J	46
563	2.6	Internal Inductance – l_i	47
564	2.7	Normalized Poloidal Magnetic Field – b_p	47
565	2.8	Current Balance – I	47
566	2.11	Greenwald Density – \bar{n}	50
567	2.15	Bootstrap Current – I_{BS}	52
568	2.20	Dilution Factor – f_D	54
569	2.21	Volume Integral – Q_V	54
570	2.23	Fusion Power – P_F	54
571	2.28	Current Drive – I_{CD}	56
572	2.30	Steady Current – I_P	57
573	2.31	Current Drive Efficiency – η_{CD}	58
574	3.1	Scanned Temperature – \bar{T}	61
575	4.75	Generalized Current – I_P	104
576	C.1	Fusion Energy – E_F	171
577	C.3	Alpha Power – P_α	173
578	C.4	Neutron Power – P_n	173

Chapter 1

Introducing Fusion Reactors

The central goal of fusion energy research is to build a profitable nuclear reactor. It has long been joked though that fusion power will always be 20-50 years away. This paper lays a framework for exploring reactor space for functional, efficient designs – based on world experiments during the last half-century. Due to the speed and simplicity of the model, hundreds of reactors can be explored in minutes (outpacing the domestic program slightly).

With this proposed model, interesting reactors can be pinpointed long before engineers hit the blueprints. This should help shorten the time until a profitable reactor, as well as illuminate ways to improve modern plasma theory. Further, it verifies the reasoning of MIT’s PSFC to invest in high field, high-temperature superconducting (HTS) tape – as this technology would lead to much smaller devices.

1.1 Treating Fusion as a Science

When people talk about fusion, they usually talk about plasma physics, and when people talk about plasma physics, they often talk about things like: the sun, lightning, and the aurora borealis. Of these three, the sun is the only nuclear reactor. However, the sun can stay on all day because the massive gravity of its fuel source helps keep

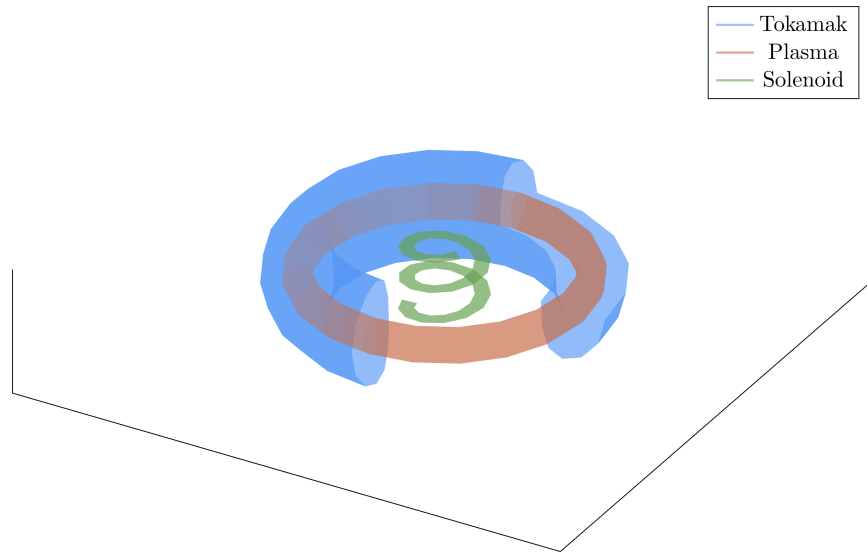


Figure 1-1: Cut-Away of Tokamak Reactor

The three main components of a magnetic fusion reactor are: the tokamak structure, the plasma fuel, and the spring-like solenoid at the center.

597 it self-contained in space. On Earth, this is not possible – the plasma fuel* needs to
598 be contained by other means (i.e. with magnets).

599 A tokamak is one of the leading candidates for a profitable fusion reactor. It shares the
600 shape of a doughnut, using magnets to keep a hula hoop of plasma swirling inside it.
601 The difficulty of keeping this plasma swirling though, is that it does not enjoy being
602 spun too fast or squeezed too hard. Conversely, the tokamak housing the plasma does
603 not like taking too much of a beating or being scaled to T-Rex sized proportions. This
604 sets the stage for tokamak reactor design – building on the various plasma physics
605 and nuclear engineering constraints of the day.

606 One of the most contentious points of building a tokamak, however, is whether it
607 will be run as: pulsed (the European approach⁹) or steady-state (the United States
608 effort⁴). Here, pulsed operation refers to how a reactor is turned on and off periodically
609 – around ten times a day. Whereas, steady state machines are meant to be left on

*Plasmas are the fourth state of matter after: solids, liquids, and gases. Fundamentally they are gaseous fluids that respond to electric and magnetic fields.

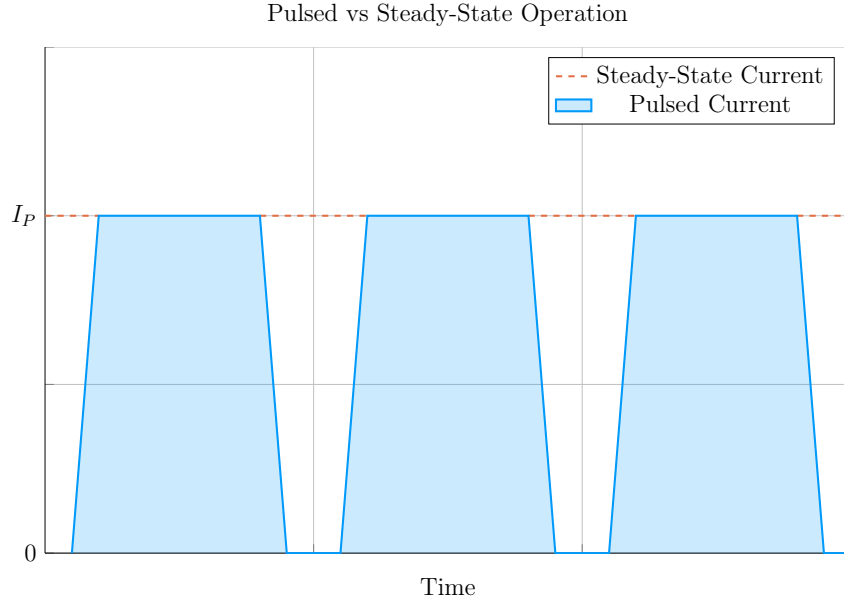


Figure 1-2: Comparison of Pulsed and Steady-State Current

Inside a pulsed reactor, current is ramped up and down several times a day – with breaks in-between. Steady state reactors are meant to stay on for weeks, months, or years.

610 nearly the entirety of their 50-year campaigns. These behaviors are shown in Fig. 1-2.

611 These two modes of operation, *pulsed* and *steady-state*, greatly influence the design
 612 through the current balance equation (derived later). What this means practically is
 613 tokamaks need current to spin their plasma hoops at some required speed and this
 614 current has to come from somewhere. Luckily, the plasma naturally enjoys spinning
 615 and provides some assistance through the bootstrap current. The remaining current
 616 must then be produced by external means.

617 The source of external current drive is what distinguishes pulsed from steady-state
 618 devices. Steady-state devices provide the required current assistance either through
 619 lasers or particle beams – this paper’s model focusing on a type of laser assistance
 620 called lower-hybrid current drive (LHCD).³ Pulsed machines, on the other hand, rely
 621 on inductive sources – which by definition require cycles of charging and discharging
 622 several times a day.*

623 The goal of this document is to show that pulsed and steady-state operation are

*These inductive sources are akin to a battery on a laptop that must be recharged every so often.

624 actually two sides of the same coin. This yields the simple conclusion that a single
 625 comprehensive model can run both modes at the flip of a switch. It even opens the
 626 opportunity of a hybrid reactor that exists somewhere in between the two.

627 1.2 Treating Fusion as a Business

628 Plasmas may be interesting, but that is not why countries build billion dollar research
 629 experiments. The ultimate goal of fusion research is to develop an energy resource
 630 that competes with coal and other base-load power sources (e.g. from hydroelectric
 631 and nuclear fission power plants). The problem is plasmas are chaotic and hard to
 632 contain, while tokamaks are expensive and slow to build. This perfect match has long
 633 put the field’s projected timeline to that of *fusion never*.¹⁰

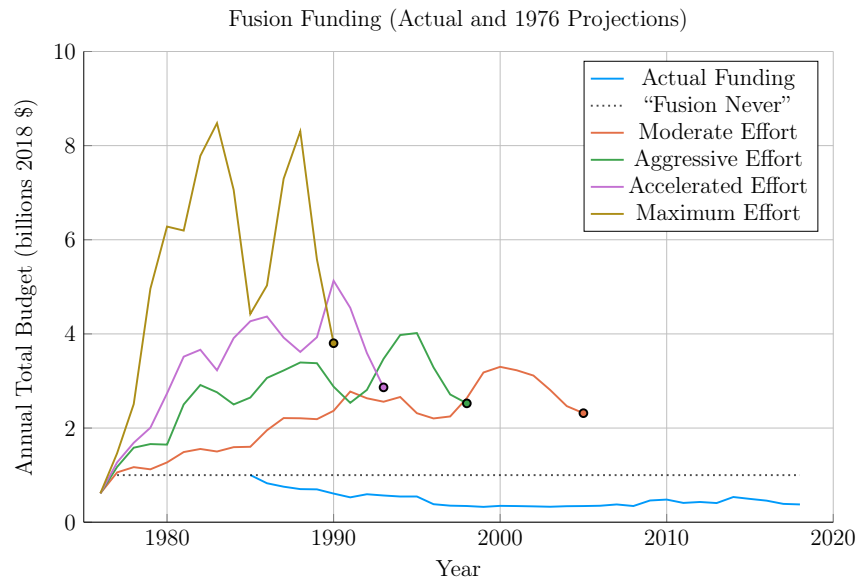


Figure 1-3: Fusion Never Funding Timeline

Comparison of Projected Timelines of Fusion from 1976 with Actual DOE Budgets.^{11,12}
 The dotted line is popularly referred to in the community as “Fusion Never.”¹³

634 The major problem with containing a plasma in a reactor is that a plasma does not
 635 want to be contained. Since the early days of fusion research, plasmas have often
 636 found escape mechanisms. When presented with a magnetic bottle, they found their

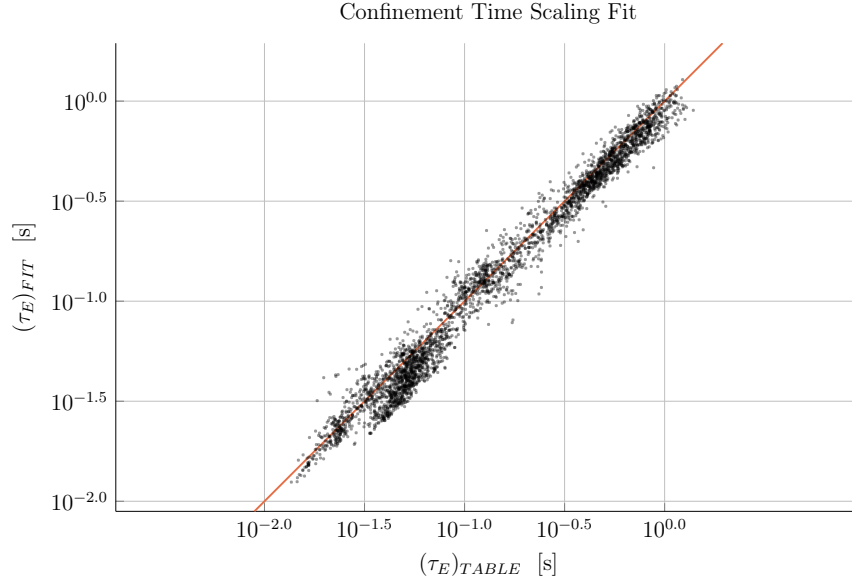


Figure 1-4: H-Mode Confinement Time Scaling

This plot shows how well the ELMy H-Mode Scaling Law does for fitting τ_E to the ITER98 database of global tokamaks. For most values, the fit is at least 80% accurate.

637 way out the top. In a tokamak, they attack the outer edges like an overinflated tire-
 638 tube. Fusion energy has seemed to remain a Tantalizing effort – within arms reach,
 639 but staunchly guarded by a shroud of instabilities.

640 The truth is plasmas are extremely chaotic: they show nonlinear behavior in almost
 641 everything they do. As of now, no theory or supercomputer-backed code can predict
 642 even something so fundamental to design as the movement of energy and particles
 643 within a tokamak. As such, the field has adopted several rules of thumb and empirical
 644 scalings – based on the last half century of experiments – which help one navigate
 645 around a plasma’s finicky behavior.

646 The two most widely used rules of thumb within the fusion design community are:
 647 the Greenwald density limit and the ELMy H-Mode confinement time scaling law.
 648 As such, the model in this document heavily utilizes the two to make a quick running
 649 code. These two relations are also why this model – which happens to be zero-
 650 dimensional – can reproduce with high fidelity the answers from three-dimensional
 651 codes, which can take days, weeks, or even months to run!

652 The use of the ELMy H-Mode scaling law also brings up another subtlety in the field.
653 To measure the movement of energy within a plasma, scaling relations are needed
654 that correlate to specific modes of plasma behavior – i.e. ones that can robustly be
655 found on a device by technicians. Currently, people rank H-Mode scalings over L-
656 Mode ones (because H stands for high confinement and L stands for low). However,
657 people often seek out other modes that can reliably be found on other machines.
658 These go by names like: I-Mode (i.e. intermediate confinement), Enhanced H-Mode,
659 and Reversed Shear modes.^{14–16}

660 Without going into too much detail, these alternate modes can be extremely valu-
661 able, as they often lead to more attractive reactors (than those made under H-Mode
662 scalings). The problem, however, is often not finding a better performing mode on a
663 single machine, but robustly finding it on other ones. This is important, because find-
664 ing a mode on multiple machines is what allows new scaling relations to be produced
665 and refined.*

666 1.3 Pricing a Fusion Reactor

667 To compare tokamaks used as fusion reactors the obvious metrics are costs. ITER –
668 the second most expensive experiment today (only behind the LHC) – has a history
669 rich in countries backing out for high price tags and rejoining only when they finally
670 get lowered.³ The problem is \$20B is a lot of money and 20 years is a long time.
671 Moreover, approximating true costs becomes even trickier when designers need to
672 project (or neglect) economies-of-scale for expensive components, such as the magnets
673 and irradiated materials.

674 As such, this paper adopts stand-ins for the conventional capital cost and cost-per-
675 watt metrics. This is done for simplicity, for both: modeling reasons as well as
676 conveying the two metrics to physicists. To begin, the relevant approximation for

*In H-Mode and L-Mode’s favor, they have been found on every machine that should see them.

capital cost – how much a tokamak costs to build – is the magnetic energy.¹⁷

$$W_M \propto R^3 B^2 \quad (1.1)$$

In this magnetic energy proportion relation, the tokamak’s major radius – R – is involved in a volumetric term (R^3) and B is the strength (in Teslas) of the hooped shape magnetic field that lays nested within the plasma’s shell (near its core). This quantity simply states that the two surefire ways to make a machine more expensive to build are: making it larger and using stronger magnets.

The next metric, the cost-per-watt, is defined by dividing the capital cost (i.e. the magnetic energy) by the main source of power output. This quantity measures how profitable a reactor will be once it is built. In a tokamak, the main power output is assumed to be fusion power, which relies on light elements (i.e. two Hydrogens) fusing into a heavier one (i.e. one Helium) – hopefully releasing enough energy to offset the expense of causing it to happen in the first place. Although fusion power will not be defined till later, it does highlight the fact that this measure of cost-per-watt actually has units of time!*

The final piece of the costing puzzle is a duty factor that levelizes the comparison of pulsed and steady-state tokamaks. As pulsed machines may be off 20% of the time, their fusion power output should be reduced by that percentage. This is accounted for in the duty factor, which is simply the ratio of the flattop – the time when pulsed machines are approximately held at steady-state – to the entire length of the pulse.

In pulsed machines, the entire pulse includes charging the inductive sources as well as flushing out the tokamak between runs. These non-flattop portions of time can last around thirty minutes (where the reactor makes no money). As steady-state machines lack these non-flattop portions, their duty factors are rightfully one. Analysis in Section 4.1.4 and discussion with several researchers, however, show that the same

*As energy per unit watt has units of time (i.e seconds).

will probably hold true for a pulsed reactor, too.

Summarizing, the cost-per-watt coupled with the duty factor provides an ad hoc pricing metric, C_W , given by:

$$C_W = \frac{W_M}{f_{Duty} \cdot P_F} \quad (1.2)$$

It serves as a cornerstone for comparing the entire landscape of tokamak reactors – whether they run in pulsed or steady-state operation. Although not a true engineering cost metric (i.e. in dollars per watt), it does provide an obvious physics meaning. Coupled with the magnetic energy stand-in for capital cost, these two costs allow researchers to pinpoint profitable and inexpensive tokamaks within reactor space.

1.4 Modeling a Fusion Reactor

Before reactors can be costed, though, they have to be modeled. Therefore the first half of this thesis is devoted to the theory behind tokamak design. A priority is placed more on a physicist’s intuition than an engineer’s costing rigor. This is justified by the nonlinearities inherent to the fusion systems and rationalized by this paper’s results matching more sophisticated frameworks with high fidelity.

What makes this paper’s model different from others in the field is the generalized handling of both modes of tokamak operation: pulsed and steady-state. This was necessitated by a desire to compare the two modes on a level playing field. What this shows is that both pulsed and steady-state tokamaks could make for profitable fusion reactors – assuming some technological advancements.

One technological advancement that could lead to major wins is improving magnet components. This is why MIT has championed high-field designs for the better part of the last century. In their latest effort, the PSFC team has explored new high-

725 temperature superconducting (HTS) tape capable of doubling the maximum achiev-
726 able field strength. What this paper shows is that this logic is indeed correct and
727 that HTS tape is all that is needed to build optimum reactors.

728 More concretely, this paper shows that new HTS tape technology is capable of low-
729 ering both pulsed and steady-state tokamak costs. Further, the benefits of doubling
730 the magnet strength bring the situation to a realm of significantly diminished rates
731 of return. HTS is thus the end goal for the conventional D-T fusion paradigm.

732 Moreover, this model shows that HTS is best utilized in different components for
733 pulsed and steady-state operation. Steady-state tokamaks favor HTS use in the D-
734 shaped magnets that circle the machine (i.e. the TF coils). Whereas pulsed devices
735 would benefit from employing HTS in the central solenoid – that produces most
736 of a reactor’s inductive current. A corollary of this is ~~the more conventional low-~~
737 ~~temperature superconducting (LTS) magnets (i.e. less expensive ones)~~~~conventional~~
738 ~~copper magnets (i.e. inexpensive ones)~~ can be used for pulsed TF coils, as their
739 improved confinement saturates at much lower field strengths.

740 Now that the problem has been thoroughly introduced, we will go over the theory
741 behind steady-state and, then, pulsed tokamaks. A couple segues will be taken along
742 the way to show how the model can be incorporated into a fusion systems code. This
743 code – Fussy.jl – is the topic of an appendix chapter and is freely available at:

744 git.io/tokamak

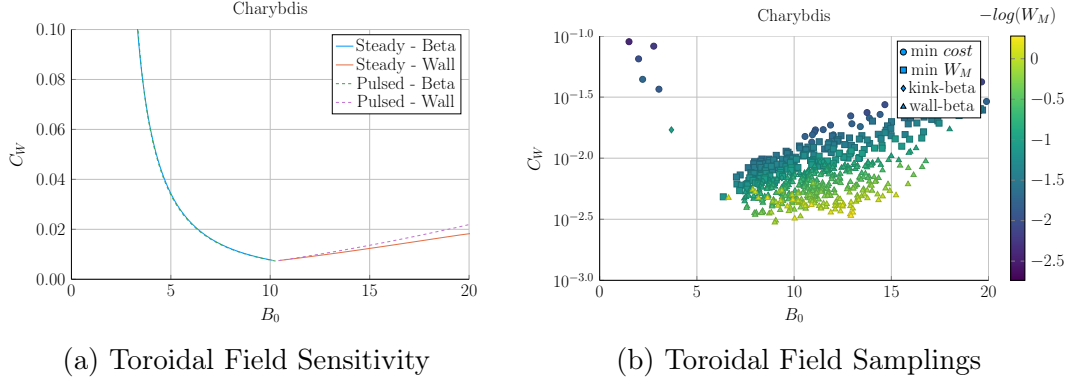


Figure 1-5: Steady State Magnet Components

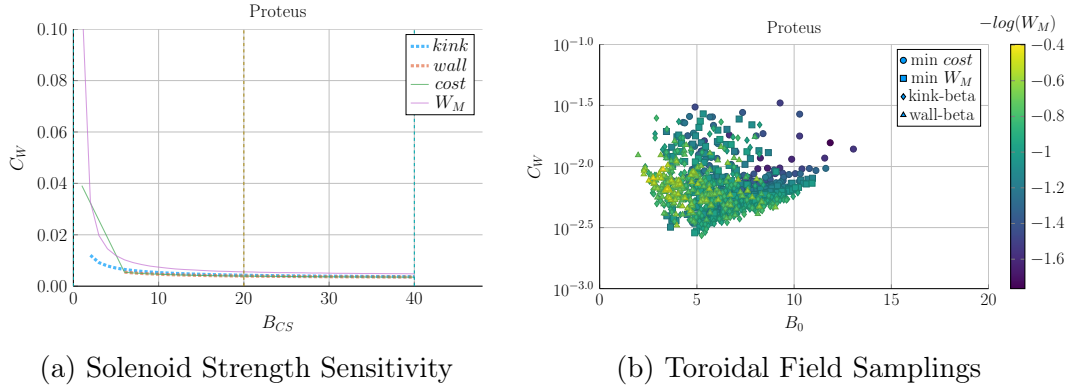


Figure 1-6: Pulsed Magnet Components

Chapter 2

Designing a Steady-State Tokamak

This chapter explores a simple model for designing steady-state tokamaks. In the next couple chapters, the model is first formalized for use in a systems code and then generalized to handle pulsed operation. These derivations highlight that the only difference between the two modes of operation is how they generate their auxiliary plasma current: LHCD for steady-state operation and inductive sources for when a reactor is purely pulsed.

Along the way, equations will be derived that get rather complicated. To remedy the situation, a distinction between `dynamicfloating` and `staticfixed` values is now given, which will allow splitting most equations into `staticfixed` and `dynamicfloating` parts. `DynamicFixed` values – i.e. the tokamak’s major radius (R_0) and magnet strength (B_0), as well as the plasma’s current (I_P), temperature (\bar{T}), and density (\bar{n}) – are first-class variables in the model (see Table 3.1). Everything is derived to relate them. `StaticFixed` values, on the other hand, can be treated as code inputs, which remain constant throughout a reactor solve. These most obviously include the various geometric and profile parameters introduced next section.

The overall structure of this chapter, then, is built around developing an equation for plasma current in a steady-state tokamak. It is shown that this value arises from balancing current in a reactor using both a plasma’s own bootstrap current (I_{BS}),

as well the tokamak's auxiliary driven current (I_{CD}). These relations necessitate geometric parameters and plasma profiles, which will be given shortly. Along the way, definitions will also be needed for the Greenwald density (N_G) and the fusion power (P_F). What is shown is that the current does not actually depend directly on the major radius (R_0) or magnet strength (B_0) of a tokamak – allowing these variables to be put off until next chapter.

2.1 Defining Plasma Parameters

As mentioned previously, the zero-dimensional model derived here can closely approximate solutions from higher-dimensional codes that might take many hoursweeks to run. The essence of boiling down three-dimensional behaviors to one dimensional profiles – and zero-dimensional averaged values – begins with defining the most important plasma parameters. These are the: current density (J), temperature (T), and density (n) of a plasma.

Solving this problem most generally usually involves decoupling the geometry of the plasma from the shaping of its nearly parabolic radial-profiles – both of which will be explained shortly.

2.1.1 Understanding Tokamak Geometry

The first thing people see when they look at a tokamak is its geometry – see Fig. 2-1. How big is it? Is it stretched out like a bicycle tire or compressed to the point of being nearly spherical? Would a slice across the major radius result in two cross-sections that were: circular, elliptic, or triangular?~~Is it stretched out like a tire or smooshed together like a bagel? If it were torn in two, would the exposed areas look like: circles, ovals, or triangles?~~

These questions lend themselves to the three important geometric variables – the inverse aspect ratio (ϵ), the elongation (κ), and the triangularity (δ). The inverse

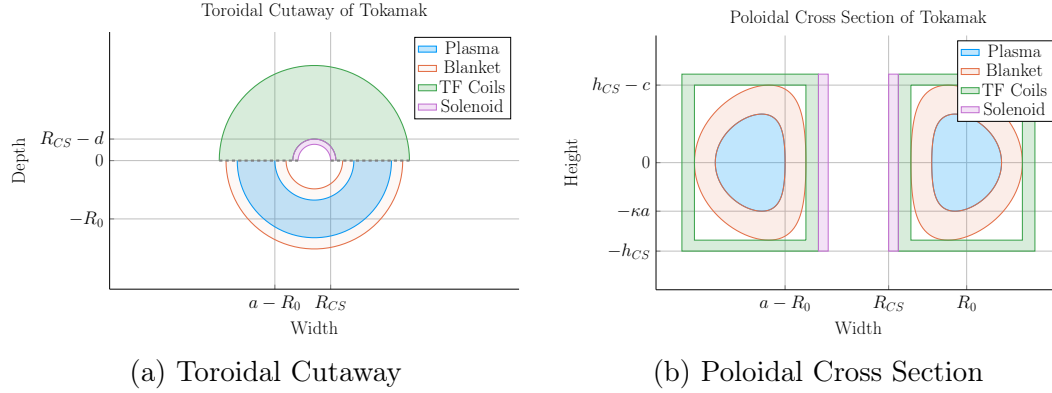


Figure 2-1: Geometry of a Tokamak

This diagram is of a tokamak's toroidal (top) view and the poloidal cross section of a slice across the major axis. Included are the four components of a reactor: the plasma, its metallic blanket, the toroidal field magnets surrounding them, and the central solenoid. These have thicknesses of a , b , c and d , respectively. R_{CS} is where the solenoid starts.

790 aspect ratio is a measure of how stretched out the device is, or formulaically:

$$a = \epsilon \cdot R_0 \quad (2.1)$$

791

792 This says that the minor radius (a), measured in meters, is related to the major radius
 793 of the machine (R_0) through ϵ . Or more tangibly, the minor radius is related to the
 794 two small ~~cross-sections~~ ~~circles~~ that ~~result from a slice across the major radius of the~~
 795 ~~machine come from tearing a bagel in two. Whereas the major radius is related to~~
 796 ~~the overall circle of the bagel when viewing it from the top.~~

797 The remaining two geometric parameters – κ and δ – are related to the shape of the
 798 torn halves. As the name hints, elongation (κ) is a measure of how stretched out
 799 the tokamak is vertically – is the cross-section a circle or an oval? The triangularity
 800 (δ) is then how much the cross-sections point outward from the center of the device.
 801 All three's effects can be seen in Fig. 2-2. ~~Their exact usage within describing flux~~
 802 ~~surfaces is shown in Appendix E.~~

803 These geometric factors allow the volumetric and surface integrals governing fusion

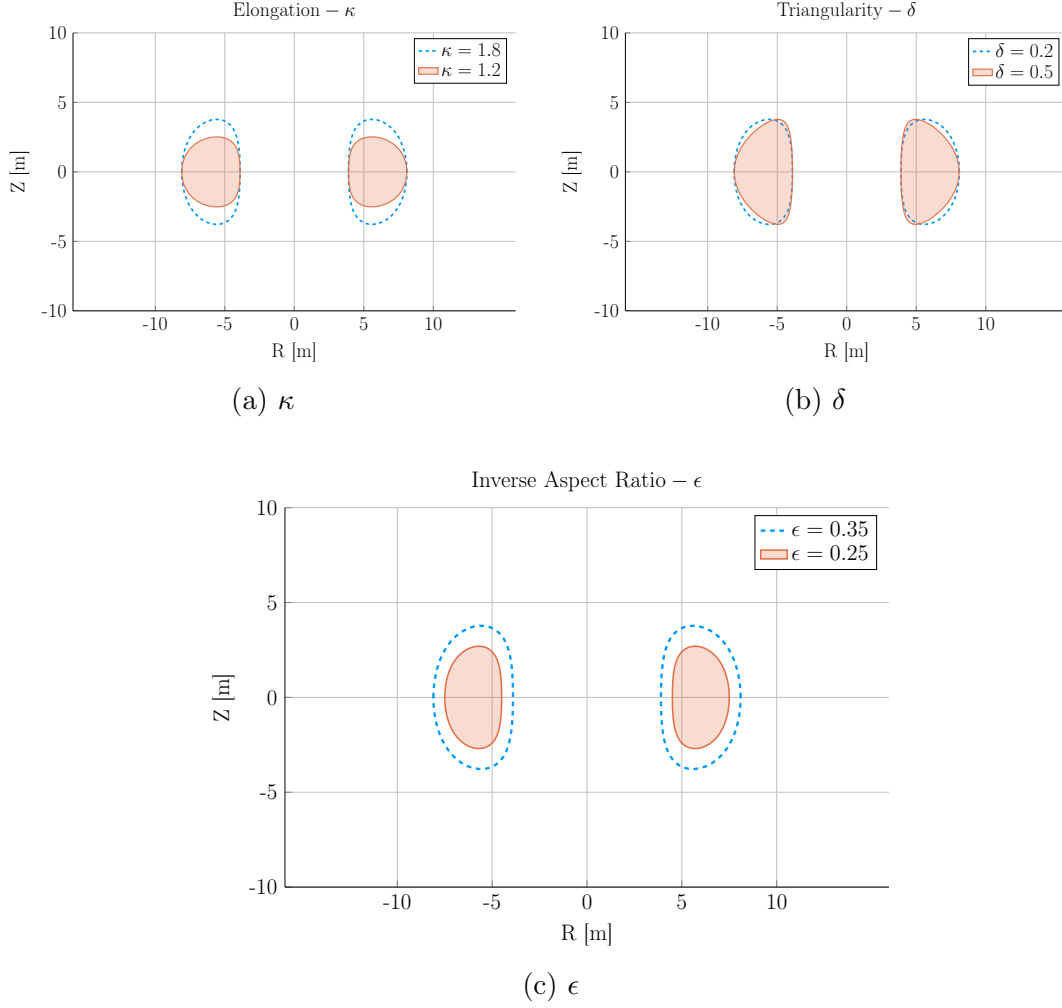


Figure 2-2: Geometric Parameters

These three geometric parameters allow the toroidal cross-sections to scale radially, stretch vertically, and become more triangular – thus improving upon simple circular slices.

power and bootstrap current to be condensed to simple radial ones – see Eqs. (E.24) and (E.25). The only remaining step is to define the radial profiles for: the density, temperature, and current of a plasma.

2.1.2 Prescribing Plasma Profiles

The first step in defining radial profiles is realizing that all three quantities are ~~essentially parabolas~~~~basically parabolas~~ – i.e. the temperature, density and current ~~density~~, shown in Section 2.1.2, are peaked at some radius (usually the center) and

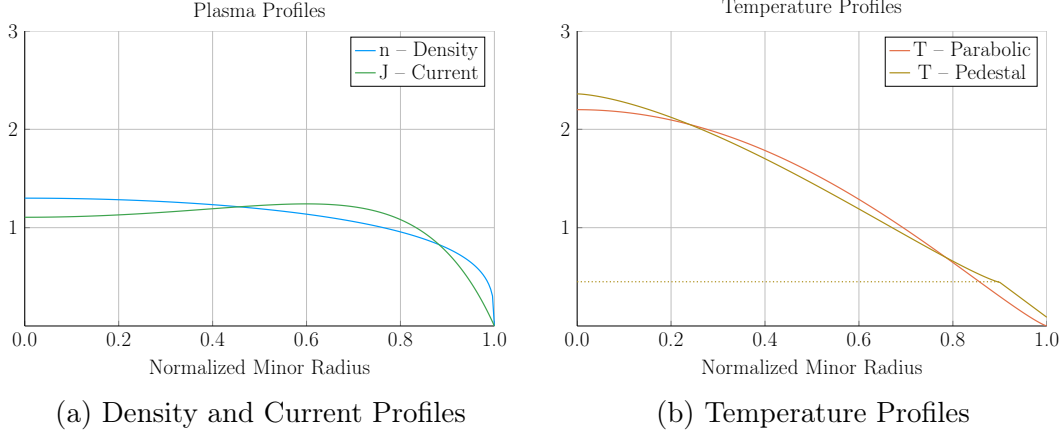


Figure 2-3: Radial Plasma Profiles

The three most fundamental ~~profiles~~^{properties} of a fusion plasma are its temperature, density, and current. These ~~profiles~~ allow the model to reduce from three dimensions to just half of one.

811 then decay to zero somewhere before the walls of the tokamak enclosure.

812 Although not self-consistent, these profiles do capture enough of the physics to ap-
813 proximate relevant phenomenon, such as transport and fusion power.¹

814 The Density Profile

815 To begin, density has the simplest profile. This is because it is relatively flat, remain-
816 ing near the average value – \bar{n} – throughout the body of the plasma until quickly
817 decaying to zero near the edge of the plasma.* For this reason, a parabolic profile
818 with a very low peaking factor – ν_n – is well suited.

$$n(\rho) = \bar{n} \cdot (1 + \nu_n) \cdot (1 - \rho^2)^{\nu_n} \quad (2.2)$$

819

820 The reason \bar{n} is referred to as the volume-averaged density is because using the volume
821 integral – given by Eq. (E.24) – over the density profile results in that value after

*Even in H-Mode plasmas where density profiles have a pedestal,¹⁸ they usually have much less of a peak than temperatures¹⁹ – especially so in a reactor setting.²⁰

822 dividing through by the volume (V):

$$\bar{n} = \frac{\int n(\mathbf{r}) d\mathbf{r}}{V} \quad (2.3)$$

823 A final point to make is this parabolic profile allows for a short closed-form relation
824 for the Greenwald density limit – substantially simplifying this fusion systems model.

825 The Temperature Profile

826 The use of a parabolic profile for the plasma temperature is slightly more dubious.
827 This is because H-Mode plasmas are actually highly peaked at the center, decaying
828 to a non-zero pedestal temperature near the edge before finally dropping sharply to
829 zero. This model chooses to forego this pedestal representation for a simple parabolic
830 one – although the pedestal approach is discussed in Appendix D. Analogous to the
831 density, the profile treats \bar{T} as the average value and ν_T as the peaking parameter.

$$T(\rho) = \bar{T} \cdot (1 + \nu_T) \cdot (1 - \rho^2)^{\nu_T} \quad (2.4)$$

832

833 The Current **Density** Profile

834 The plasma current **density** is the third profile and cannot safely be represented by a
835 simple parabola. This is because having an adequate bootstrap current relies heavily
836 on a profile being peaked off-axis – i.e. at some radius not at the center. This hollow
837 profile can then be modeled with the commonly given plasma internal inductance (l_i).
838 Concretely, the current's hollow profile is described by:

$$J(\rho) = \bar{J} \cdot \frac{\gamma^2 \cdot (1 - \rho^2) \cdot e^{\gamma \rho^2}}{e^\gamma - 1 - \gamma} \quad (2.5)$$

839

840 The intermediate γ quantity can then be numerically solved for from the plasma
 841 internal inductance using the following relations – with b_p representing the normalized
 842 poloidal magnetic field. **These are derived in Appendix F.**

$$l_i = \frac{4\kappa}{1 + \kappa^2} \int_0^1 b_p^2 \frac{d\rho}{\rho} \quad (2.6)$$

843

$$b_p(\rho) = \frac{-e^{\gamma\rho^2}(\gamma\rho^2 - 1 - \gamma) - 1 - \gamma}{\rho(e^\gamma - 1 - \gamma)} \quad (2.7)$$

844

845 Combined, these three geometric parameters and profiles lay the foundation for this
 846 zero-dimensional fusion systems model.

847 2.2 Solving the Steady Current

848 As suggested, one of the most important equations in a fusion reactor is current
 849 balance. In steady-state operation, all of a plasma's current (I_P) must come from
 850 a combination of its own bootstrap current (I_{BS}), as well as auxiliary current drive
 851 (I_{CD}). This can be represented mathematically as:

$$I_P = I_{BS} + I_{CD} \quad (2.8)$$

852

853 The goal is then to write equations for bootstrap current and driven current. This
 854 will make heavy use of the Greenwald density limit. **The steady current will then**
 855 **be**~~Without spoiling too much, the steady current is~~ shown to be only a function of
 856 temperature! In other words, this current is independent of a tokamak's geometry
 857 and magnet strength. As will be pointed out then, though, a subtlety arises that will
 858 bring the two back into the picture – self-consistency in the current drive efficiency
 859 (η_{CD}).

2.2.1 Enforcing the Greenwald Density Limit

The Greenwald density limit is a density limit that applies to all tokamaks ~~ubiquitous in the field of fusion energy~~. It sets a hard limit on the density and how it scales with current and reactor size. Although currently lacking a true first-principles theoretical explanation, it does have a real meaning within the design context. Operate at too low a density and run the risk of never entering H-Mode. Run the density too high, and cause the tokamak's plasma to ~~disrupt~~~~disrupt catastrophically!~~ These conclusions can be seen in Fig. 2-4.

As no theoretical backing exists, the Greenwald density limit can simply be written (with citation) as:²

$$\hat{n} = N_G \cdot \left(\frac{I_P}{\pi a^2} \right) \quad (2.9)$$

Here, \hat{n} has units of $10^{20} \frac{\text{particles}}{\text{m}^3}$, N_G is the Greenwald density fraction, and I_P is again the plasma current (measured in mega-amps). ~~and π has its usual meaning (3.141592653...)~~. The final variable is then the minor radius – a – which was previously defined through:

$$a = \epsilon \cdot R_0 \quad (2.1)$$

The next step is transforming the *line-averaged* density (\hat{n}) into the *volume-averaged* version (\bar{n}) used in this model. Harnessing the simplicity of the density's parabolic profile allows this relation to be written in a closed form as:

$$\hat{n} = \frac{\sqrt{\pi}}{2} \cdot \left(\frac{\Gamma(\nu_n + 2)}{\Gamma(\nu_n + \frac{3}{2})} \right) \cdot \bar{n} \quad (2.10)$$

Where $\Gamma(\dots)$ represents the gamma function: the non-integer analogue of the factorial function.

Combining these pieces allows the volume-averaged density to be written in standard-

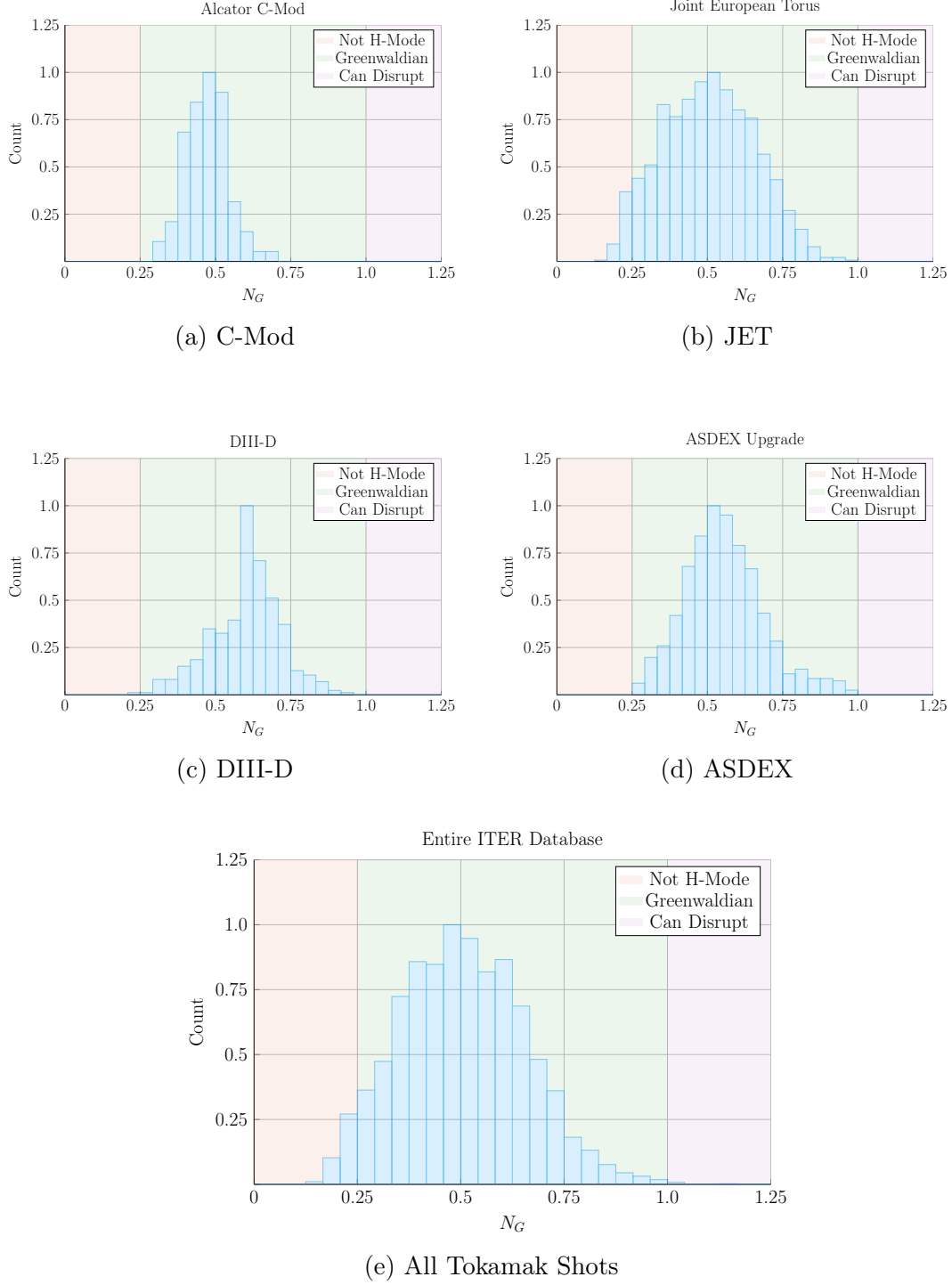


Figure 2-4: Greenwald Density Limit

The Greenwald Density Limit is a robust metric of what densities an H-Mode plasma can attain. Although empirical in nature, it accurately predicts when a tokamak will undergo degraded plasma transport.²~~it is an indicator for good transport regimes.~~

879 ized units (~~i.e. the ones we use~~) as:

$$\bar{n} = K_n \cdot \left(\frac{I_P}{R_0^2} \right) \quad (2.11)$$

880

$$K_n = \frac{2N_G}{\epsilon^2 \pi^{3/2}} \cdot \left(\frac{\Gamma(\nu_n + \frac{3}{2})}{\Gamma(\nu_n + 2)} \right) \quad (2.12)$$

881 The format of the previous equation pair will be used throughout the remainder of
 882 the paper. The top equation relates ~~dynamicfloating~~ variables (i.e. \bar{n} , I_P , and R_0),
 883 while the ~~staticfixed~~-value coefficient (K_n) lumps together ~~staticfixed~~ quantities, such
 884 as: N_G , ϵ , 2, π , and ν_n .

885 2.2.2 Declaring the Bootstrap Current

886 The first term to define in current balance, Eq. (2.8), is the bootstrap current. This
 887 bootstrap current is a mechanism of tokamak plasmas that helps supply some of
 888 the current needed to keep a plasma in ~~equilibriumstable~~. Its underlying behavior
 889 stems from particles stuck in banana-shaped orbits on the outer edges of the device
 890 propelling the majority species along their helical trajectories around the tokamak.
 891 ~~From a hand-waving perspective, it involves particles stuck in banana-shaped orbits~~
 892 ~~on the outer edges of a tokamak behaving like racing-game style speed boosts that~~
 893 ~~accelerate charged particles along their hooped-shaped race tracks.~~

894 Utilizing the surface integral from Eq. (E.25), the bootstrap current (I_{BS}) can be
 895 written in terms of the temperature and density profiles: ~~To get an equation for~~
 896 ~~bootstrap current, we must first introduce the surface integral—made possible from~~
 897 ~~our previous choice of geometric parameters:—~~

898 ~~Here, Q is an arbitrary function of the normalized radius (ρ) and g is a geometric~~
 899 ~~factor (of order 1):~~

900 This allows the bootstrap current (I_{BS}) to be written in terms of the temperature
 901 and density profiles:

$$I_{BS} = 2\pi a^2 \kappa g \int_0^1 J_{BS} \rho d\rho \quad (2.13)$$

902

$$\begin{aligned} J_{BS} &= f\left(n, T, \frac{dn}{d\rho}, \frac{dT}{d\rho}\right) \\ &\equiv 4.88 \cdot \left(\frac{r}{R_0}\right) \cdot \left(\frac{nT}{B_\theta}\right) \cdot \left(\frac{1}{n} \frac{dn}{dr} + 0.055 \frac{1}{T} \frac{dT}{dr}\right) \end{aligned} \quad (2.14)$$

903 The second definition for the bootstrap current density – J_{BS} – comes from using
 904 well known theoretical results plus several simplifying assumptions, including the
 905 large aspect limit.

906 For a more formal look into this J_{BS} function, check the appendix section on pedestal
 907 temperatures. The point to make now is that it depends on the the profiles' derivatives,
 908 leading to one major discrepancy in the model.

909 As shown later in the results, bootstrap fractions are often under-predicted by this
 910 model. This is due to parabolic profiles (i.e. for temperature) having much less steep
 911 declines near the edge (i.e. in their derivatives) than characteristic H-Mode profiles
 912 with pedestals. This implies that the area most positively impacted by a pedestal
 913 profile for temperature would be the bootstrap current derivation. The instructions
 914 to do so are given in Appendix D.4.

915 Getting back on track—and without completeness—the bootstrap current can now
 916 be written in proportionality form as:

917 Recognizing that the last term is basically the inverse of the Greenwald density (see
 918 Eq. 2.11), allows the proportionality to be written in the following form. Note that
 919 this implies the bootstrap current is only a function of temperature!

920 In standardized units, this proportionality can be written as a concrete relation of
 921 the form:

922 Finally, summarizing the results of Appendix F, the bootstrap current is found to be

only a function of temperature! In standardized units, it can be written as:

$$I_{BS} = K_{BS} \cdot \bar{T} \quad (2.15)$$

$$K_{BS} = 4.879 \cdot K_n \cdot \left(\frac{1 + \kappa^2}{2} \right) \cdot \epsilon^{5/2} \cdot H_{BS} \quad (2.16)$$

$$H_{BS} = (1 + \nu_n)(1 + \nu_T)(\nu_n + 0.054\nu_T) \int_0^1 \frac{\rho^{5/2} (1 - \rho^2)^{\nu_n + \nu_T - 1}}{b_p} d\rho \quad (2.17)$$

Quickly noting, this H_{BS} term serves as the analogue of ~~static~~**fixed**-value coefficients (e.g. K_{BS} and K_n) when they contain an integral. And b_p represents the poloidal magnet strength given by Eq. 2.7.

2.2.3 Deriving the Fusion Power

~~The next segue on our journey to solving for the steady current is deriving the fusion power (P_F), which appears in current drive. This requires a more first-principles approach than those used up until now. As such, a quick background is given to motivate the parameters it adds—i.e. the dilution factor (f_D) and the Bosch-Hale fusion reactivity (σv).~~

~~The natural place to start when talking about fusion is the binding-energy per nucleon plot (see Fig. N). As can be seen, the function reaches a maximum value around the element Iron ($A=56$). What this means at a basic level is: elements lighter than iron can *fuse* into a heavier one (i.e. hydrogens into helium), whereas heavier elements can *fission* into lighter ones (e.g. uranium into krypton and barium). This is what differentiates fission (uranium-fueled) reactors from fusion (hydrogen-fueled) ones. For fusion reactors, the most common reaction in a first-generation tokamak will be: What this reaction describes is two isotopes of hydrogen—i.e. deuterium and tritium—fusing into a heavier element, helium, while simultaneously ejecting a neutron. The entire energy of the fusion reaction (E_F) is then divvied up 80-20 between the neutron~~

945 and helium, respectively. Quantitatively, the helium (hereafter referred to as an alpha
946 particle) receives 3.5 MeV.

947 The final point to make before returning to the fusion power derivation is the main
948 difference between the two fusion products: helium (i.e. the alpha particle) and the
949 neutron. First, neutrons lack a charge — they are neutral. This means they cannot
950 be confined with magnetic fields. As such, they simply move in straight lines until
951 they collide with other particles. As the structure of a tokamak is mainly metal, the
952 neutron is much more likely to collide there than the gaseous plasma, which is orders
953 of magnitude less dense. Conversely, alpha particles are charged — when stripped of
954 their electrons — and can therefore be kept within the plasma using magnets. What
955 this means practically is that of the 17.6 MeV that comes from every fusion reaction,
956 only 3.5 MeV remains inside the plasma (within the helium particle species).

957 The next segue on our journey to solving for the steady current is deriving the fusion
958 power (P_F), which appears in current drive. A comprehensive introduction to this is
959 given in Appendix C. Summarized, though, a formula for
960 hand, the fusion power from a D-T reaction – in megawatts – is given by the following
961 volume integral:[?] –Jeff Freidberg’s textbook through the following volume integral:–

$$P_F = \int E_F n_D n_T \langle \sigma v \rangle d\mathbf{r} \quad (2.18)$$

962

$$E_F = 17.6 \text{ MeV} \quad (2.19)$$

963 The E_F quantity is the energy created from a deuterium-tritium fusion reaction. The
964 n_D and n_T in this equation then represent the density of the deuterium and tritium
965 ions, respectively. Assuming a 50-50 mix of the two, they can be related to the
966 electron density – i.e. the one used in this model – through the dilution factor (f_D).
967 This dilution factor represents the decrease in available fuel from part of the plasma
968 actually being composed of non-hydrogen gasses:

$$n_D = n_T = f_D \cdot \left(\frac{n}{2}\right) \quad (2.20)$$

969

970 The fusion reactivity, $\langle\sigma v\rangle$, is then a nonlinear function of the temperature, T , which
 971 the model approximates using the Bosch-Hale tabulation (described in the appendix).
 972 As this tabulated value appears inside an integral, it seems important to point out
 973 that the temperature is now the most difficult ~~dynamic~~~~floating~~ variable to handle –
 974 over R_0 , B_0 , \bar{n} , and I_P . This will come into play when the model is formalized next
 975 chapter.

976 The next step in the derivation of fusion power is transforming the three-dimensional
 977 volume integral (see Eq. 2.18) into a zero-dimension averaged value. First, the volume
 978 analogue of the previously given surface-area integral is:

$$Q_V = 4\pi^2 R_0 a^2 \kappa g \int_0^1 Q(\rho) \rho d\rho \quad (2.21)$$

979 Where again, Q is an arbitrary function of ρ and g is a geometric factor approximately
 980 equal to one. The fusion power can now be rewritten as:

$$P_F = \pi^2 E_F f_D^2 R_0 a^2 \kappa g \int_0^1 n^2 \langle\sigma v\rangle \rho d\rho \quad (2.22)$$

981 In standardized units, this becomes:

$$P_F = K_F \cdot \bar{n}^2 \cdot R_0^3 \cdot (\sigma v) \quad (2.23)$$

982

$$K_F = 278.3 \cdot f_D^2 \cdot (\epsilon^2 \kappa g) \quad (2.24)$$

983 Where the standardized fusion reactivity is now,

$$(\sigma v) = 10^{21} (1 + \nu_n)^2 \int_0^1 (1 - \rho^2)^{2\nu_n} \langle\sigma v\rangle \rho d\rho \quad (2.25)$$

984 ~~As mentioned before, this fusion power is divvied up 80-20 between the neutron and~~

985 ~~alpha particle. These relations will be used shortly. For now, they can be described~~
986 ~~mathematically as:~~

987 At this point, the current drive needed for steady-state can now be defined.

988 2.2.4 Using Current Drive

989 As may have been lost along the way, ~~this chapter's the current~~ mission is to define
990 a formula for steady current – from the current balance equation for steady-state
991 tokamaks:

$$I_P = I_{BS} + I_{CD} \quad (2.8)$$

992 In standardized units, the equation for current drive is often given in the literature
993 as:²¹

$$I_{CD} = \eta_{CD} \cdot \left(\frac{P_H}{\bar{n}R_0} \right) \quad (2.26)$$

994 Here, η_{CD} is the current drive efficiency with units $\left(\frac{\text{MA}}{\text{MW-m}^2} \right)$ and P_H is the heating
995 power in megawatts driven by LHCD (and absorbed by the plasma).

996 Let it be known, though, that driving current in a plasma is hard! In fact, pulsed
997 reactor designers (i.e. European fusion researchers) think it is so difficult, they may
998 choose to forego it completely – focusing only on inductive sources that necessitate
999 reactor fatigue and downtime.

1000 A common current drive efficiency (η_{CD}) seen in many designs is 0.3 ± 0.1 in the
1001 standard units. It is however inherently a function of all the plasma parameters –
1002 with subtlety put off until the discussion of self-consistency. For now it assumed to
1003 have some constant/~~static~~~~fixed~~ value.

1004 The remaining step in deriving an equation for driven current (I_{CD}) is a formula for
1005 the heating power (P_H). The way fusion systems models – like this one – handle the
1006 heating power is through the physics gain factor, Q. Sometimes referred to as big Q,
1007 this value represents how many times over the heating power (P_H) is amplified as it

1008 is transformed into fusion power (P_F):

$$P_H = \frac{P_F}{Q} \quad (2.27)$$

1009 Now, utilizing the previously defined Greenwald density and fusion power:

$$\bar{n} = K_n \cdot \left(\frac{I_P}{R_0^2} \right) \quad (2.11)$$

1010

$$P_F = K_F \cdot \bar{n}^2 \cdot R_0^3 \cdot (\sigma v) \quad (2.23)$$

1011 The current from LHCD can be written as:

$$I_{CD} = K_{CD} \cdot I_P \cdot (\sigma v) \quad (2.28)$$

1012

$$K_{CD} = (K_F K_n) \cdot \frac{\eta_{CD}}{Q} \quad (2.29)$$

1013 As η_{CD} and Q appear within a ~~staticfixed~~ coefficient, it is implied that both re-
1014 main constant throughout a solve. This subtlety is lifted when handling η_{CD} self-
1015 consistently, which will be discussed shortly. However, even in that context, it proves
1016 beneficial to still think of η_{CD} as a sequence of ~~staticfixed~~ variables – set by the model
1017 rather than the user.

1018 2.2.5 Completing the Steady Current

1019 ~~TheAs hinted along the way, the~~ goal of this ~~chaptersection~~ has been to derive a
1020 simple formula for steady current (I_P). The problem started with current balance in
1021 a steady-state reactor:

$$I_P = I_{BS} + I_{CD} \quad (2.8)$$

1022 Two equations were then found for the bootstrap (I_{BS}) and driven (I_{CD}) current:

$$I_{BS} = K_{BS} \cdot \bar{T} \quad (2.15)$$

1023

$$I_{CD} = K_{CD} \cdot I_P \cdot (\sigma v) \quad (2.28)$$

1024 Combining these three equations and solving for the total plasma current (I_P) – in
1025 mega-amps – yields:

$$I_P = \frac{K_{BS} \bar{T}}{1 - K_{CD}(\sigma v)} \quad (2.30)$$

1026

1027 This is the answer we have been seeking!

1028 As mentioned before, this simple formula appears to only depend on temperature!*

1029 Apparently, the plasma should have the same current at some temperature (i.e. $\bar{T} =$
1030 15 keV), regardless of the size of the machine or the strength of its magnets. This
1031 has the important corollary that each temperature maps to only one current value.
1032 Further, each temperature would then map to a single magnet strength, capital cost,
1033 etc. (as shown next chapter).

1034 As has become a mantra, though, the subtlety of this behavior lies in the self-
1035 consistency of the current-drive efficiency – η_{CD} .

1036 2.3 Handling Current Drive Self-Consistently

1037 Although a thorough description of the wave theory behind lower-hybrid current
1038 drive (LHCD) is well outside the scope of this text, it does motivate the solving of
1039 a tokamak's major radius (R_0) and field strength (B_0). It also shows how what was
1040 once a simple problem has now transformed into a rather complex one – a common
1041 occurrence with plasmas.

*This dependence only on temperature refers to dynamic variables. The plasma current can still be highly volatile to many of the static variables, such as: ϵ , κ , N_G , f_D , ν_n , l_i , etc.

1042 The logic behind finding a self-consistent current-drive efficiency is starting at some
 1043 plausible value (i.e. $\eta_{CD} = 0.3$), solving for the steady current – i.e. $I_P = f(\bar{T})$ – and
 1044 then somehow iteratively creeping towards a value deemed self-consistent. What this
 1045 means is that in addition to the solver described in the last section, there needs to be
 1046 a black-box function that solutions are piped through to get better guesses at η_{CD} .
 1047 The black-box function we use is a variation of the Ehst-Karney model.²²

1048 As mentioned, a self-consistent η_{CD} is found once a trip through the Ehst-Karney
 1049 black-box results in the same η_{CD} as was piped in – to some tolerable level of error.
 1050 This consistency incorporates an explicit dependence on the tokamak configuration.
 1051 Mathematically,

$$\tilde{\eta}_{CD} = f(R_0, B_0, \bar{n}, \bar{T}, I_P) \quad (2.31)$$

1052

1053 As such, to recalculate it after every solution of the steady current requires a value
 1054 for both B_0 and R_0 – the targets of this model’s primary and ~~limiting~~~~secondary~~
 1055 constraints. These will be the highlight of the next chapter.

1056 Chapter 3

1057 Formalizing the Systems Model

1058 The goal of this chapter is to take a step back from the steady current derivation and
1059 see the larger picture behind reactor design. As such, a more in-depth description of
1060 ~~staticfixed~~ and ~~dynamicfloating~~ variables is given. This discussion of ~~dynamicfloating~~
1061 variables will then lend itself to a description of the framework underpinning the
1062 fusion systems model. As such, we will now need formulas for the radius and magnet
1063 strength of the tokamak. Moving forward, the current will ~~then~~ remain a connecting
1064 piece as we ~~redirect focusswitch-gears~~ to pulsed tokamaks and compare ~~the underlying~~
1065 ~~solvers of the two schemes.the two schemes' underlying solvers.~~

1066 The end result of this analysis will then be equations that allow the density (\bar{n}),
1067 current (I_P), major radius (R_0), and magnet strength (B_0) to be written as functions
1068 of the temperature (\bar{T}) and static variables (e.g. ν_n , N_G , f_D). These formulas are
1069 the product of applying constraints required for all tokamak reactors with several
1070 other limiting constraints. The constraints relevant to all tokamak reactors are: the
1071 Greenwald limit, current balance, and power balance. Limit constraints then include:
1072 the Troyon beta limit, the kink safety factor, the wall loading limit, the maximum
1073 power constraint, and the heat loading limit.

1074 Actual methodologies for solving for the five dynamic variables simultaneously – i.e.
1075 \bar{T} , \bar{n} , I_P , R_0 , B_0 – are put off until Chapter 5.

1076 3.1 Explaining StaticFixed Variables

1077 In this model, `staticfixed` variables are ones that remain constant while solving for a
1078 reactor. These include geometric scalings (i.e. ϵ , δ , κ), profile parameters (i.e. ν_n ,
1079 ν_T , l_i), and a `couple dozens` of physics constants related to pulsed and steady-
1080 state design (e.g. Q , N_G , f_D). For a complete list of `staticfixed` variables, consult
1081 `Appendix A`. The point to make now is that this model treats `staticfixed`
1082 variables as `immutable` objects. As such they often reside in `staticfixed`
1083 coefficients – K_{\square} – which are treated as constants.

1084 3.2 Connecting DynamicFloating Variables

1085 `DynamicFloating` variables – \bar{T} , \bar{n} , I_P , R_0 , B_0 – are the first-class variables of this
1086 fusion systems model. They represent the fundamental properties of a plasma and
1087 tokamak (which constitute a fusion reactor). As such, they will be reintroduced one
1088 at a time, explaining how they fit into the model – and which `equations` are capable
1089 of representing them.

Table 3.1: Dynamic Variables

Symbol	Name	Units
I_P	Plasma Current	MA
\bar{T}	Plasma Temperature	keV
\bar{n}	Electron Density	10^{20} m^{-3}
R_0	Major Radius	m
B_0	Magnetic Field	T

1090 Bluntly, this fusion systems model is a simple algebra problem: solve five equations
1091 with five unknowns (i.e. \bar{T} , \bar{n} , I_P , R_0 , B_0). Although this naive approach would work,
1092 we can do a little better by `collapsing` these five equations down to just one.
1093 This was already done while deriving the steady current. It just happened that the
1094 current was not directly dependent on the tokamak size (R_0) or magnet strength (B_0).
1095 This will prove more challenging for the generalized current needed for pulsed oper-

1096 ation. Even so, this equation will still be ~~reducedboiled-down~~ to one equation with a
 1097 single unknown – I_P . A solution to which can be solved much faster than the naive
 1098 5 equation approach. This is one reason the model is so fast.

1099 The Plasma Temperature – \bar{T}

1100 The plasma temperature, measured in keV (kilo-electron-volts), is one of the most
 1101 ~~nonlinearfinicky~~ variables in the fusion systems ~~frameworkmodel~~. It first proved trou-
 1102 blesome when it was shown that a pedestal profile – not a parabolic one used here
 1103 – would be needed for an accurate calculation of bootstrap current. The ~~black-~~
 1104 ~~boxunusual~~ tabulation for reactivity – (σv) – which appeared in fusion power only
 1105 further exposed this nonlinearity.

1106 Acknowledging that temperature is the most difficult to handle parameter prompts its
 1107 use as the scanned variable. What this means practically is scanning temperatures ~~is~~
 1108 ~~the most straightforward method to produceproduces~~ curves of reactors. By example,
 1109 a scan may be run over the average temperatures (\bar{T}): 10, 15, 20, 25, and 30 keV –
 1110 ~~where each correspondseorresponding~~ to its own reactor ~~with its own field strength~~
 1111 (B_0), plasma current (I_P), etc. In equation form, this becomes:

$$\bar{T} = \text{const.} \quad (3.1)$$

1112 The constant value, here,~~Where the constant~~ happens to be 10 keV in one run, 15
 1113 keV for the next, and 30 keV in the fifth.

1114 The Plasma Density – \bar{n}

1115 The Greenwald density limit is a constraint with a simple form that applies to all
 1116 tokamak reactors.~~The cornerstone of this fusion systems model has always been the~~
 1117 ~~application of the Greenwald density limit from square one.~~ It is for this reason – as
 1118 well as being a good approximation – that a parabolic profile was rationalized over a

1119 pedestal (H-Mode) one. Repeated, the Greenwald density limit is:

$$\bar{n} = K_n \cdot \frac{I_P}{R_0^2} \quad (2.11)$$

1120 This is an exceptionally simple relationship and why it guided the model. Unlike the
1121 next three variables, it is actually used in their derivations. ~~Therefore, any reactor~~
1122 ~~found through this model is considered a *Greenwaldian Reactor*—one held at the~~
1123 ~~Greenwald density limit.~~

1124 The Plasma Current – I_P

1125 The plasma current is what separates steady-state from pulsed operation. From
1126 before, the steady current was found to be:

$$I_P = \frac{K_{BS}\bar{T}}{1 - K_{CD}(\sigma v)} \quad (2.30)$$

1127 This was derived by setting the total current equal to the two sources of current:
1128 bootstrap and current drive. Or in fractional form,

$$I_P = I_{BS} + I_{CD} \rightarrow 1 = f_{BS} + f_{CD} \quad (3.2)$$

1129 This says that the current fractions of bootstrap and current drive must sum to one.
1130 As shown next chapter, inductive sources can be included into this current balance:

$$1 = f_{BS} + f_{CD} + f_{ID} \quad (3.3)$$

1131

1132 This equation shows how steady-state and pulsed operation can coexist (see Fig. 3-1).
1133 The final point to make is reducing the model to being purely pulsed – i.e. neglecting
1134 the current drive:

$$1 = f_{BS} + f_{ID} \quad (3.4)$$

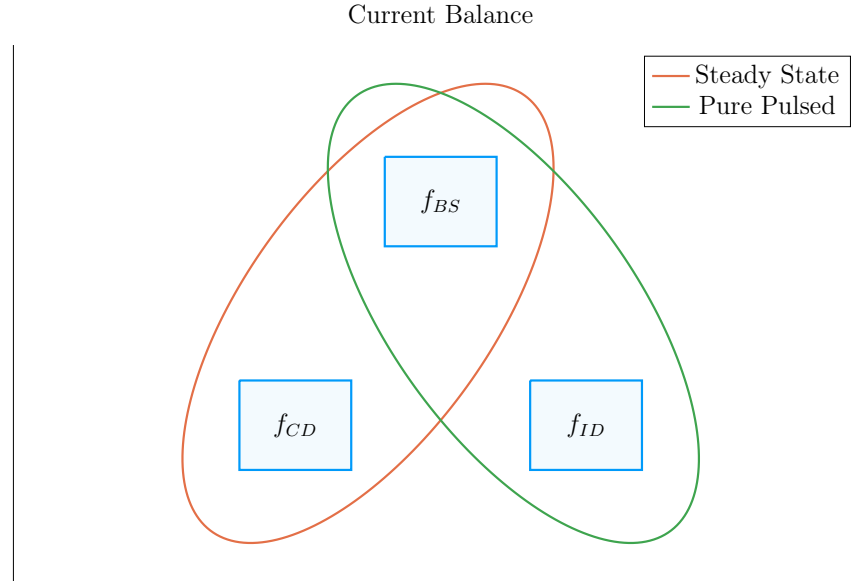


Figure 3-1: Current Balance in a Tokamak

In a tokamak, there needs to be a certain amount of current – and that current has to come from somewhere. All good reactors have an adequate bootstrap current. What provides the remaining current is what distinguishes steady state from pulsed operation.

Therefore, the next chapter will generalize the steady current to allow pulsed operation, and then simplify it to the purely pulsed case. Just as steady current faced self-consistency issues with η_{CD} , this current will also involve its own root solving conundrum – the description of which will be given in the following two chapters.

The Tokamak Magnet Strength – B_0

The tokamak magnet strength has no ~~uniqueobvious~~ equation to eliminate it. With foresight, the one this model ~~useschooses-to-use~~ is the power balance inherent to everyin-a reactor. Similar to current balance, power balance is what separates a reactor from a ~~device incapable of producing net electricitytoaster~~. As such, it is referred throughout this document as: the primary constraint. It will be derived later this chapter.

1146 The Tokamak Major Radius – R_0

1147 Much like the magnet strength, the major radius has no ~~unique~~~~obvious~~ relation to
1148 express it. ~~The model therefore uses this equation to handle a reactor's various~~~~This is~~
1149 ~~convenient, because the model still has yet to resolve one of its most pressing issues:~~
1150 physical and engineering-based constraints. This ~~laundry~~ list of requirements further
1151 restricts reactor space to the curves shown in the results section. Collectively, these
1152 are referred to as the ~~limiting~~~~secondary~~ constraints – discussed later this chapter.
1153 ~~These~~~~By miraele, these~~ constraints all just happen to depend on the size of the reactor
1154 – the reason they are chosen to ~~represent~~~~substitute out~~ the radius.

1155 3.3 Enforcing Power Balance

1156 What separates a reactor from a ~~device incapable of producing net electricity~~~~toaster~~
1157 is power balance. ~~Within a tokamak, it~~~~It~~ accounts for how the power going into
1158 a plasma's core exactly matches the power coming out of it. To approximate this
1159 conservation equation, two sets of power will be introduced: the sources and the
1160 sinks.

1161 The sources have mainly been introduced at this point – they include the alpha
1162 power (P_α) ~~from fusion reactions~~ and the heating power (P_H), as well as a new ohmic
1163 power term (P_Ω). The remaining two powers – the sinks – then appear through the
1164 radiation and heat conduction losses, which will be given shortly. In equation form,
1165 power balance becomes:

$$\sum_{sources} P = \sum_{sinks} P \quad (3.5)$$

1166 or expanded to fit this model:

$$P_\alpha + P_H + P_\Omega = P_{BR} + P_\kappa \quad (3.6)$$

1167 For clarity, the left-hand side of this equality are the sources. Whereas the remaining

1168 two are sinks, i.e. Bremsstrahlung radiation (P_{BR}) and heat conduction losses (P_{κ}).

1169 3.3.1 Collecting Power Sources

1170 As suggested, the two dominant sources of power in a tokamak are: alpha power
1171 (P_{α}) and auxiliary heating (P_H). From Appendix C, it was determined that alpha
1172 particles (i.e. helium nuclei) carry around 20% of the total fusion power; or as we put
1173 it mathematically:

$$P_{\alpha} = \frac{P_F}{5} \quad (3.7)$$

1174 Additionally, it was determined that the heating power is what was eventually am-
1175 plified into fusion power – or through equation:

$$P_H = \frac{P_F}{Q} \quad (3.8)$$

1176 The final source term then is the ohmic power (P_{Ω}). This is identical to how copper
1177 wires in a home heat up as current runs through them. From a simple circuits
1178 picture, the power across the plasma is related to its current and resistance – in our
1179 standardized units – through:

$$P_{\Omega} = 10^6 \cdot I_P^2 \cdot R_P \quad (3.9)$$

1180 ~~Here, the resistance of the plasma is unlike any material humans encounter on a~~
1181 ~~daily basis—actually decreasing with temperature. This~~The fusion systems model
1182 handles the plasma resistance (R_P) with the neoclassical Spitzer resistivity. Through
1183 equation,³

$$R_P = \frac{K_{RP}}{R_0 \bar{T}^{3/2}} \quad (3.10)$$

1184

$$K_{RP} = 5.6e-8 \cdot \left(\frac{Z_{eff}}{\epsilon^2 \kappa} \right) \cdot \left(\frac{1}{1 - 1.31\sqrt{\epsilon} + 0.46\epsilon} \right) \quad (3.11)$$

1185 Combined with the Greenwald limit, ohmic power can be written more compactly as,

$$P_{\Omega} = K_{\Omega} \cdot \left(\frac{\bar{n}^2 R_0^3}{T^{3/2}} \right) \quad (3.12)$$

1186

$$K_{\Omega} = 10^6 \cdot \frac{K_{RP}}{K_n^2} \quad (3.13)$$

1187 With the sources defined, we are now in a position to discuss the two sink terms used
1188 in this model's power balance.

1189 3.3.2 Approximating Radiation Losses

1190 All nuclear reactors emit radiation. From a power balance perspective, this means
1191 some power has to always be reserved to recoup from its losses – measured in megawatts.
1192 In a fusion reactor, the three most important types of radiation are: Bremsstrahlung
1193 radiation, line radiation, and synchrotron radiation.

1194 ~~This Without going into too much detail, this~~ model chooses to only model Bremsstrahlung
1195 radiation – as it usually dominates within the plasma's core. ~~Within most designs,~~
1196 ~~Bremsstrahlung radiation outweighs the other two's contribution, to core power bal-~~
1197 ~~ance, two-to-one.~~^{4,5} However, adding the effects of line-radiation and synchrotron
1198 radiation would drive results closer to real-world experiments. For example, line-
1199 radiation would better account for the ~~effects of~~ heavy impurities that ~~are emitted~~
1200 ~~from the divertor plate and first wall appear as pieces of a tokamak fall into the plasma.~~
1201 For clarity, Bremsstrahlung – or breaking – radiation is what occurs when a charged
1202 particle (e.g. an electron) is accelerated by some means. In a tokamak, this happens
1203 all the time as ~~electrons collide with the ion species.~~⁶ ~~charged particles are flung around~~
1204 ~~and around the machine.~~ This term can be ~~As given in Jeff Freidberg's book, this term~~
1205 ~~is~~ described by the volume integral:³

$$P_{BR} = \int S_{BR} d\mathbf{r} \quad (3.14)$$

1206 ~~Where~~Here, the radiation power density (S_{BR}) is given by:

$$S_{BR} = \left(\frac{\sqrt{2}}{3\sqrt{\pi^5}} \cdot \frac{e^6}{\epsilon_0^2 c^3 h m_e^{3/2}} \right) \cdot (Z_{eff} n^2 T^{1/2}) \quad (3.15)$$

1207 The constants in the left set of parentheses all have their usual physics meanings (i.e.
1208 c is the speed of light and m_e is the mass of an electron). What is new is the effective
1209 charge: Z_{eff} .

1210 The effective charge is a scheme for ~~reducing~~collapsing the charge ~~each ion~~that ~~each~~
1211 ~~partiele~~ has to a ~~single representative~~effective value. Fundamental charge, here, is
1212 what: neutrons lack, electrons and hydrogen have one of, and helium has two. As
1213 such, a plasma with a purely deuterium and tritium fuel would have an effective
1214 charge of one. This value would then quickly rise if a Tungsten tile – with 74 units
1215 of charge – were to fall into the plasma core from the walls of the tokamak.

1216 Using the volume integral – seen in the derivation of fusion power – allows the
1217 Bremsstrahlung power to be written in standardized units as:

$$P_{BR} = K_{BR} \bar{n}^2 \bar{T}^{1/2} R_0^3 \quad (3.16)$$

1218

$$K_{BR} = 0.1056 \frac{(1 + \nu_n)^2 (1 + \nu_T)^{1/2}}{1 + 2\nu_n + 0.5\nu_T} Z_{eff} \epsilon^2 \kappa g \quad (3.17)$$

1219 This power term represents the radiation power losses involved in power balance. All
1220 that is needed now is a formula for heat conduction losses – ~~one of the most difficult~~
1221 ~~plasma behavior~~the ~~hardest plasma behavior~~ to model to date.

1222 3.3.3 Estimating Heat Conduction Losses

1223 Heat is energy that ~~moves about randomly~~lacks ~~direction~~ on a microscopic level.
1224 Macroscopically, it generally moves from hotter areas to colder ones. As hinted by
1225 the plasma profile for temperature, heat emanates from the center of a plasma and
1226 migrates towards the walls of its tokamak enclosure. It therefore ~~is a critical~~seems ~~an~~

1227 ~~important~~ quantity to calculate when balancing power in a plasma's core.

1228 The difficulty of estimating heat conduction, though, lies in the ~~nonlinear behavior~~~~chaotic~~
1229 ~~nature~~ of plasmas – no theory or ~~quick-running code~~~~computation~~~~today~~ can properly
1230 model it. As such, reactor designers have turned towards experimentalists for empir-
1231 ical scaling laws based on the dozen or so strongest tokamaks in the world. These are
1232 collectively referred to as confinement time scalings, i.e. the ELMy H-Mode Scaling
1233 Law.

1234 The derivation of this heat conduction loss term (P_κ) starts in a manner similar to
1235 the previous powers. To begin, an equation for P_κ ~~can be found using the following~~
1236 ~~volume integral:~~³~~is given in Jeff Freidberg's book as:~~

$$P_\kappa = \frac{1}{\tau_E} \int U d\mathbf{r} \quad (3.18)$$

1237 This volume integral includes two new terms: the confinement time (τ_E) and the
1238 internal energy (U). Before explaining these terms, a qualitative description is in
1239 order. As mentioned previously, the heat – or microscopically random – energy is
1240 captured by the internal energy (U). Then the confinement time (τ_E) is how long
1241 it would take for the heat to ~~undergo an e-folding~~~~completely leave the device~~ if the
1242 ~~device~~~~system~~ were suddenly turned off.

1243 A formula for confinement time will be delayed till the end of this section, when it is
1244 needed to solve for the magnetic field (B_0). The internal energy (U), however, can be
1245 given now as it has its typical physics meaning. This assumes that all three plasma
1246 species are held nearly at the same temperature (T) as the electrons:

$$U = \frac{3}{2} (n + n_D + n_T) T \quad (3.19)$$

1247 Here again, n_D and n_T – the density of deuterium and tritium, respectively – are
1248 related to the electron density (used in this model) through the dilution factor, which

1249 assumes a 50-50 mix of D-T fuel:

$$n_D = n_T = f_D \cdot \left(\frac{n}{2} \right) \quad (3.20)$$

1250 ~~After several substitutions,Foregoing the mathematical rigor of previous sections,~~ the
1251 equations here can be combined to form an equation for P_κ – the heat conduction
1252 losses – in standardized units:

$$P_\kappa = K_\kappa \frac{R_0^3 \bar{n} \bar{T}}{\tau_E} \quad (3.21)$$

1253

$$K_\kappa = 0.4744 (1 + f_D) \frac{(1 + \nu_n)(1 + \nu_T)}{1 + \nu_n + \nu_T} (\epsilon^2 \kappa g) \quad (3.22)$$

1254 Now that all five terms have been defined in power balance, the next step is expanding
1255 it and solving for the tokamak’s toroidal magnetic field strength: B_0 .

1256 3.3.4 Writing the Lawson ~~ParameterCriterion~~

1257 Before ~~arriving at a formula forlocking in the primary constraint—i.e.~~ the magnet
1258 strength (B_0) ~~usingequation from~~ power ~~balance,balance~~ – it seems appropriate to
1259 take a detour and explain an intermediate solution: the Lawson ~~ParameterCriterion~~.
1260 Within the fusion community, the Lawson ~~ParameterCriterion~~ is the cornerstone in
1261 any argument on the possibility of a ~~tokamak everdesign~~ being used as a ~~reactor.react~~
1262 ~~(and not just some grandiose toaster).~~

1263 An equation for the Lawson ~~ParameterCriterion~~ – sometimes referred to as the *triple*
1264 *product* – is easily found in the literature as:

$$n \cdot T \cdot \tau_E = \frac{60}{E_F} \cdot \frac{T^2}{\langle \sigma v \rangle} \quad (3.23)$$

1265 Similar to the steady current derived earlier, the right-hand side is only dependent
1266 on temperature. Further, as the left-hand side is a measure of difficult to achieve

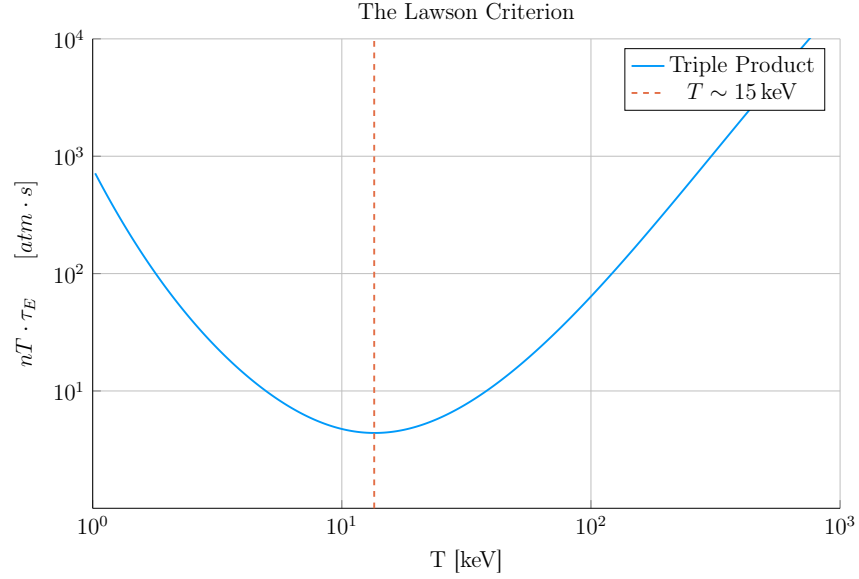


Figure 3-2: Power Balance in a Reactor

Power balance is what differentiates a reactor from a radiator. When cast as the Lawson ~~Parameter Criterion~~ for fusion, it explains why D-T plasmas often have a temperature around 15 keV.

parameters, the goal is to minimize both sides. As shown in Fig. 3-2, this occurs when the plasma temperature is around 15 keV – a fact well known to many fusion engineers. As will be seen, this is a simplified result of our model. This is why $\bar{T} = 15$ keV is not always the optimum temperature – but usually is in the right neighborhood for reasonable reactor designs.

As all the terms in power balance have already been defined, the starting point will be simply repeating the standardized equations for all five included powers.

$$P_{\alpha} = \frac{P_F}{5} \quad (3.7)$$

$$P_H = \frac{P_F}{Q} \quad (3.8)$$

$$P_{\Omega} = K_{\Omega} \cdot \left(\frac{\bar{n}^2 R_0^3}{\bar{T}^{3/2}} \right) \quad (3.12)$$

$$P_{BR} = K_{BR} \bar{n}^2 \bar{T}^{1/2} R_0^3 \quad (3.16)$$

1277

$$P_\kappa = K_\kappa \frac{R_0^3 \bar{n} \bar{T}}{\tau_E} \quad (3.21)$$

1278 With the fusion power again being,

$$P_F = K_F \cdot \bar{n}^2 \cdot R_0^3 \cdot (\sigma v) \quad (2.23)$$

1279 These can then be substituted into power balance:

$$P_\alpha + P_H + P_\Omega = P_{BR} + P_\kappa \quad (3.6)$$

1280 After a couple lines of algebra, power balance can be rewritten in a form analogous
1281 to the triple product:

$$\bar{n} \cdot \bar{T} \cdot \tau_E = \frac{K_\kappa \bar{T}^2}{\left(K_P (\sigma v) + K_{OH} \bar{T}^{-3/2} \right) - K_{BR} \bar{T}^{1/2}} \quad (3.24)$$

1282

$$K_P = K_F \cdot \left(\frac{5 + Q}{5 \times Q} \right) \quad (3.25)$$

1283 As expected, this shares a form ~~As can be seen, this is remarkably~~ similar to the simple
1284 Lawson ~~Parameter~~ **Criterion**:

$$n \cdot T \cdot \tau_E = \frac{60}{E_F} \cdot \frac{T^2}{\langle \sigma v \rangle} \quad (3.23)$$

1285 The main difference is this model does not ignore ohmic power and radiation losses
1286 completely. The inclusion of radiation for example sometimes bars a range of temper-
1287 atures from being physically realizable.* With this intermediate relation in place, the
1288 goal is now to give a formula for the confinement time and solve it for the magnetic
1289 field strength (B_0) – thus giving the Primary Constraint.

*The denominator of Eq 3.24 has discontinuities when the $K_{BR} \bar{T}^{1/2}$ term exactly equals the parenthesised one. Therefore, valid reactors only exist outside the discontinuities, when the entire triple product is finite and positive.

3.3.5 Finalizing the Primary Constraint

The goal now is to transform the Lawson ~~Parameter Criterion~~ into an equation for magnet strength (B_0). This choice to solve the equation for B_0 was motivated by the goals of analysis and how it will fit ~~completely arbitrary, only motivated by the foresight of how it fits~~ into the fusion systems model. To solve the primary constraint, the confinement time scaling law will need to be introduced. At the end, a ~~convoluted messy~~ – albeit highly useful – relation will be the reward.

The energy confinement time – τ_E – is one of the most ~~difficult to obtain~~ ~~elusive~~ terms in all of fusion energy. It is an attempt to ~~reduce boil-down~~ all the ~~nonlinear behavior~~ ~~chaotic nature~~ of plasmas into a simple measure of how fast its internal energy would be ejected from the tokamak if the device was instantaneously shut down. As such, reactor designers have turned toward experimentalists for empirical scalings based on the world’s tokamaks. These all share a form similar to:

$$\tau_E = K_\tau H \frac{I_P^{\alpha_I} R_0^{\alpha_R} a^{\alpha_a} \kappa^{\alpha_\kappa} \bar{n}^{\alpha_n} B_0^{\alpha_B} A^{\alpha_A}}{P_{src}^{\alpha_P}} \quad (3.26)$$

This ~~regressional fit~~ ~~mouthful of a formula~~ is how the field actually designs machines (i.e. ITER). Let it be known, though, that ~~fits of this kind~~ ~~these fits~~ often do remarkable well, having relative errors less than 20% on interpolated data. The new terms in this equation are: P_{src} , K_τ , H , A , and the α_\square factors.

First, the loss power is a metric used in the engineering community to quantify the power being transported out of the “core” of the plasma by charged particles (i.e. not the neutrons).⁷ To optimize fits, experimentalists have defined this as a combination of the source power terms:

$$P_{src} = P_\alpha + P_H + P_\Omega \quad (3.27)$$

~~However, many have argued that the term should actually be replaced by its correct physics meaning – the conductive heat loss power. As this model uses the ELMy H-Mode scaling law, which is standard in the field, this alternative definition will not be used.~~ Moving on, K_τ is simply a constant fit-makers use in their scalings.

Whereas H is the ~~enhancement factor over the empirical fit. (H-Mode) scaling factor~~
~~—the analogue of K_τ used by reactor designers. This H factor can be used to~~
~~artificially boost the confinement of a machine (i.e. it adds a little bit of magic).~~
~~Next, Continuing,~~ A is the average mass number of the fuel source, in atomic mass
units. For a 50-50 D-T fuel, this is 2.5, as deuterium weighs two amus and tritium
weighs three. Lastly, the alpha factors (e.g. α_n , α_a , α_P) are fitting parameters that
represent each variable's relative importance in the scaling.

For ELMy H-Mode, this confinement scaling law can be written as:

$$\tau_E = 0.145 H \frac{I_P^{0.93} R_0^{1.39} a^{0.58} \kappa^{0.78} \bar{n}^{0.41} B_0^{0.15} A^{0.19}}{P_{src}^{0.69}} \quad (3.28)$$

~~However, similar scaling laws~~~~Where similar ones~~ can be ~~writtengiven~~ for L-Mode,
I-Mode, etc. One final remark to make before moving on is that even these fits
have subtleties. The value of κ , for example, may have a slightly different geometric
meaning from tokamak to tokamak. And the exact definition of loss power — P_{src} —
introduces an even larger area of discrepancy. ~~Although not actually used, a better~~
~~fit for our model might be one from the author:~~

Returning to the problem at hand, though, this model's Lawson ~~ParameterCriterion~~
(eq. 3.24) can be simplified after expanding the left-hand side using the Greenwald
density and substituting in a confinement time scaling law. ~~After a few lines of~~
~~algebra, this can be transformed~~~~Albeit a little cumbersome, this can be wrangled~~
into a ~~formulaan equation~~ for B_0 !

$$B_0 = \left(\frac{G_{PB}}{K_{PB}} \cdot \left(I_P^{\alpha_I^*} R_0^{\alpha_R^*} \right)^{-1} \right)^{\frac{1}{\alpha_B}} \quad (3.29)$$

1334

$$G_{PB} = \frac{\bar{T} \cdot \left(K_P(\sigma v) + K_\Omega \bar{T}^{-3/2} \right)^{\alpha_P}}{\left(K_P(\sigma v) + K_\Omega \bar{T}^{-3/2} - K_{BR} \bar{T}^{1/2} \right)} \quad (3.30)$$

1335

$$K_{PB} = H \cdot \left(\frac{K_\tau K_n^{\alpha_n^*}}{K_\kappa} \right) \cdot (\epsilon^{\alpha_a} \kappa^{\alpha_\kappa} A^{\alpha_A}) \quad (3.31)$$

1336 Where we have added new starred alpha values for the density, current, and major
1337 radius:

$$\alpha_n^* = 1 + \alpha_n - 2\alpha_P \quad (3.32)$$

1338

$$\alpha_I^* = \alpha_I + \alpha_n^* \quad (3.33)$$

1339

$$\alpha_R^* = \alpha_R + \alpha_a - 2\alpha_n^* - 3\alpha_p \quad (3.34)$$

1340 ~~Again, if the alternate definition for heat loss (\tilde{P}_{abs}) were used, another definition for~~
1341 ~~G_{PB} would arise. Quickly reemphasizing, though, these tilded values are not actually~~
1342 ~~used in the model:~~

1343 This equation for B_0 – derived from power balance – is thus the primary constraint
1344 for reactor designs. It is the first step in connecting the plasma (i.e. \bar{n} , \bar{T} , and I_P) to
1345 its tokamak enclosure (i.e. B_0 and R_0). The remaining step is finding an equation –
1346 or in this case, equations – for the major radius of the device. These radius equations
1347 will collectively be referred to as: the ~~limiting constraints.Secondary Constraints.~~

1348 ~~Before moving onto the Secondary Constraint, it is worth noting that this power~~
1349 ~~balance equation can be written in a triple product form analogous to the Lawson~~
1350 ~~ParameterCriterion. For this reason, we will refer to it as the Freidberg Triple~~
1351 ~~Product:~~

1352 ~~As is readily apparent, this has a shape similar to the Lawson ParameterCriterion.~~
1353 ~~Again, the goal is operate when the right hand side reaches an approximate minimum.~~
1354 ~~This corresponds to when the left hand side is also minimized—where each term~~
1355 ~~represents one of the difficult to achieve quantities of a tokamak fusion reactor.~~

1356 3.4 Collecting ~~LimitingSecondary~~ Constraints

1357 As of now, the only missing equation within our list of ~~staticfixed~~ variables – i.e.
1358 R_0 , B_0 , \bar{T} , \bar{n} , and I_P – is for the major radius of the tokamak. This equation will
1359 come from around five potential limits, each either physical or engineering-based.
1360 These limits will then correspond to different curves through reactor space. As will
1361 be shown, many of these reactors will be invalid (as they violate at least one of the
1362 other limits). ~~Our analysis is always based on selecting the most stringent criterion.~~

1363 Before tackling the subject of finding reactors that exist on the fine line of satisfying
1364 every ~~limitingsecondary~~ constraints, though, it is essential to collect them one-by-one.
1365 These are: the Troyon Beta Limit, the Kink Safety Factor, the Wall Loading Limit,
1366 the Power Cap Constraint, and the Heat Loading Limit.

1367 The goal of this section is to solve for each of these constraints on the major radius. As
1368 with the primary constraint, this choice of solving for R_0 was ~~not completely unique,~~
1369 ~~just motivated by physics and engineering concerns.completely arbitrary.~~ It just so
1370 happens that each limit described here depends on the size of a reactor – which is
1371 not true for the magnetic field strength.

1372 3.4.1 Introducing the Beta Limit

1373 The Beta Limit is the most important ~~limitingsecondary~~ constraint – especially for
1374 steady-state reactors. It sets a maximum on the amount of pressure a plasma is
1375 willing to tolerate. As with future ~~limitingsecondary~~ constraints, literature-based
1376 equations will be transformed into formulas for R_0 . Each will then contain some
1377 limiting quantity that can be handled by a ~~staticfixed~~ variable – as β_N will be used
1378 shortly.

1379 The starting point for the beta limit is to define the important plasma physics quan-
1380 tity: β – the plasma beta. This value is a ratio between a plasma’s internal pressure
1381 and the pressure exerted on it by the tokamak’s magnetic configuration. Mathemat-

1382 ically,³

$$\beta = \frac{\text{plasma pressure}}{\text{magnetic pressure}} = \frac{\bar{p}}{\left(\frac{B_0^2}{2\mu_0}\right)} \quad (3.35)$$

1383 Using this model's temperature and density profiles, the volume-averaged pressure
1384 (\bar{p}) can be written in units of atmospheres (i.e. atm) as:

$$\bar{p} = 0.1581 (1 + f_D) \frac{(1 + \nu_n)(1 + \nu_T)}{1 + \nu_n + \nu_T} \bar{n} \bar{T} \quad (3.36)$$

1385 Moving forward, the final step is plugging this definition for plasma beta into the
1386 ~~physics-based~~ Troyon Beta Limit derived using standard MHD stability analysis. ~~Limit.~~
1387 ~~Although outside the scope of this text, it is a stability limit set by treating plasmas~~
1388 ~~as charge-carrying fluids.~~ This equation can be written in the following form, where
1389 β_N is the normalized plasma beta – i.e. a ~~staticfixed~~ variable usually set between 2%
1390 and 4%.²³

$$\beta = \beta_N \frac{I_P}{aB_0} \quad (3.37)$$

1391 Substituting the plasma β from eq. 3.35, into this relation results in the model's first
1392 equation for tokamak radius:

$$R_0 = \frac{K_{TB} \bar{T}}{B_0} \quad (3.38)$$

1393

$$K_{TB} = 4.027 \times 10^{-2} \cdot \left(\frac{K_n \epsilon}{\beta_N} \right) \cdot (1 + f_D) \cdot \frac{(1 + \nu_n)(1 + \nu_T)}{1 + \nu_n + \nu_T} \quad (3.39)$$

1394 As mentioned, this is often the dominating constraint in a steady-state reactor. The
1395 often dominating constraint for pulsed designs – the kink safety factor – will be the
1396 focus of the next subsection.

1397 3.4.2 Giving the Kink Safety Factor

1398 Just like how the Troyon Beta Limit set a fluids-based maximum on plasma pressure,
1399 the Kink Safety Factor sets one on the plasma's current. This constraint usually
1400 only appears in pulsed designs, as it is assumed that getting to this high a current in

1401 steady-state (with only LHCD) would prove extremely impractical.

1402 The starting point, again, is an equation from the literature for the kink condition:^{7,24}

$$q_{*95} = 5\epsilon^2 \cdot \frac{R_0 B_0}{I_P} \cdot \left(\frac{1 + \kappa^2 \cdot (1 + 2\delta^2 - 1.2\delta^3)}{2} \right) \quad (3.40)$$

1403 Here the safety factor – q_{*95} – ~~is subscripted by 95, an identifier that this value is~~
1404 ~~taken at the 95% flux surface (i.e. near the statistically drawn edge of the plasma).~~
1405 ~~It~~ typically has values around 3. ~~Next, the f_q variable is a geometric scaling factor:⁷~~

1406 Combined, the kink safety factor can now be written in standardized units as:

$$R_0 = \frac{K_{SF} I_P}{B_0} \quad (3.41)$$

1407

$$K_{SF} = \frac{q_{*95}}{5\epsilon^2} \cdot \left(\frac{2}{1 + \kappa^2 \cdot (1 + 2\delta^2 - 1.2\delta^3)} \right) \quad (3.42)$$

1408 This relation is the ~~limitingsecondary~~ constraint important for most pulsed reactor
1409 designs. As with the Beta Limit, the two are derived through plasma physics alone.
1410 The remaining ~~limitingsecondary~~ constraints, however, are engineering-based in origin
1411 – these include: the Wall Loading Limit, the Power Cap Constraint, and the Heat
1412 Loading Limit. Each will be defined shortly.

1413 3.4.3 Working under the Wall Loading Limit

1414 The first engineering-based ~~limitingsecondary~~ constraint – the wall loading limit –
1415 will prove to be an important quantity when determining the magnet strength at
1416 which reactor costs ~~beginfirst-start~~ to increase. As hinted, its definition originates
1417 from nuclear engineering concerns: it is a measure of the maximum neutron damage
1418 a tokamak's walls can take over the lifetime of the machine.*

1419 The first step in deriving a ~~limitingsecondary~~ constraint for wall loading is a de-

*For clarity, the wall loading limit should actually be a energy fluence limit. It is converted to an instantaneous power limit for ease of design purposes.

1420 scription of the problem it models. In a reactor, fusion reactions typically make
 1421 high-energy neutrons – with around 14.1 MeV of kinetic energy – that ~~collide with~~
 1422 ~~the tokamak enclosure continually blast the inner wall of the tokamak.~~ Therefore a
 1423 ~~simple quick-and-dirty~~ metric would be limiting the amount of neutron power that
 1424 can be unloaded on the surface area of a tokamak. This can be written as:²⁵

$$P_W = \frac{P_n}{S_P} \quad (3.43)$$

$$S_P = 4\pi^2 a R_0 \cdot \frac{(1 + \frac{2}{\pi} (\kappa^2 - 1))}{\kappa} \quad (3.44)$$

1426 Here, S_P is the surface area of the tokamak's inner wall and P_n is the neutron power
 1427 derived in the subsection on fusion power. The quantity, P_W , then serves a role
 1428 analogous to β_N for the beta limit and q_{*95} for the kink safety factor – it is a ~~static fixed~~
 1429 variable representing the maximum allowed wall loading. For fusion reactors, P_W is
 1430 assumed to be around 2-4 $\frac{\text{MW}}{\text{m}^2}$. It will be shown that the wall loading limit is important
 1431 in any tokamak – regardless of operating mode (i.e. steady-state or pulsed).

1432 Finishing this ~~limiting secondary~~ constraint, the Wall Loading limit can be written in
 1433 standardized units as:

$$R_0 = K_{WL} \cdot I_P^{\frac{2}{3}} \cdot (\sigma v)^{\frac{1}{3}} \quad (3.45)$$

$$K_{WL} = \left(\frac{K_F K_n^2}{5\pi^2 P_W} \cdot \frac{\kappa}{\epsilon} \cdot \frac{1}{1 + \frac{2}{\pi} \cdot (\kappa^2 - 1)} \right)^{\frac{1}{3}} \quad (3.46)$$

1435 3.4.4 Setting a Maximum Power Cap

1436 As opposed to the previous three ~~limiting secondary~~ constraints, the maximum power
 1437 cap is more of a ~~constraint set by economic competitiveness. rule-of-thumb.~~ Because
 1438 no reactor – coal, solar, or otherwise – has a 4000 MW reactor, neither should fusion.*
 1439 It makes sense from a practical position after realizing the long history of tokamaks
 1440 being delayed, underfunded, or completely canceled. Mathematically, this has the

*Note that this 4000 MW (electric) is a maximum. A 1000 MW reactor would obviously not violate this constraint. Instead it would likely be pressing on either the kink or beta limit.

1441 simple form:

$$P_E \leq P_{CAP} \quad (3.47)$$

1442 Here, P_{CAP} is the maximum allowed power output of the reactor. Similar to the other
1443 limiting quantities, P_{CAP} is treated as a ~~staticfixed~~ variable (i.e. set to 4000 MW).
1444 The electrical power output of the reactor (P_E) is then related to the fusion power
1445 through:³

$$P_E = 1.273 \eta_T \cdot P_F \quad (3.48)$$

1446 ~~The constant in front (i.e. 1.273) represents some extra power the reactor makes~~
1447 ~~as more fuel is bred when the fusion neutrons pass through a tokamak (inside its~~
1448 ~~still-undiscussed blanket region).~~ The variable η_T is the thermal efficiency of the
1449 reactor – which is usually found to be around 40%. ~~And the constant in front (i.e.~~
1450 ~~1.273) represents some extra power the reactor makes as fuel is bred by the fusion~~
1451 ~~neutrons passing through a tokamak’s lithium-filled blanket. Explicitly this results~~
1452 ~~from including the energy released by lithium-6 as it undergoes neutron capture (E_{Li}).~~

1453

$$1.273 = \frac{E_F + E_{Li}}{E_F} \quad (3.49)$$

1454

$$E_{Li} = 4.8 \text{ MeV} \quad (3.50)$$

1455 Substituting in fusion power and solving for the major radius results in:

$$R_0 = K_{PC} \cdot I_P^2 \cdot (\sigma v) \quad (3.51)$$

1456

$$K_{PC} = K_F K_n^2 \cdot \left(\frac{1.273 \eta_T}{P_{max}} \right) \quad (3.52)$$

1457 This ~~limitingsecondary~~ constraint can be used to create curves of reactors, although
1458 it is mainly used as a stopping point for designs – i.e. if you get to the power-cap
1459 regime, you have gone too far. This is different than the next constraint, which is
1460 ~~fundamentally an unsolved problem within~~~~basically a glorified warning sign in~~ the
1461 ~~moderneontemporary~~ tokamak design paradigm.⁸

1462 3.4.5 Listing the Heat Loading Limit

1463 Fusion plasmas are hot. The commonly given relation is one electron volt
1464 is around 20,000 °F – which makes 15 keV around a quarter-billion Fahrenheit. Although
1465 slightly a tad deceptive, heat damage to melting a tokamak is an all too real concern.
1466 The problem is there is currently no solution to the problem. Although researchers
1467 have explored various types of heat divertors, none have been shown to withstand the
1468 gigawatts-per-square-meter of heat emitted from a reactor-size tokamak.⁸ Further, as
1469 it is not as glamorous as plasma physics, attempts to tackle the problem head-on have
1470 often gone unfunded.⁸

1471 As such, this model takes an approach similar to the research community, calculating
1472 it at the end as a manual check on the difficulty of building such a device – but not
1473 using it to explicitly guide design. As such, this model takes the approach that we are
1474 no worse than the rest of the field. We almost completely ignore the heat loading limit
1475 and just refer to it at the end, saying "and then this magic divertor will have to deal
1476 with solar corona levels of heat." After which, discussion will quickly be redirected
1477 to happier concerns. For completeness though, a limiting secondary con-
1478 straint will still be derived. The first step is giving the heat load limit commonly
1479 found in the literature:²⁵

$$q_{DV} = \frac{K_{DV}}{K_F} \cdot \frac{P_F I_P^{1.2}}{R_0^{2.2}} \quad (3.53)$$

$$K_{DV} = \frac{18.31 \times 10^{-3}}{\epsilon^{1.2}} \cdot K_P \cdot \left(\frac{2}{1 + \kappa^2} \right)^{0.6} \quad (3.54)$$

1481 This is the heat load that impinges on an extended leg, double null divertor – primarily
1482 from the outer midplane of the plasma core. After a simple rearrangement and
1483 substitution for fusion power, this becomes:

$$R_0 = K_{DH} \cdot I_P \cdot (\sigma v)^{\frac{1}{3.2}} \quad (3.55)$$

$$K_{DH} = \left(\frac{K_{DV} K_n^2}{q_{DV}} \right)^{\frac{1}{3.2}} \quad (3.56)$$

1485 At this point all the ~~limitingsecondary~~ constraints have been defined. The next step
1486 is taking a step back and motivating the derivation of a current equation suitable for
1487 pulsed tokamaks.

1488 3.5 Summarizing the Fusion Systems Model

1489 ~~Stepping back, this~~This chapter focused on the bigger picture behind designing a
1490 zero-dimension fusion systems model. It started with a description of various design
1491 parameters and then ~~moved onto~~~~sequed into~~ explaining the five relations needed to
1492 close the model – i.e. for \bar{T} , \bar{n} , I_P , B_0 , and R_0 .

1493 Before ~~moving onto~~ generalizing the steady current to ~~allow modeling~~~~model~~ pulsed
1494 reactors, ~~though~~, a quick recap of the equations will prove beneficial. The first variable
1495 ~~described~~~~tackled~~ was temperature – i.e. scan five evenly-spaced \bar{T} values between 10
1496 and 30 keV. This was then quickly followed by the Greenwald density limit – the ~~a~~
1497 ~~simple relation assumed to apply to all fusion reactors.~~~~cornerstone of this framework.~~
1498 Through equations, these two were written as:

$$\bar{T} = \text{const.} \quad (3.1)$$

1499

$$\bar{n} = K_n \cdot \frac{I_P}{R_0^2} \quad (2.11)$$

1500 The next variable handled was the steady current:

$$I_P = \frac{K_{BS}\bar{T}}{1 - K_{CD}(\sigma v)} \quad (2.30)$$

1501 As was mentioned then, this only directly depends on temperature, but is strongly af-
1502 fected by a tokamak's configuration – R_0 and B_0 - through the current drive efficiency
1503 (η_{CD}). For pulsed reactors, this equation proves too simple as it ignores inductive
1504 current. To remedy the situation, current balance will be revisited next chapter. The
1505 main point to make now, though, is that the R_0 and B_0 dependence will be made

1506 explicit.

1507 Moving on, the remaining equations were the primary and ~~limitingsecondary~~ con-
1508 straints for B_0 and R_0 , respectively. It was through these relations that a tokamak's
1509 configuration was brought back into the fold. The choice of solving the two con-
1510 straints for their respective variables was ~~not completely uniquecompletely arbitrary~~
1511 – motivated only by the foresight of how they fit into the model. Repeated below,
1512 they served as the proper vehicles for closing the system of equations. ~~The next step~~
1513 ~~now is to learn how to generalize the current formula and design a pulsed tokamak~~
1514 ~~reactor.~~

$$B_0 = \left(\frac{G_{PB}}{K_{PB}} \cdot \left(I_P^{\alpha_I^*} R_0^{\alpha_R^*} \right)^{-1} \right)^{\frac{1}{\alpha_B}} \quad (3.29)$$

$$R_0 = \frac{K_{TB} \bar{T}}{B_0} \quad (3.38)$$

1515

$$R_0 = \frac{K_{SF} I_P}{B_0} \quad (3.41)$$

$$R_0 = K_{WL} \cdot I_P^{\frac{2}{3}} \cdot (\sigma v)^{\frac{1}{3}} \quad (3.45)$$

1516

$$R_0 = K_{PC} \cdot I_P^2 \cdot (\sigma v) \quad (3.51)$$

1517

$$R_0 = K_{DH} \cdot I_P \cdot (\sigma v)^{\frac{1}{3.2}} \quad (3.55)$$

1518 The next step now is to learn how to generalize the current formula and design a
1519 pulsed tokamak reactor (see Chapter 4). After this is done, Chapter 5 will pick up
1520 where this chapter leaves off – transforming this fusion systems model into a simple
1521 reactor solver.

1522 Chapter 4

1523 Designing a Pulsed Tokamak

1524 Pulsed tokamaks are the flagship of the European fusion reactor design effort. As such,
1525 this paper's model will now be generalized to accommodate this mode of operation.
1526 Fundamentally, this involves transforming current balance into flux balance – adding
1527 inductive (pulsed) sources to stand alongside the LHCD (steady-state) ones.

1528 The first step in generalizing current balance will be understanding the problem from
1529 a basic electrical engineering perspective – i.e. with circuit analysis. The resulting
1530 equation will then be transformed into the flux balance seen in other models from
1531 the literature. All that will need to be done then is solving the problem for plasma
1532 current (I_P) and simplifying it for various situations – e.g. steady-state operation.

1533 This generalized plasma current will then be found to be a function of the other
1534 dynamic variables (i.e. R_0 , B_0 , and \bar{T}). This, of course, is more difficult to handle
1535 computationally than the steady current, which only directly depended on tempera-
1536 ture (\bar{T}). Discussion about solving this new root solving problem will be the topic of
1537 the next chapter.

1538 4.1 Modeling Plasmas as Circuits

1539 Although it may have been lost along the way, what makes plasmas so interesting and
1540 versatile – in comparison to gases – is their ability to respond to electric and magnetic
1541 fields. It seems natural then to model plasma current from a circuits perspective (i.e.
1542 with resistors, voltage sources, and inductors). By name, this circuit is referred to as
1543 a transformer where: the plasma is the secondary and the yet-to-be discussed central
1544 solenoid (of the tokamak) is the primary.

1545 The first step in deriving a current equation is to determine the circuit equations
1546 that govern pulsed operation in a tokamak. This will be done in two steps. First, we
1547 will draw a circuit diagram and write the equations that describe it. Next, we will
1548 use a simple schematic for how current evolves in a transformer to boil the resulting
1549 differential equations into simple algebraic ones – as is the hallmark of our model.

1550 4.1.1 Drawing the Circuit Diagram

1551 Understanding a circuit always starts with drawing a simple diagram, see Fig. 4-1.
1552 This figure depicts the transformer governing pulsed reactor. The left sub-circuit
1553 is the transformer’s primary – the central solenoid component of the tokamak that
1554 provides most of the inductive current. Whereas, the right sub-circuit is the plasma
1555 acting as the transformer’s secondary. The central solenoid, here, is then a helically-
1556 spiraled metal coil that fits within the inner ring of the doughnut. For now, every
1557 other flux source (besides this central solenoid) is neglected.

1558 This is described by the standard circuits involving voltage sources, resistors, and
1559 inductors: ~~Hopefully without scaring the reader too much, the circuit equations—~~
1560 ~~when only modeling voltage sources, resistors, and inductors—are described by:~~

$$V_i = \sum_j^n \frac{d}{dt} (M_{ij} I_j) + I_i R_i \quad , \quad \forall i = 1, 2, \dots, n \quad (4.1)$$

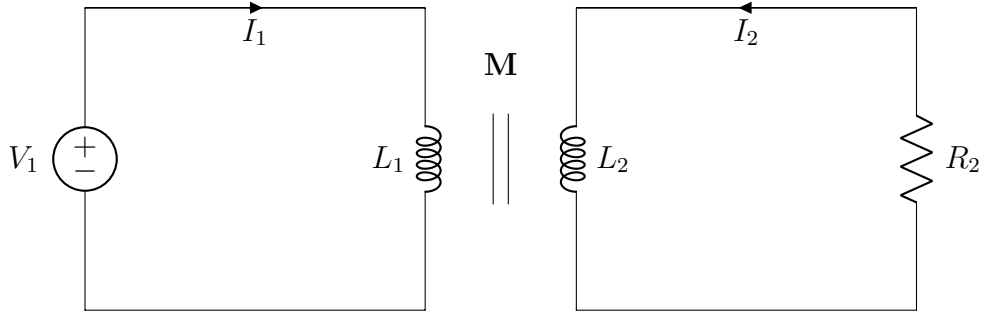


Figure 4-1: A Simple Plasma Transformer Description

1561 Without going into the inductances (M) and resistances (R), the variable n is the
 1562 number of sub-circuits, here being 2. Whereas, the variables i and j are the indices
 1563 of sub-circuits (i.e. 1 for the primary, 2 for the secondary). For illustrative purposes,
 1564 this would boil down to the following relation for a battery attached to a lightbulb:

$$V = IR \quad (4.2)$$

1565 Back to the transformer diagram, the equations for the two subcircuits can be ex-
 1566 panded and greatly simplified. Besides ignoring every inductive source other than the
 1567 central solenoid, the next powerful assumption is treating the solenoid as a supercon-
 1568 ductor (i.e. with negligible resistance). Lastly, the inductances between components
 1569 and themselves are held constant – independent of time. This allows the coupled
 1570 transformer equations to be written as:

$$V_1 = L_1 \dot{I}_1 - M \dot{I}_2 \quad (4.3)$$

$$-I_2 R_P = L_2 \dot{I}_2 - M \dot{I}_1 \quad (4.4)$$

1571 With I_1 and I_2 going in opposite directions. Note, here, that the subscript on M
 1572 has been dropped, as there are only two components. This was done in conjunction
 1573 to adding internal (self-)inductance terms. Mathematically, the mapping between

1574 variables is:

$$M = M_{12} = M_{21} \quad (4.5)$$

1575

$$L_1 = M_{11} \quad (4.6)$$

1576

$$L_2 = M_{22} \quad (4.7)$$

1577 Repeated, the one subscript represents the primary – the central solenoid – and the
 1578 two stands for the plasma as the transformer’s secondary. Exact definitions for the
 1579 inductances will be put off till the end of the next subsection.

1580 4.1.2 Plotting Pulse Profiles

1581 Up until now, little has been discussed that has a time dependence. For steady-state
 1582 tokamaks, this did not occur because it is an extreme case where pulses basically last
 1583 the duration of the machine’s lifespan (i.e. around 50 years). By definition, though,
 1584 a pulsed machine has pulses – with around ten scheduled per day. For this reason, a
 1585 fusion pulse is now investigated in detail.

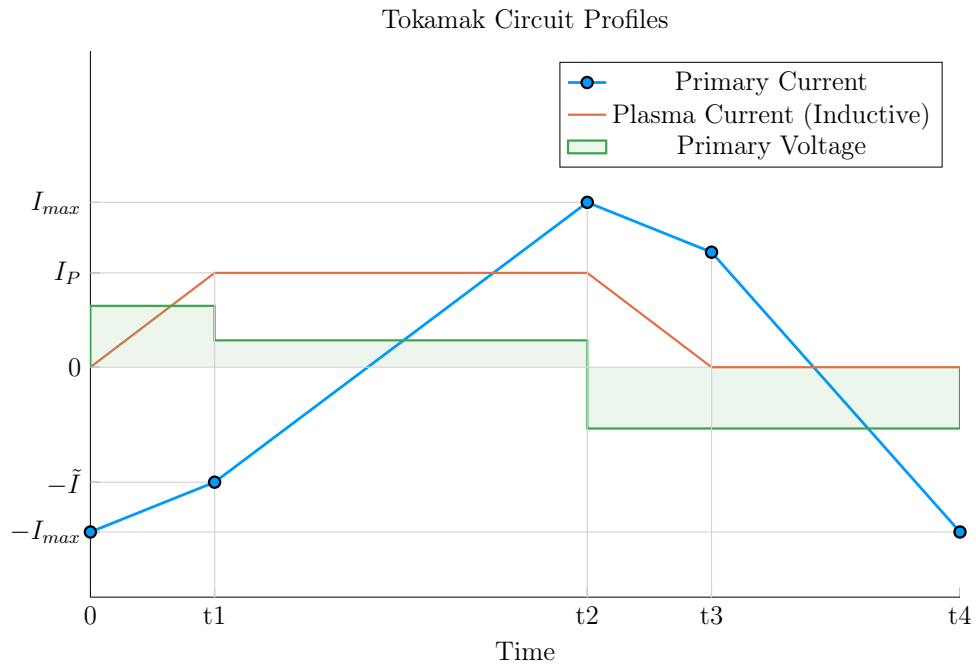


Figure 4-2: Time Evolution of Circuit Profiles

Transformer pulses between the central solenoid and the plasma occur on the timescale of hours. During this time, a plasma is brought up to some quasi-steady-state current (I_P^*) for around an hour and then ramped back down using the available flux in the solenoid (measured in volt-seconds). For clarity, each pulse is subdivided into four phases: ramp-up, flattop, ramp-down, and dwell. Pictorially represented in Fig. 4-2, these divisions allow a simple scheme for transforming the coupled circuit differential equations – from Eqs. (4.3) and (4.4) – into simple algebraic formulas.

Along the way, we will approximate derivatives with linear piecewise functions. Using t_i to represent the initial time and t_f as the final one, these can be written as:

$$\dot{I} = \frac{I(t_f) - I(t_i)}{t_f - t_i} \quad (4.8)$$

In tabular form, the data from Fig. 4-2 can be written in this piecewise fashion as:

Table 4.1: Piecewise Linear Scheme for Pulsed Operation

(a) Currents			(b) Voltage			
Time	I_1	I_2	Phase	t_i	t_f	V_1
0	$-I_{max}$	0	Ramp-Up	0	t_1	$+V_{max}$
t1	$-\tilde{I}$	I_P^*	Flattop	t_1	t_2	$+\tilde{V}$
t2	$+I_{max}$	I_P^*	Ramp-Down	t_2	t_3	$-V_{max}$
t3	$+\tilde{I}$	0	Dwell	t_3	t_4	$-V_{max}$
t4	$-I_{max}$	0				

The exact definitions for the plasma's inductive current (I_P^*) and the maximum voltage in the central solenoid (V_{max}) will be put off until the end of the section.

The Ramp-Up Phase – RU

The first phase in every plasma pulse is the ramp-up. During ramp-up, the central solenoid starts discharging from its fully charged values, as the plasma is brought to its quasi-steady-state current. As this occurs on the timescale of minutes – not hours – resistive effects of the plasma can safely be ignored. This results in the ramp-up equations becoming:

$$V_{max} = \frac{1}{\tau_{RU}} \cdot \left(L_1 \cdot (I_{max} - \tilde{I}) - M \cdot I_{ID} \right) \quad (4.9)$$

$$0 = \frac{1}{\tau_{RU}} \cdot \left(M \cdot (I_{max} - \tilde{I}) - L_2 \cdot I_{ID} \right) \quad (4.10)$$

1604 Simplifying these equations will be done shortly, for now the new terms are what
 1605 is important. The maximum voltage of the solenoid is V_{max} – usually measured in
 1606 kilovolts. Next, I_{max} is the solenoid’s current at the beginning of ramp-up. Whereas
 1607 \tilde{I} is the magnitude of the current once the plasma is at its flattop inductive-drive
 1608 current – I_{ID} . The τ_{RU} quantity, then, is the duration of time it takes to ramp-up
 1609 (i.e. RU). Again, L_1 and L_2 are the microhenry-scale internal inductances of the
 1610 solenoid and plasma, respectively, and M is the mutual inductance between them.

1611 The last step in discussing ramp-up is giving the two important formulas that come
 1612 from it:

$$\tilde{I} = I_{max} - I_{ID} \cdot \left(\frac{L_2}{M} \right) \quad (4.11)$$

$$\tau_{RU} = \frac{I_{ID}}{V_{max}} \cdot \left(\frac{L_1 L_2 - M^2}{M} \right) \quad (4.12)$$

1614 The Flattop Phase – FT

1615 The most important phase in any reactor’s pulse is flattop – the quasi-steady-state
 1616 time when the tokamak is making electricity (and money). Flattops are assumed
 1617 to last a couple of hours for a profitable machine, during which the central solenoid
 1618 completely discharges to overcome a plasma’s resistive losses – keeping it in a quasi-
 1619 steady-state mode of operation. In a steady-state reactor, this phases constitutes the
 1620 entirety of the pulse.

1621 Although the resistance cannot be safely neglected for flattop – as it was for ramp-up –
 1622 the plasma’s inductive current (I_{ID}) is assumed constant. This leads to its derivative
 1623 in equations cancelling out! Mathematically,

$$\tilde{V} = \frac{L_1}{\tau_{FT}} \cdot (I_{max} + \tilde{I}) \quad (4.13)$$

$$I_{ID}R_P = \frac{M}{\tau_{FT}} \cdot (I_{max} + \tilde{I}) \quad (4.14)$$

As with ramp-up, the simplifications will be given shortly. The new terms here, however, are an intermediate voltage for the central solenoid (\tilde{V}), and the duration of the flattop (τ_{FT}). The resistance term was given in Eq. (3.10). Solutions can then be found by substituting \tilde{I} – from Eq. (4.11) – into the flattop equations:

$$\tilde{V} = I_{ID}R_P \cdot \left(\frac{L_1}{M} \right) \quad (4.15)$$

$$\tau_{FT} = \frac{I_{max} \cdot 2M - I_{ID} \cdot L_2}{I_{ID}R_P} \quad (4.16)$$

The Ramp-Down Phase – RD

Due to the simplicity – and symmetry – of this model’s reactor pulse, ramp-down is the exact mirror of ramp-up. It takes the same amount of time and results in the same algebraic equations. For brevity, this will just be represented as:

$$\tau_{RD} = \tau_{RU} \quad (4.17)$$

For clarity, this is the time when a plasma’s current is brought down from its flattop value to zero.

The Dwell Phase – DW

Where the first three phases had little ambiguity, the dwell phase changes definition from model to model. For now, it is assumed to be the time it takes the central solenoid to reset after a plasma has been completely ramped-down to an off-mode. To get a more realistic duty factor for cost estimates, it could include an evacuation

time, set to last around thirty minutes. During this evacuation, a plasma is vacuumed out of a device as it undergoes some inter-pulse maintenance.

Ignoring evacuation for now, the dwell phase involves resetting the central solenoid when the plasma's current is negligible. This fundamentally means the secondary of the transformer is nonexistent – the central solenoid is the entire circuit. In equation form,

$$V_{max} = \frac{L_1}{\tau_{DW}} \cdot (I_{max} + \tilde{I}) \quad (4.18)$$

Or substituting in \tilde{I} and solving for τ_{DW} ,

$$\tau_{DW} = \frac{L_1}{M} \cdot \frac{(I_{max} \cdot 2M - I_{ID} \cdot L_2)}{V_{max}} \quad (4.19)$$

4.1.3 Specifying Circuit Variables

The goal now is to collect the results from the four phases and introduce the inductance, resistance, voltage, and current terms relevant to our model. This will motivate recasting the problem as flux balance in a reactor – the form commonly used in the literature (and discussed next section).

First, collecting the phase durations in one place:

$$\tau_{RU} = \frac{I_{ID}}{V_{max}} \cdot \left(\frac{L_1 L_2 - M^2}{M} \right) \quad (4.12)$$

$$\tau_{FT} = \frac{I_{max} \cdot 2M - I_{ID} \cdot L_2}{I_{ID} R_P} \quad (4.16)$$

$$\tau_{RD} = \tau_{RU} \quad (4.17)$$

$$\tau_{DW} = \frac{L_1}{M} \cdot \frac{(I_{max} \cdot 2M - I_{ID} \cdot L_2)}{V_{max}} \quad (4.19)$$

These can be used in the definition of the duty-factor: the fraction of time a reactor

1654 is putting electricity on the grid. Formulaically,

$$f_{duty} = \frac{\tau_{FT}}{\tau_{pulse}} \quad (4.20)$$

1655

$$\tau_{pulse} = \tau_{RU} + \tau_{FT} + \tau_{RD} + \tau_{DW} \quad (4.21)$$

1656 As will turn out, the solving of pulsed current actually only involves Eq. (4.16).
 1657 What is interesting about this, is that there is no explicit dependence on ramp-down
 1658 or dwell! Whereas ramp-up passes \tilde{I} to the flattop phase, the other two are just
 1659 involved in calculating the duty factor.

1660 The remainder of this subsection will then be defining the following circuit variables:
 1661 I_{ID} , I_{max} , V_{max} , L_1 , L_2 , and M . Again, the resistance was defined last chapter as:

$$R_P = \frac{K_{RP}}{R_0 \bar{T}^{3/2}} \quad (3.10)$$

1662 **The Inductive Current – I_{ID}**

1663 The inductive current is the source of current that separates pulsed from steady-state
 1664 operation. Quickly fitting it into the previous definitions of current balance – see
 1665 Eq. (3.3):

$$I_{ID} = I_P - (I_{BS} + I_{CD}) \quad (4.22)$$

1666 As before, I_P is the total plasma current in mega-amps, I_{BS} is the bootstrap current,
 1667 and I_{CD} is the current from LHCD (i.e. lower hybrid current drive). For this model,
 1668 the relation can be rewritten as:

$$I_{ID} = I_P \cdot \left(1 - K_{CD}(\sigma v)\right) - K_{BS} \bar{T} \quad (4.23)$$

1669 The Central Solenoid Maximums – V_{max} and I_{max}

1670 For this simple model, the central solenoid has two maximum values: the voltage and
1671 current. The voltage is the easier to give value. Literature values have this around:²⁶

$$V_{max} \approx 5 \text{ kV} \quad (4.24)$$

1672 The maximum current, on the other hand, can be defined through Ampere's Law on
1673 a helically-shaped central solenoid:¹⁷

$$I_{max} = \frac{B_{CS} h_{CS}}{N \mu_0} \quad (4.25)$$

1674 Here, B_{CS} is a magnetic field strength the central solenoid is assumed to operate at
1675 (i.e. 12 T), h_{CS} is the height of the solenoid, N is the number of loops, and μ_0 has its
1676 usual physics meaning (i.e. $40 \pi \frac{\mu\text{H}}{\text{m}}$). As will be seen, the value of N does not directly
1677 affect the model, as it cancels out in the final flux balance. The height of the central
1678 solenoid will be the focus of an upcoming section on improving tokamak geometry.

1679 The Central Solenoid Inductance – L_1

1680 For a central solenoid with circular cross-sections of finite thickness (d), the inductance
1681 can be written as:²³

$$L_1 = G_{LT} \cdot \left(\frac{\mu_0 \pi N^2}{h_{CS}} \right) \quad (4.26)$$

1682

$$G_{LT} = \frac{R_{CS}^2 + R_{CS} \cdot (R_{CS} + d) + (R_{CS} + d)^2}{3} \quad (4.27)$$

1683 Note that R_{CS} is the inner radius of the central solenoid and $(R_{CS} + d)$ is the outer
1684 one. In the limit where d is negligible, this says that the inductance is quadratically
1685 dependent on the radius of the central solenoid:

$$\lim_{d \rightarrow 0} G_{LT} = G_{LT}^\dagger = R_{CS}^2 \quad (4.28)$$

1686 The formulas for both R_{CS} and d will be defined in a few sections.

1687 The Plasma Inductance – L_2

1688 The plasma inductance is a composite of several different terms, but overall scales
1689 with radius. Through equation,

$$L_2 = K_{LP} R_0 \quad (4.29)$$

1690 This ~~static~~~~fixed~~ coefficient – K_{LP} – then combines three inductive behaviors of the
1691 plasma. The first is its own self inductance (through l_i).³ The next is a resistive
1692 component through the Ejima coefficient, C_{ejima} , which is usually set to $\sim \frac{1}{3}$.⁷ And
1693 lastly, a geometric component – involving ϵ and κ – is given by the Hirshman-Neilson
1694 model.²⁷ Mathematically,

$$K_{LP} = \mu_0 \cdot \left(\frac{l_i}{2} + C_{ejima} + \frac{(b_{HN} - a_{HN})(1 - \epsilon)}{(1 - \epsilon) + \kappa d_{HN}} \right) \quad (4.30)$$

1695 Here the HN values come from the 1985 Hirshman-Neilson paper:

$$a_{HN}(\epsilon) = 2.0 + 9.25\sqrt{\epsilon} - 1.21 \epsilon \quad (4.31)$$

1696

$$b_{HN}(\epsilon) = \ln(8/\epsilon) \cdot (1 + 1.81\sqrt{\epsilon} + 2.05 \epsilon) \quad (4.32)$$

1697

$$d_{HN}(\epsilon) = 0.73\sqrt{\epsilon} \cdot (1 + 2\epsilon^4 - 6\epsilon^5 + 3.7\epsilon^6) \quad (4.33)$$

1698 The Mutual Inductance – M

1699 The mutual inductance – M – represents the coupling between the solenoid primary
1700 and the plasma secondary. A common method for treating this mutual inductance is
1701 through a coupling coefficient, k , that links the two self-inductances. Formulaically,

$$M = k \sqrt{L_1 L_2} \quad (4.34)$$

1702 The value of the coupling coefficient, k , is always less than (or equal to) 1, but usually
 1703 has a value around one-third. With all the equations defined, we are now at a position
 1704 to explain one of the larger nuances of this fusion systems framework: declaring the
 1705 pulse length of a tokamak.

1706 4.1.4 ConstructingReasoning the Pulse Length

1707 This subsection focuses on a quantitative estimate for how to select a pulse length.
 1708 As no fusion reactor exists in the world today, the writers believe this is an acceptable
 1709 calculation. Further, the resulting length of two hours matches the durations of other
 1710 studies in the literature.

1711 Starting at the end, our goal is to find the pulse length of a tokamak reactor in seconds
 1712 – as dictated by cyclical stress concerns. The first piece of information is the expected
 1713 lifetime of the central solenoid, $N \approx 10$ years. The next is the desired number of shots
 1714 the machine will likely have, $M \approx 50,000$ shots.* This gives the ballpark estimate of
 1715 around 10 pulses a day – or a flattop pulse length of two hours.

1716 With the pulse length defined, we are now in a position to justify neglecting the duty
 1717 factor for pulsed reactors in this model. Using expectedballpark reactor values – while
 1718 assuming the central solenoid has around 4000 turns – leads to the following scalings:

$$\tau_{FT} \sim \tau_{pulse} \sim \text{O}(\text{hours}) \quad (4.35)$$

1719

$$\tau_{RU} \sim \tau_{RD} \sim \tau_{DW} \sim \text{O}(\text{mins}) \quad (4.36)$$

1720 As such, even pulsed tokamak reactors should have a duty factor of around unity:

$$f_{duty} \approx 1 \quad (4.37)$$

1721 This analysis of course would change if the central solenoid became an inexpensive

*This 50,000 shots comes from multiplying the number of pulses run at Diii-D per year by the expected lifetime of the central solenoid (10 years).²⁸

1722 component to replace. For example, if a tokamak had a new one installed annually,
 1723 the pulse length could shorten to be on the order of minutes.

1724 Now that all the terms in a pulsed circuit have been explored, we will move on to
 1725 rearranging the flattop equation to reproduce flux balance. This will then naturally
 1726 lead to a generalized current equation – which is the main result of the chapter.

1727 4.2 Producing Salvaging Flux Balance

1728 The goal of this section is to arrive at a conservation equation for flux balance that
 1729 mirrors the ones in the literature. The fusion systems model this one attempts to
 1730 follow most is the PROCESS code.⁷ In a manner similar to power balance, flux
 1731 balance can be written as:

$$\sum_{sources} \Phi = \sum_{sinks} \Phi \quad (4.38)$$

1732 4.2.1 Rearranging the Circuit Equation

1733 The way to arrive at flux balance from the circuit equation is to rearrange the flattop
 1734 phase’s duration equation:

$$\tau_{FT} = \frac{I_{max} \cdot 2M - I_{ID} \cdot L_2}{I_{ID} R_P} \quad (4.16)$$

1735 Multiplying by the right-hand side’s denominator and moving the negative term over
 1736 yields:

$$2MI_{max} = I_{ID} \cdot (L_2 + R_P \tau_{FT}) \quad (4.39)$$

1737 This equation is flux balance, where the left-hand side are the sources (e.g. the central
 1738 solenoid), and the other terms are the sinks (i.e. ramp-up and flattop). The source
 1739 term can currently be encapsulated in:

$$\Phi_{CS} = 2MI_{max} \quad (4.40)$$

1740 The sinks, namely the ramp-up inductive losses (Φ_{RU}) and the flattop resistive losses
 1741 (Φ_{FT}), are what drain up the flux. Again, ramp-down and dwell are not included as
 1742 sinks because flux balance only tracks till the end of flattop. They come into play
 1743 when measuring the cost of electricity – through the duty factor from Eq. (4.20).
 1744 Relabeling terms, flux balance can now be rewritten as:

$$\Phi_{CS} = \Phi_{RU} + \Phi_{FT} \quad (4.41)$$

1745 With the ramp-up and flattop flux given respectively by:

$$\Phi_{RU} = L_2 \cdot I_{ID} \quad (4.42)$$

1746

$$\Phi_{FT} = (R_P \tau_{FT}) \cdot I_{ID} \quad (4.43)$$

1747 On comparing these quantities to the ones from the PROCESS team, Φ_{RU} and Φ_{FT}
 1748 are exactly the same. The source terms, on the other hand, are off for two reasons
 1749 – both related to the central solenoid being the only source term in flux balance.
 1750 This can partially be remedied by adding the second most dominant source of flux
 1751 a posteriori – i.e. the PF coils. The second, and inherently limiting factor, is the
 1752 simplicity of the current model. All that can be shown to this regard is that the Φ_{CS}
 1753 terms does reasonably predict the values from the PROCESS code.

1754 4.2.2 AddingImporting Poloidal Field Coils

1755 Adding the effect of PF coils – belts of current driving plates on the outer edges of
 1756 the tokamak – leads to as much as a 50% improvement^{5,7} ~~a second-order improvement~~
 1757 over relying solely on the central solenoid for flux generation. From the literature,
 1758 this can be modeled as:²³

$$\Phi_{PF} = \pi B_V \cdot (R_0^2 - (R_{CS} + d)^2) \quad (4.44)$$

1759 Where again R_{CS} and d are the inner radius and thickness of the central solenoid,
 1760 respectively. These will be the topic of the next section.

1761 Moving forward, the vertical field – B_V – is a magnetic field oriented up-and-down
 1762 with the ground. It is needed to prevent a tokamak plasma from ~~drifting radially~~~~spinning~~
 1763 out of the machine. From the literature, the magnitude of this vertical field (~~valid for~~
 1764 ~~a circular plasma~~) is given by:⁷

$$|B_V| = \frac{\mu_0 I_P}{4\pi R_0} \cdot \left(\ln \left(\frac{8}{\epsilon} \right) + \beta_p + \frac{l_i}{2} - \frac{3}{2} \right) \quad (4.45)$$

1765 Analogous to the previously covered plasma beta, the poloidal beta can be represented
 1766 by:²⁹

$$\beta_p = \frac{\bar{p}}{\left(\frac{\overline{B_p}^2}{2\mu_0} \right)} \quad (4.46)$$

1767 Where the average poloidal magnetic field comes from a simple application of Am-
 1768 pere's law:

$$\overline{B_p} = \frac{\mu_0 I_P}{l_p} \quad (4.47)$$

1769 The variable l_p is then the perimeter of the tokamak's cross-sectional halves:

$$l_p = 2\pi a \cdot \sqrt{g_p} \quad (4.48)$$

1770 Here, g_p is another geometric scaling factor,

$$g_p = \frac{1 + \kappa^2(1 + 2\delta^2 - 1.2\delta^3)}{2} \quad (4.49)$$

1771 ~~After a few lines of algebra~~~~Boiled down~~, this relation for the magnitude of the vertical
 1772 magnetic field can be written in standardized units as:

$$|B_V| = \left(\frac{1}{10 \cdot R_0} \right) \cdot (K_{VI} I_P + K_{VT} \overline{T}) \quad (4.50)$$

1773

$$K_{VT} = K_n \cdot (\epsilon^2 g_P) \cdot (1 + f_D) \frac{(1 + \nu_n)(1 + \nu_T)}{1 + \nu_n + \nu_T} \quad (4.51)$$

$$K_{VI} = \ln \left(\frac{8}{\epsilon} \right) + \frac{l_i}{2} - \frac{3}{2} \quad (4.52)$$

1774 For clarity, this will be plugged into the new PF coil flux contribution (Φ_{PF}):

$$\Phi_{PF} = \pi B_V \cdot (R_0^2 - (R_{CS} + d)^2) \quad (4.44)$$

1775 Which then gets plugged into a more complete flux balance:

$$\Phi_{CS} + \Phi_{PF} = \Phi_{RU} + \Phi_{FT} \quad (4.53)$$

1776 The R_{CS} and d terms found in Φ_{PF} will now be discussed as they are needed for this
1777 more sophisticated tokamak geometry.

1778 4.3 Improving Tokamak Geometry

1779 From before, this fusion systems model has been said to depend on the major and
1780 minor radius – R_0 and a , respectively – and along the way, various geometric param-
1781 eters have been defined (e.g. ϵ , κ , δ) to describe the geometry further. Now three
1782 more thicknesses will be added: b , c , and d . Additionally, two fundamental dimension
1783 corresponding to the solenoid will be given: the radius (R_{CS}) and height (h_{CS}). These
1784 are the topics of this section.

1785 4.3.1 Defining Central Solenoid Dimensions

1786 The best way to conceptualize tokamak geometry is through cartoon – see Fig. E-2.
1787 What this says is there is a gap at the very center of a tokamak. This gap extends
1788 radially outwards to R_{CS} meters where the ~~spiraledslinky-shaped~~ central solenoid –
1789 of thickness d – begins. Between the outer edge of the solenoid and the wall of the
1790 torus (i.e. the doughnut) are the blanket and toroidal field (TF) coils.

1791 The blanket and TF coils have thicknesses of b and c , respectively. Before defining

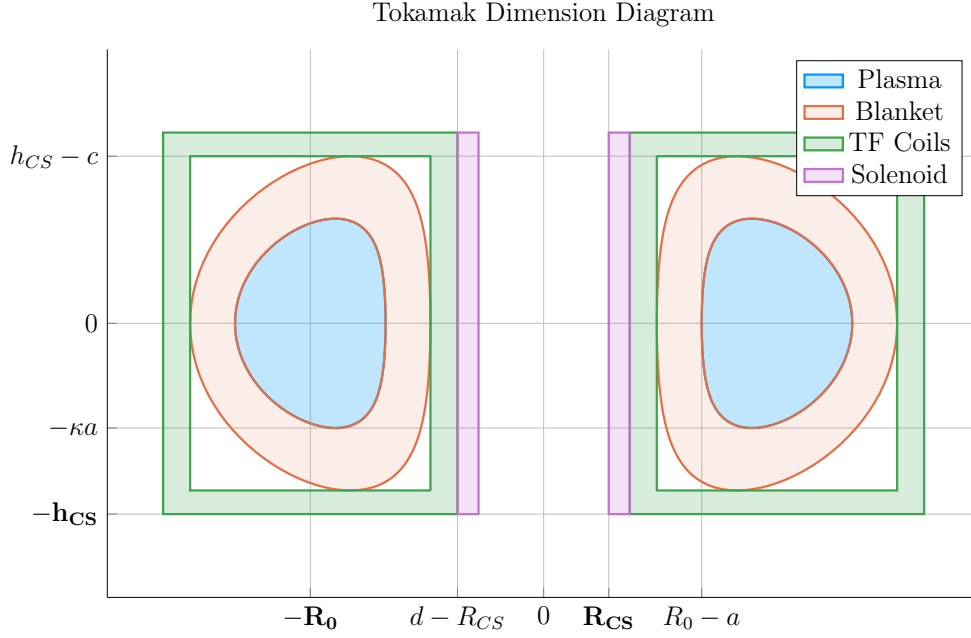


Figure 4-3: Dimensions of Tokamak Cross-Section

1792 b , c , and d , though, it proves fruitful to relate all the quantities in equations for the
 1793 inner radius (R_{CS}) and height (h_{CS}) of the central solenoid.

$$R_{CS} = R_0 - (a + b + c + d) \quad (4.54)$$

1794

$$h_{CS} = 2 \cdot (\kappa a + b + c) \quad (4.55)$$

1795 Again, this relation is pictorially represented in Fig. E-2. The next step is defining:
 1796 b , c , and d – to close the variable loop.

1797 4.3.2 CalculatingMeasuring Component Thicknesses

1798 In between the inner surface of the central solenoid and the major radius of the
 1799 tokamak are four thicknesses: a , b , c , and d . This subsection will go over them
 1800 one-by-one.

1801 The Minor Radius – a

1802 The minor radius was the first of these thicknesses we encountered. To calculate it,
1803 we introduced the inverse aspect ratio (ϵ) to relate it to the major radius (R_0):

$$a = \epsilon \cdot R_0 \quad (2.1)$$

1804 The Blanket Thickness – b

1805 The blanket is an area between the TF coils and the torus that is **strongly** composed
1806 **mainly** of lithium. It serves to both: protect the superconducting magnet structures
1807 from neutron damage, as well as breed **a little** more tritium fuel from stray fusion
1808 neutrons. In equation form, the blanket thickness is given by:²⁵

$$b = 1.23 + 0.074 \ln P_W \quad (4.56)$$

1809 ~~Here, the constant term (i.e. 1.23) is approximately the mean-free-path of fusion~~
1810 ~~neutrons through lithium-7—the thickness of lithium needed to reduce the population~~
1811 ~~of neutrons by $\sim 65\%$. Here, P_W While the second term, which includes P_W , is a~~
1812 ~~correction to account for extra wall loading (as discussed in Section 3.4.3~~
1813 ~~the secondary constraint section).~~

1814 Moving forward, the remaining two thicknesses – c and d – are handled differently,
1815 estimating structural steel portions as well as magnetic current-carrying ones.

1816 The Toroidal Field Coil Thickness – c

1817 The thickness of the TF coils – c – is a little beyond the scope of this paper. It does,
1818 however, have a form that combines a structural steel component with a magnetic
1819 portion. From **a previous model**~~one of Jeff's previous models~~, this can be given as:²⁵

$$c = G_{CI}R_0 + G_{CO} \quad (4.57)$$

$$G_{CI} = \frac{B_0^2}{4\mu_0\sigma_{TF}} \cdot \frac{1}{(1 - \epsilon_b)} \cdot \left(\frac{4\epsilon_b}{1 + \epsilon_b} + \ln \left(\frac{1 + \epsilon_b}{1 - \epsilon_b} \right) \right) \quad (4.58)$$

1820

$$G_{CO} = \frac{B_0}{\mu_0 J_{TF}} \cdot \frac{1}{(1 - \epsilon_b)} \quad (4.59)$$

1821 The critical stress – σ_{TF} in G_{CI} implies it depends on the structural component,
 1822 whereas the maximum current density – J_{TF} – implies a magnetic predisposition
 1823 in G_{CO} . The use of G_{\square} in these quantities, instead of K_{\square} is because they include
 1824 the toroidal magnetic field strength – B_0 . For this reason, they are referred to as
 1825 **dynamicfloating** coefficients. Lastly, the term ϵ_b represents the blanket inverse aspect
 1826 ratio that combines the minor radius with the blanket thickness:

$$\epsilon_b = \frac{a + b}{R_0} \quad (4.60)$$

1827 The Central Solenoid Thickness – d

1828 Finishing this discussion where we started, the central solenoid's thickness – d – has
 1829 a form similar to the TF coil's (i.e. c). In mathematical form, this can be represented
 1830 as:²⁵

$$d = K_{DR}R_{CS} + K_{DO} \quad (4.61)$$

1831

$$K_{DR} = \frac{3B_{CS}^2}{6\mu_0\sigma_{CS} - B_{CS}^2} \quad (4.62)$$

1832

$$K_{DO} = \frac{6B_{CS}\sigma_{CS}}{6\mu_0\sigma_{CS} - B_{CS}^2} \cdot \left(\frac{1}{J_{OH}} \right) \quad (4.63)$$

1833 Here, the use of K_{\square} for the coefficients signifies their use as **staticfixed** coefficients.
 1834 Therefore, B_{CS} must be treated as a **staticfixed** variable representing the magnetic
 1835 field strength in the central solenoid. For prospective solenoids using high temperature
 1836 superconducting (HTS) tape, B_{CS} may be around 20 T. The values of σ_{CS} and J_{CS}
 1837 have similar meanings to the ones for TF coils. These are collected in a table below
 1838 with example values representative of our model.

1839 Before moving on, it seems important to say that although K_{DI} and K_{DO} do not
 1840 depend on **dynamicfloating** variables, R_{CS} most definitely does. This is what makes

Table 4.2: Example TF Coils and Central Solenoid Critical Values

(a) Stresses [MPa]			(b) Current Densities [MA/m ²]		
Item	Symbol	Limit	Item	Symbol	Limit
Solenoid	σ_{CS}	600 300	Solenoid	J_{CS}	100 50
TF Coils	σ_{TF}	600	TF Coils	J_{TF}	200

the central solenoid's thickness difficult.

4.3.3 Revisiting Central Solenoid Dimensions

Now that the various thicknesses have been defined (i.e. a , b , c , and d), the equations for the solenoid's dimensions (i.e. R_{CS} and h_{CS}), can now be revisited and simplified. From before,

$$R_{CS} = R_0 - (a + b + c + d) \quad (4.54)$$

$$h_{CS} = 2 \cdot (\kappa a + b + c) \quad (4.55)$$

Utilizing the four thicknesses from before, these can now be expanded to simple formulas. Repeating the thicknesses:

$$a = \epsilon \cdot R_0 \quad (2.1)$$

$$b = 1.23 + 0.074 \ln P_W \quad (4.56)$$

$$c = G_{CI}R_0 + G_{CO} \quad (4.57)$$

$$d = K_{DR}R_{CS} + K_{DO} \quad (4.61)$$

Plugging these into the central solenoid's dimensions results in:

$$h_{CS} = 2 \cdot (R_0 \cdot (\epsilon\kappa + G_{CI}) + (b + G_{CO})) \quad (4.64)$$

$$R_{CS} = \frac{1}{1 + K_{DR}} \cdot (R_0 \cdot (1 - \epsilon - G_{CI}) - (K_{DO} + b + G_{CO})) \quad (4.65)$$

These are the complete central solenoid dimension formulas. To make them more tractable to the reader, they will now be simplified one step at a time. (The same

1849 simplification exercise will be done again after the generalized current is derived later
 1850 this chapter.)

1851 The first simplification to make while estimating central solenoid dimensions is to
 1852 neglect the magnetic current-carrying portions of the central solenoid and TF coils.
 1853 This results in:

$$\lim_{\substack{G_{CO} \rightarrow 0 \\ K_{DO} \rightarrow 0}} h_{CS} = h_{CS}^{\dagger} = 2R_0 \cdot (K_{EK} + \epsilon_b + G_{CI}) \quad (4.66)$$

1854

$$\lim_{\substack{G_{CO} \rightarrow 0 \\ K_{DO} \rightarrow 0}} R_{CS} = R_{CS}^{\dagger} = \frac{R_0}{1 + K_{DR}} \cdot (1 - \epsilon_b - G_{CI}) \quad (4.67)$$

1855 The new ~~static~~~~fixed~~ coefficient, here, is:

$$K_{EK} = \epsilon \cdot (\kappa - 1) \quad (4.68)$$

1856 The next simplification is ignoring the TF coil thickness – and thus magnetic field
 1857 dependence – altogether:

$$\lim_{G_{CI} \rightarrow 0} h_{CS}^{\dagger} = h_{CS}^{\ddagger} = 2R_0 \cdot (K_{EK} + \epsilon_b) \quad (4.69)$$

1858

$$\lim_{G_{CI} \rightarrow 0} R_{CS}^{\dagger} = R_{CS}^{\ddagger} = \frac{R_0}{1 + K_{DR}} \cdot (1 - \epsilon_b) \quad (4.70)$$

1859 These oversimplifications will be used later this chapter while simplifying the gener-
 1860 alized current equation to something more tractable. For now, they highlight how the
 1861 dimensions change as different components are neglected. The next step is bringing
 1862 plasma physics back into the flux balance equation and solving for the generalized
 1863 current.

1864 4.4 Piecing Together the Generalized Current

1865 The goal of this section is to quickly expand flux balance using all the defined quan-
 1866 tities and then massage it into an equation for plasma current – which is suitable for

1867 root solving. This starts with a restatement of flux balance in a reactor:

$$\Phi_{CS} + \Phi_{PF} = \Phi_{RU} + \Phi_{FT} \quad (4.53)$$

1868

$$\Phi_{CS} = 2MI_{max} \quad (4.40)$$

1869

$$\Phi_{PF} = \pi B_V \cdot (R_0^2 - (R_{CS} + d)^2) \quad (4.44)$$

1870

$$\Phi_{RU} = L_2 \cdot I_{ID} \quad (4.42)$$

1871

$$\Phi_{FT} = (R_P \tau_{FT}) \cdot I_{ID} \quad (4.43)$$

1872 The first step is realizing that the central solenoid flux can now be rewritten using
1873 the new geometry in a standardized form:

$$\Phi_{CS} = K_{CS} \cdot \sqrt{R_0 G_{LT} h_{CS}} \quad (4.71)$$

1874

$$K_{CS} = 2k B_{CS} \cdot \sqrt{\frac{\pi K_{LP}}{\mu_0}} \quad (4.72)$$

1875 Next, we will slightly simplify the PF coil flux using a ~~dynamicfloating~~ variable coef-
1876 ficient:

$$\Phi_{PF} = G_V \cdot \frac{K_{VI} I_P + K_{VT} \bar{T}}{R_0} \quad (4.73)$$

1877

$$G_V = \frac{\pi}{10} \cdot (R_0^2 - (R_{CS} + d)^2) \quad (4.74)$$

1878 This allows us to rewrite the generalized current as:

$$I_P = \frac{(K_{BS} + G_{IU}/G_{IP}) \cdot \bar{T}}{1 - K_{CD}(\sigma v) - G_{ID}/G_{IP}} \quad (4.75)$$

1879

$$G_{IU} = K_{VT} G_V + K_{CS} R_0^{3/2} \cdot \frac{\sqrt{h_{CS} G_{LT}}}{\bar{T}} \quad (4.76)$$

1880

$$G_{ID} = K_{VI} G_V \quad (4.77)$$

1881

$$G_{IP} = K_{LP} R_0^2 + \frac{K_{RP} \tau_{FT}}{\bar{T}^{3/2}} \quad (4.78)$$

1882 As we will show in the next section, this form not only has a form remarkably similar
 1883 to the steady current – it reduces to it in the limit of infinitely long pulses!

1884 4.5 Simplifying the Generalized Current

1885 This section focuses on making various simplifications to the generalized current:

$$I_P = \frac{(K_{BS} + G_{IU}/G_{IP}) \cdot \bar{T}}{1 - K_{CD}(\sigma v) - G_{ID}/G_{IP}} \quad (4.75)$$

1886 As promised, this will start with the trivial simplification of the generalized current
 1887 into steady state. Next it will move on to a basic simplification for the purely pulsed
 1888 case. These two activities should shed some light on how to interpret the equation in
 1889 the more complicated hybrid case.

1890 4.5.1 Recovering the Steady Current

1891 The place to start with the steady current is the ~~dynamic~~~~floating~~ coefficient, G_{IP} :

$$G_{IP} = K_{LP}R_0^2 + \frac{K_{RP} \tau_{FT}}{\bar{T}^{3/2}} \quad (4.78)$$

1892 As can be seen, as $\tau_{FT} \rightarrow \infty$, so does the coefficient,

$$\lim_{\tau_{FT} \rightarrow \infty} G_{IP} = \infty \quad (4.79)$$

1893 Because G_{IU} and G_{ID} remain constant, their contribution to plasma current becomes
 1894 insignificant in this limit. Concretely,

$$\lim_{\tau_{FT} \rightarrow \infty} I_P = \frac{K_{BS} \bar{T}}{1 - K_{CD}(\sigma v)} \quad (4.80)$$

1895 This is precisely the steady current given by Eq. (2.30)! The generalized current
 1896 automatically works when modeling steady-state tokamaks.*

1897 4.5.2 Extracting the Pulsed Current

1898 For pulsed reactors, we have to ~~resolve a similar problem~~~~play a similar game~~ – except
 1899 now τ_{FT} is expected to be a reasonably sized number (i.e. 2 hours).

1900 With an aim at intuition, the reactor is first treated as purely pulsed – having no
 1901 current drive assistance:

$$\lim_{\eta_{CD} \rightarrow 0} I_P = \frac{(K_{BS} + G_{IU}/G_{IP}) \cdot \bar{T}}{1 - (G_{ID}/G_{IP})} \quad (4.81)$$

1902 Next, for simplicity-sake, the PF coil contribution to flux balance is assumed negligi-
 1903 ble, as it was always just a correction term:

$$\lim_{\Phi_{PF} \ll \Phi_{CS}} G_{IU} = K_{CS} R_0^{3/2} \cdot \frac{\sqrt{h_{CS} G_{LT}}}{\bar{T}} \quad (4.82)$$

$$\lim_{\Phi_{PF} \ll \Phi_{CS}} G_{ID} = 0 \quad (4.83)$$

1905 Piecing this altogether, we can write a new current for this highly simplified case,

$$I_P^\dagger = K_{BS} \bar{T} + \frac{K_{CS} R_0^{3/2} \cdot \sqrt{h_{CS} G_{LT}}}{K_{LP} R_0^2 + K_{RP} \tau_{FT} \bar{T}^{-3/2}} \quad (4.84)$$

1906 As this is not quite simple enough, these previous simplifications will be incorporated:

$$G_{LT}^\dagger = R_{CS}^2 \quad (4.28)$$

$$h_{CS}^\dagger = 2R_0 \cdot (K_{EK} + \epsilon_b) \quad (4.69)$$

$$R_{CS}^\dagger = \frac{R_0}{1 + K_{DR}} \cdot (1 - \epsilon_b) \quad (4.70)$$

*It should be noted that this is much harder when setting τ_{FT} to a large, but finite number – as η_{CD} still needs to be solved self-consistently.

1909 Taking these into consideration results in the following current formula:

$$I_P^\dagger = K_{BS} \bar{T} + \left(\frac{K_{CS} R_0^3}{K_{LP} R_0^2 + K_{RP} \tau_{FT} \bar{T}^{-3/2}} \cdot \frac{(1 - \epsilon_b) \cdot \sqrt{2(K_{EK} + \epsilon_b)}}{1 + K_{DR}} \right) \quad (4.85)$$

1910 In the limit that the pulse length drops to zero (and bootstrap current is negligible),

$$\lim_{\tau_{FT} \rightarrow 0} I_P^\dagger = R_0 \cdot \left(\frac{K_{CS}}{K_{LP}} \cdot \frac{(1 - \epsilon_b) \cdot \sqrt{2(K_{EK} + \epsilon_b)}}{1 + K_{DR}} \right) \quad (4.86)$$

1911 This implies that a purely pulsed current scales with major radius to leading order.

1912 4.5.3 Rationalizing the Generalized Current

1913 From the previous two subsections, we arrived at equations for infinitely large and
1914 infinitely small pulse lengths:

$$\lim_{\tau_{FT} \rightarrow \infty} I_P = \frac{K_{BS} \bar{T}}{1 - K_{CD}(\sigma v)} \quad (4.80)$$

1915

$$\lim_{\tau_{FT} \rightarrow 0} I_P^\dagger = R_0 \cdot \left(\frac{K_{CS}}{K_{LP}} \cdot \frac{(1 - \epsilon_b) \cdot \sqrt{2(K_{EK} + \epsilon_b)}}{1 + K_{DR}} \right) \quad (4.86)$$

1916 What these imply at an intuitive level is that at small pulses, current scales with the
1917 major radius. While for long pulses, current sales with plasma temperature. In the
1918 general case, of course, the problem becomes much harder to predict.

Chapter 5

Completing the Systems Model

As opposed to previous chapters, this one will focus on the numerics behind the fusion systems model. A simple algebra will lead to a generalized solver for exploring reactor space for low cost and interesting machines. This will then naturally segue into a discussion of how plots are made and should be interpreted. The remaining chapters will then decouple the presentation of results from their analytic conclusions.

5.1 Describing a Simple Algebra

In essence, ~~Boiled-down~~, the systems model used here is a simple algebra problem – given five equations, solve for five unknowns. The goal is then to pick the five equations that best represent modern fusion reactor design. This selection should also be done in such a way that actually reduces the system of equations to a simple univariate root solving equation (i.e. one equation with one unknown). As will be shown in the results, this model does ~~reasonably~~ ~~remarkably~~ well: matching year-long modeling campaigns in seconds.

The logical place to start in a discussion of this algebra problem is with the three equations fundamental to all reactor-grade tokamaks – both in steady-state and pulsed operation. These are: the Greenwald density limit, power balance, and current bal-

1937 ance. The Greenwald density's importance was hinted early on when it was used to
1938 simplify every equation derived thereafter.

$$\bar{n} = K_n \cdot \frac{I_P}{R_0^2} \quad (2.11)$$

1939 The two balance equations ~~proved to be~~proved slightly more complicated.~~dubious.~~ As
1940 was ~~shown, shown previously,~~ current balance ~~— the stability requirement for tokamaks~~
1941 ~~— was the more difficult of the two — bringing most peculiar. It brought~~ forth the notion
1942 of self-consistency for steady-state machines and a highly-coupled multi-root equation
1943 for pulsed ones. As such, ~~current balance this equation~~ stands as the ~~equation one~~
1944 everything ~~is substituted else will be substituted~~ into to ~~do a final setup for a~~ univariate
1945 root solve.

$$I_P = \frac{(K_{BS} + G_{IV}/G_{IP}) \cdot \bar{T}}{1 - K_{CD}(\sigma v) - G_{ID}/G_{IP}} \quad (4.75)$$

1946 Although slightly buried in Eq. (4.75), the right-hand side actually depends on all the
1947 quantities (including I_P through the ~~wall loading term in~~ blanket thickness). Through
1948 equation,

$$I_P = f(I_P, \bar{T}, R_0, B_0) \quad (5.1)$$

1949 The remaining equation common to all reactor-grade tokamaks is power balance —
1950 the relation that ~~quantifies its net electricity production capabilities. separates power~~
1951 ~~plants from toasters.~~ Due to the use of the ELMy H-Mode scaling law for modeling
1952 the diffusion coefficient, this had the complicated form of:

$$R_0^{\alpha_R} \cdot B_0^{\alpha_B} \cdot I_P^{\alpha_I} = \frac{G_{PB}}{K_{PB}} \quad (5.2)$$

1953 Although being rather cumbersome, this equation actually remains relatively simple
1954 in that all three quantities on the left-hand side are separable. To close the system,
1955 two more equations of this form are needed. These have the following form and will
1956 be described next.

$$R_0^{\gamma_R} \cdot B_0^{\gamma_B} \cdot I_P^{\gamma_I} = G(\bar{T}) \quad (5.3)$$

5.2 Generalizing Previous Equations

Where the equations defined up to this point in the chapter are shared among all fusion reactors, the remaining two equations – needed to close the system – must be **partially** chosen by the user. These **user-supplied** equations come in three **varieties:flavors:** limits, **intermediatederived** quantities, and **dynamicfloating** variables. By convention, we enforce that at least one limit must be used. The other constraint can then come from any of the three defined collections, which we will refer to as the closure equation.

Table 5.1: Main Equation Bank

To close the system of equations for potential reactors, different equations can be used to lock down tokamak designs. These include physics and engineering limits (L), as well as ways to set **dynamic (D)floating-(F)** or **intermediate (I)derived-(D)** variables to constant values.

Variable	Category	$G(\bar{T})$	γ_R	γ_B	γ_I
Power Balance	-	G_{PB}/K_{PB}	α_R^*	α_B	α_I^*
Beta (β_N)	L	$K_{TB}\bar{T}$	1	1	0
Kink (q_{*95})	L	K_{KF}	1	1	-1
Wall Loading (P_W)	L	$K_{WL}(\sigma v)^{1/3}$	1	0	$-2/3$
Power Cap (P_E)	L	$K_{PC}(\sigma v)$	1	0	-2
Heat Loading (q_{DV})	L	$K_{DV}(\sigma v)^{1/3.2}$	1	0	-1
Major Radius (R_0)	D	$(R_0)_{const}$	1	0	0
Magnet Strength (B_0)	D	$(B_0)_{const}$	0	1	0
Plasma Current (I_P)	D	$(I_P)_{const}$	0	0	1
Plasma Temperature (\bar{T})	D	$(\bar{T})_{const}/\bar{T}$	0	0	0
Electron Density (\bar{n})	D	$(\bar{n})_{const}/K_n$	-2	0	1
Plasma Pressure (\bar{p})	I	$(\bar{p})_{const}/K_n K_{nT} \bar{T}$	-2	0	1
Bootstrap Current (f_{BS})	I	$(f_{BS})_{const}/K_{BS} \bar{T}$	0	0	-1
Fusion Power (P_F)	I	$(P_F)_{const}/K_F K_n^2(\sigma v)$	-1	0	2
Magnetic Energy (W_M)	I	$(W_M)_{const}/K_{WM}$	3	2	0
Cost per Watt (C_W)	I	$(C_W)_{const} \cdot (K_F K_n^2(\sigma v)/K_{WM})$	4	2	-2

1964 5.2.1 Including Limiting Constraints~~Rehashing the Limits~~

1965 The limits category is composed of the limiting constraints given in Chapter 3.~~simply~~
1966 ~~a rebranding of the secondary constraints given previously.~~ These include the physics
1967 derived limits from MHD theory – i.e. the beta limit (β_N) and the kink safety
1968 factor (q_{*95}) – which for clarity, set maximums on the allowed plasma pressure and
1969 ~~current, velocity,~~ respectively. Additionally, there were several engineering limits also
1970 described: wall loading, heat loading, and maximum power capacity. For this paper,
1971 wall loading from neutrons (P_W) is assumed to be important, whereas the other two
1972 engineering limits are not allowed to explicitly guide designs.

1973 Combined all these limits, as well as the yet to be defined ~~dynamic float~~ and ~~intermediatederived~~
1974 equations, are given in Table 5.1. These share a remarkably similar form to power
1975 balance when put into a generalized, separable state. This hints at why the major
1976 radius (R_0), the toroidal field strength (B_0), and the plasma current (I_P) can easily
1977 be separated and substituted out of the current balance equation.

1978 Before moving on, it proves useful to explain the two limits not used to explicitly guide
1979 reactor design – divertor heat loading and the maximum power capacity. The simpler
1980 of the two to reason is the heat loading limit. Although removing the gigawatts-~~per-~~
1981 ~~square-meter~~ of heat is extremely difficult, it remains an unsolved problem worthy of
1982 its own research ~~machine.~~⁸ ~~machine, but currently neglected financially.~~ As such, it is
1983 only kept to provide a human-interpreted measure of difficulty. The power cap, on the
1984 other hand, is just handled informally. If a reactor surpasses it (i.e. $P_E > 4000MW$),
1985 it is considered invalid.

1986 While the maximum power cap informally sets a maximum major radius for a ma-
1987 chine, there also exists an implicit minimum major radius. This minimum occurs due
1988 to the hole-size constraint – i.e. at some point there is no longer enough room on the
1989 inside of the machine to store the central solenoid, blanket, and TF coils.

1990 At this point, we can now explain how various quantities in the systems model
1991 can be set to user-given constant values. This basically allows users to treat one

dynamicfloating variable as a staticfixed one (e.g. the temperature and bootstrap fraction).

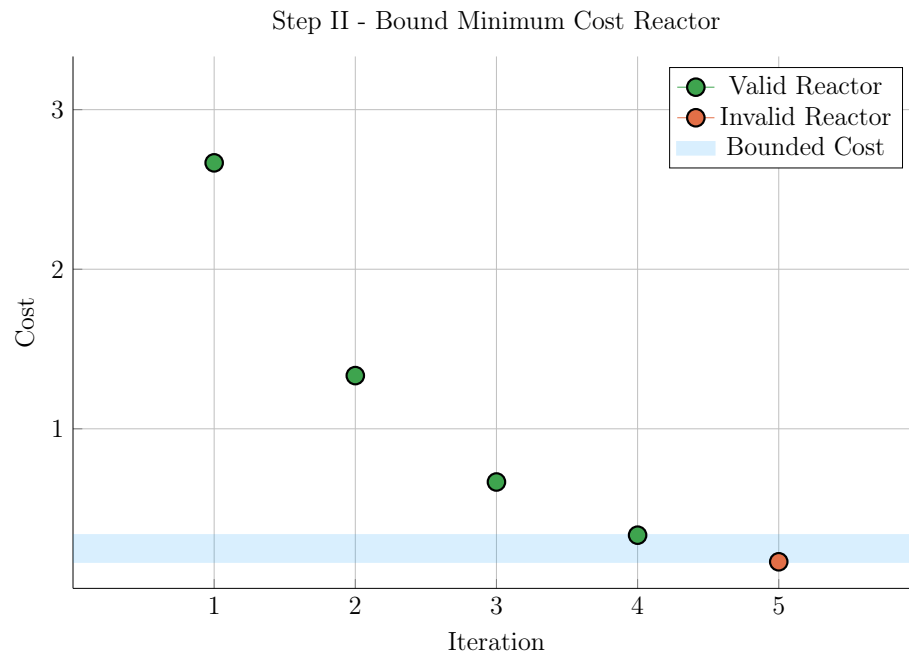
5.2.2 Minimizing IntermediateDerived Quantities

Whereas the limits from the previous section represented constraints with real physics and engineering repercussions, the intermediatederived quantities here are just used to find when reactors reach certain user-supplied values. Most notable are the capital cost (through the magnetic energy – W_M) and the cost-per-watt (C_W). The model also, however, allows easily setting values for the bootstrap fraction, plasma pressure, and fusion power. As mentioned previously, they are given in Table 5.1 through a generalized representation of the form:

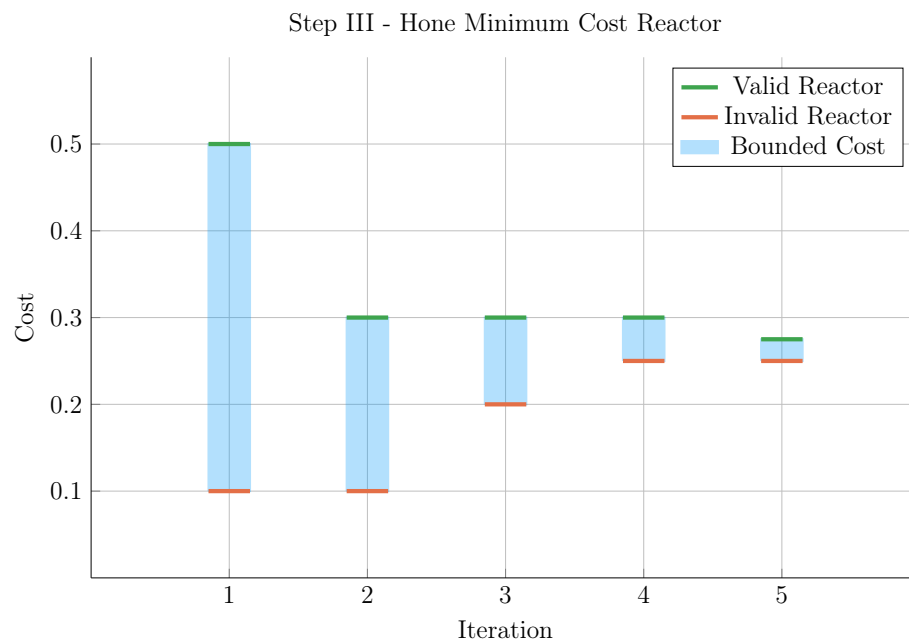
$$R_0^{\gamma_R} \cdot B_0^{\gamma_B} \cdot I_P^{\gamma_I} = G(\bar{T}) \quad (5.3)$$

What this collection of variables is really useful for, though, is finding minimum cost reactors – both in a capital context as well as a cost-per-watt one. ~~ThisWithout boring the reader, this~~ is done in a three stage process. ~~The first of which is to find a valid reactor – i.e. one that satisfies every limiting constraint. Practically, this is done by searching over a range of scanned temperatures. First, some valid reactor is found: it does not matter if it is good, just valid. This of course can be found by systematically throwing darts at a dart board—see ??.~~

After a valid reactor is found, its cost is recorded leading to a drill-down stage. In this step, the cost is continuously halved until a valid reactor cannot be found. Once this invalid reactor is reached, it sets a bound on the minimum cost reactor. As such, the final stage is a simple bisection step where the minimum cost is honed down to some acceptable margin of error – see Fig. 5-1.



(a) Minimize Step II



(b) Minimize Step III

Figure 5-1: Minimize Cost Step II/III – Optimize Reactor

2014 5.2.3 Pinning ~~DynamicFloating~~ Variables

2015 The remaining collection of closure equations is for the five ~~dynamicfloating~~ variables
2016 in the systems model: R_0 , B_0 , \bar{n} , \bar{T} , and I_P . As we are making equations of the
2017 following form, the formulas for R_0 , B_0 , and I_P are trivial.

$$R_0^{\gamma_R} \cdot B_0^{\gamma_B} \cdot I_P^{\gamma_I} = G(\bar{T}) \quad (5.3)$$

2018 Next, the equation for \bar{n} – shown in Table 5.1 – is just a simple undoing of the Green-
2019 wald density limit. The remaining equation is then from the original temperature
2020 equation:

$$\bar{T} = \text{const.} \quad (3.1)$$

2021 As was assumed earlier, this is sort of a default equation for the systems model. By
2022 this, we mean reactor curves can be created by scanning over temperatures, i.e. set
2023 $\bar{T} = 5$ keV in one run, 10 in the next, etc. This temperature equation also brings up
2024 a ~~difficulty for the algebraic solver, as it does not depend on: subtlety of the model, as~~
2025 ~~it does not depend on~~ current, radius, or magnet strength. ~~Overcoming this difficulty~~
2026 ~~is discussed next subsection.~~

2027 5.2.4 Detailing the Equation Solver

2028 The algorithm that motivated this generalized equation approach most notably bi-
2029 furcates in the situation where the closure equation does not depend on R_0 , B_0 , or I_P
2030 (i.e. ~~for~~ the temperature equation). The two scenarios are given in Eqs. (5.4) to (5.10)
2031 – where at least R_0 and B_0 are substituted out of the system. In the temperature
2032 case, I_P is not needed to be explicitly removed.

2033 Concretely, the root solve for the temperature scenario is for the current, whereas it
2034 is for the temperature in all other cases. The nomenclature in the code is a *match*
2035 for Scenario I (i.e. root solving for plasma temperature), and a *solve* for Scenario II
2036 (i.e. root solving for plasma current).

2037 Scenario I – Match for \bar{T}

$$R_0(\bar{T}) = \left(G_1^{(\gamma_{B,2} \gamma_{I,3} - \gamma_{B,3} \gamma_{I,2})} \cdot G_2^{(\gamma_{B,3} \gamma_{I,1} - \gamma_{B,1} \gamma_{I,3})} \cdot G_3^{(\gamma_{B,1} \gamma_{I,2} - \gamma_{B,2} \gamma_{I,1})} \right)^{\frac{1}{\gamma_{RBI}}} \quad (5.4)$$

$$B_0(\bar{T}) = \left(G_1^{(\gamma_{I,2} \gamma_{R,3} - \gamma_{I,3} \gamma_{R,2})} \cdot G_2^{(\gamma_{I,3} \gamma_{R,1} - \gamma_{I,1} \gamma_{R,3})} \cdot G_3^{(\gamma_{I,1} \gamma_{R,2} - \gamma_{I,2} \gamma_{R,1})} \right)^{\frac{1}{\gamma_{RBI}}} \quad (5.5)$$

$$I_P(\bar{T}) = \left(G_1^{(\gamma_{R,2} \gamma_{B,3} - \gamma_{R,3} \gamma_{B,2})} \cdot G_2^{(\gamma_{R,3} \gamma_{B,1} - \gamma_{R,1} \gamma_{B,3})} \cdot G_3^{(\gamma_{R,1} \gamma_{B,2} - \gamma_{R,2} \gamma_{B,1})} \right)^{\frac{1}{\gamma_{RBI}}} \quad (5.6)$$

$$\begin{aligned} \gamma_{RBI} = & (\gamma_{R,1} \gamma_{B,2} \gamma_{I,3} + \gamma_{R,2} \gamma_{B,3} \gamma_{I,1} + \gamma_{R,3} \gamma_{B,1} \gamma_{I,2}) - \\ & (\gamma_{R,1} \gamma_{B,3} \gamma_{I,2} + \gamma_{R,2} \gamma_{B,1} \gamma_{I,3} + \gamma_{R,3} \gamma_{B,2} \gamma_{I,1}) \end{aligned} \quad (5.7)$$

2040 Scenario II – Solve for I_P

$$R_0(\bar{T}) = \left(G_1^{\gamma_{B,2}} \cdot G_2^{-\gamma_{B,1}} \cdot I_P^{(\gamma_{B,1} \gamma_{I,2} - \gamma_{B,2} \gamma_{I,1})} \right)^{\frac{1}{\gamma_{RBT}}} \quad (5.8)$$

$$B_0(\bar{T}) = \left(G_1^{-\gamma_{R,2}} \cdot G_2^{\gamma_{R,1}} \cdot I_P^{(\gamma_{I,1} \gamma_{R,2} - \gamma_{I,2} \gamma_{R,1})} \right)^{\frac{1}{\gamma_{RBT}}} \quad (5.9)$$

$$\gamma_{RBT} = \gamma_{R,1} \gamma_{B,2} - \gamma_{R,2} \gamma_{B,1} \quad (5.10)$$

2043 5.3 Wrapping up the Logic

2044 As stated at the beginning of the chapter, this systems model basically ~~reducesboils~~
 2045 ~~down~~ to a simple 5 equation/5 unknown algebra problem. The Greenwald density was
 2046 implicitly used in the initial derive to simplify the logic. The current balance was then
 2047 delegated to be the root solve equation. Lastly, three equations were needed to remove
 2048 the major radius and magnet strength, as well as either the current or temperature.
 2049 These 16 equations were given in Table 5.1 with the generalized solution given in
 2050 Eqs. (5.4) to (5.10).

2051 This now sets the stage for the most interesting part of the document – the results.
 2052 ~~TheseIn true Dickens fashion, they~~ will come in several forms. The first result type
 2053 ~~we will encounter~~ will be temperature ~~scans thatscans. These~~ allow us to validate the

2054 model ~~against other~~~~by comparing it to several~~ designs from the literature. These are
 2055 ~~created using~~~~These will use~~ the Scenario II solver.

2056 ~~The~~~~Moving onto examples of the~~ Scenario I matcher ~~will then be used to create~~~~are~~
 2057 sensitivity studies and Monte Carlo samplings. The simple one variable sensitivities
 2058 will reveal local trends from sweeping various ~~static~~~~fixed~~ (i.e. input) variables –
 2059 namely H , κ , B_{CS} , etc. – ~~one at a time~~. Whereas the samplings will highlight global
 2060 trends as many ~~static~~~~fixed~~/input variables are allowed to vary simultaneously.

2061 These Scenario I ~~matchers~~~~flavors~~ are further subdivided in regards to the nature of
 2062 their closure equation. The first ~~type~~~~flavor~~ comes from finding so called two limit
 2063 solutions, which live at the point where the beta and kink (or wall) limits are just
 2064 marginally satisfied. The second main type is then minimum cost reactors – measured
 2065 in either a capital cost or cost-per-watt context. These will be used in depth next
 2066 chapter.

2067 Chapter 6

2068 Presenting the Code Results

2069 Now that our fusion systems model has been formulated and completed, the next
2070 logical step is to code it up and run it to produce interesting data. To this, the code
2071 for this document – Fussy.jl – is available at git.io/tokamak (with a short guide given
2072 in the Appendix). The results will be given shortly.

2073 Before accosting the reader with some twenty plots and tables, though, it makes sense
2074 to first warn them what they are getting into. This chapter has three sections. The
2075 first is an attempt to test how good the model is by comparing it with other codes
2076 in the field.^{7,9,26} Next, we will develop two prototype reactors that pit steady-state
2077 against pulsed operation on a levelized playing field.

2078 This chapter will then conclude with a discussion on how best to lower the costs
2079 of a tokamak reactor. In line with the MIT mission, this will highlight how using
2080 stronger magnets leads to more compact, efficient machines. The new piece of insight,
2081 then, is how to optimally incorporate high-temperature superconducting (HTS) tape
2082 technology – the miracle found in the ARC design family.

2083 Without spoiling too much for the reader, we will show that HTS tape should be used
2084 in the TF coils for steady-state tokamaks (i.e. B_0), whereas it should only be appear
2085 in the central solenoid (i.e. B_{CS}) for pulsed ones. This is a fundamentally new result!

2086 6.1 Validating Code with other Models

2087 When you develop a new model, the first thing you have to do is check that it makes
2088 sensical results. The goal is not to go overboard, though, by: comparing it with
2089 too many models or requiring perfect matches with all their results. To this, we
2090 will compare Fussy.jl with five designs coming from three separate research teams
2091 – hopefully casting a wide enough net through reactor-space to prove sufficient. It
2092 should be noted that for how simple this model is, it does a remarkable job matching
2093 these more sophisticated frameworks. It also highlights how discrepancies arise in
2094 this highly non-linear computational problem.

2095 The first reactor design that will provide a basis for comparison is the ARC reactor.
2096 As it was also designed by MIT researchers, the fit is shown to be almost exact. This
2097 of course probably involves a fair amount of inherent biases stemming from how this
2098 ecosystem operates and produces engineers – most notably as the core of this code
2099 comes from Jeff’s ongoing interest in the problem.

2100 The next set of reactor designs come from the ARIES four-act study. This ARIES
2101 team is a United States effort to reevaluate the problem of designing a fusion reac-
2102 tor around once a decade. The most recent study focused on how tokamaks shape
2103 up as you assume optimistic and conservative physics and engineering parameters.
2104 Although our model recovers their results, it does highlight one peculiarity of their
2105 algorithm – reliance on the minimum achievable value of H .

2106 The final series of reactors comes from the major codebase used among European
2107 fusion systems experts: PROCESS. As such, this group actually gives an example for
2108 pulsed vs. steady-state tokamaks. Although these designs have the most discrepancies
2109 with our model, discussion will be given that remedy some of the shortcomings. These
2110 basically boil down to: alternative definitions for heat loss appearing in the ELMy
2111 H-Mode Scaling, as well as the simplified nature of our flux balance equation – which
2112 only accounts for central solenoid and PF coil source terms.

2113 6.1.1 Comparing with the PSFC Arc Reactor

2114 As mentioned, this model matches the results from the ARC design almost perfectly.
 2115 This probably stems from how both models were developed within the MIT commu-
 2116 nity. The points to make now, though, is even with how well the results match, there
 2117 are two notable discrepancies: the fusion power (P_F) and bootstrap current fraction
 2118 (f_{BS}). These mainly arise from the use of simple parabolic profiles for temperature.

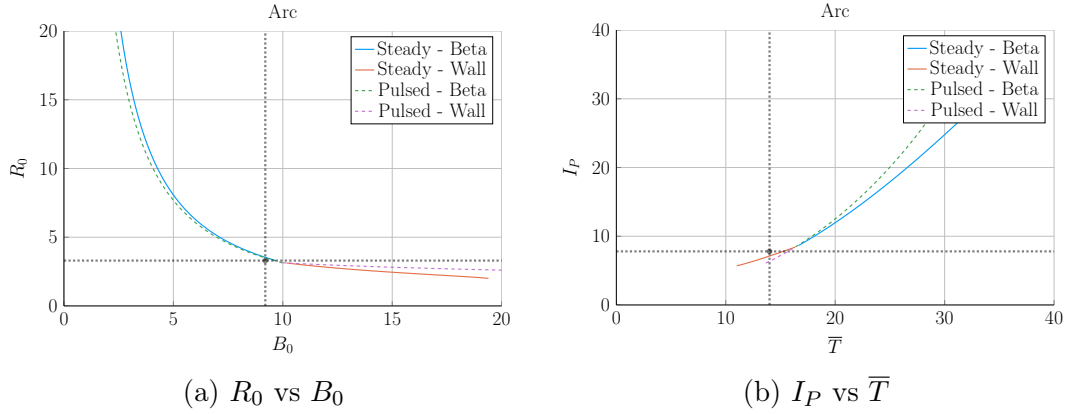


Figure 6-1: Arc Model Comparison

Table 6.1: Arc Variables

(a) Input Variables

Input	Value
H	1.8
Q	13.6
N_G	0.67
ϵ	0.333
κ_{95}	1.84
δ_{95}	0.333
ν_n	0.385
ν_T	0.929
l_i	0.67
A	2.5
Z_{eff}	1.2
f_D	0.9
τ_{FT}	1.6e9
B_{CS}	12.77

(b) Output Variables

Output	Original	Fussy.jl
R_0	3.3	3.4
B_0	9.2	9.5
I_P	7.8	8.8
\bar{n}	1.3	1.3
\bar{T}	14.0	16.8
β_N	0.026	-
q_{95}	7.2	6.1
P_W	2.5	2.2
f_{BS}	0.63	0.56
f_{CD}	0.37	0.44
f_{ID}	-	-
V	141	157
P_F	525	726
η_{CD}	0.321	0.316

2119 6.1.2 Contrasting with the Aries Act Studies

2120 Moving on, the Aries Act study focuses on how steady-state reactors would look under
 2121 both a conservative and optimistic perspective. This is highlighted in Fig. 6-2, which
 2122 shows how costs decrease as the H factor is allowed to increase. Notice that for every
 2123 value of H, the ACT I study (i.e. the optimistic act) has a lower cost than the design
 2124 from ACT II (i.e. the conservative one).

2125 This figure also highlights another peculiarity of the ARIES study – a reliance on the
 2126 minimum possible value of H. Note that just left of the reactor point on both plots
 2127 is a highly erratic portion of the curve. As such, if even a slightly smaller value of H
 2128 were used in either case, a quite distinct reactor would occur. This is not a robust
 2129 way to design machines. A better approach would be to build with some safety factor
 2130 – i.e. at a slightly more magical version of H. This can be seen in ARC’s H-Sweep.

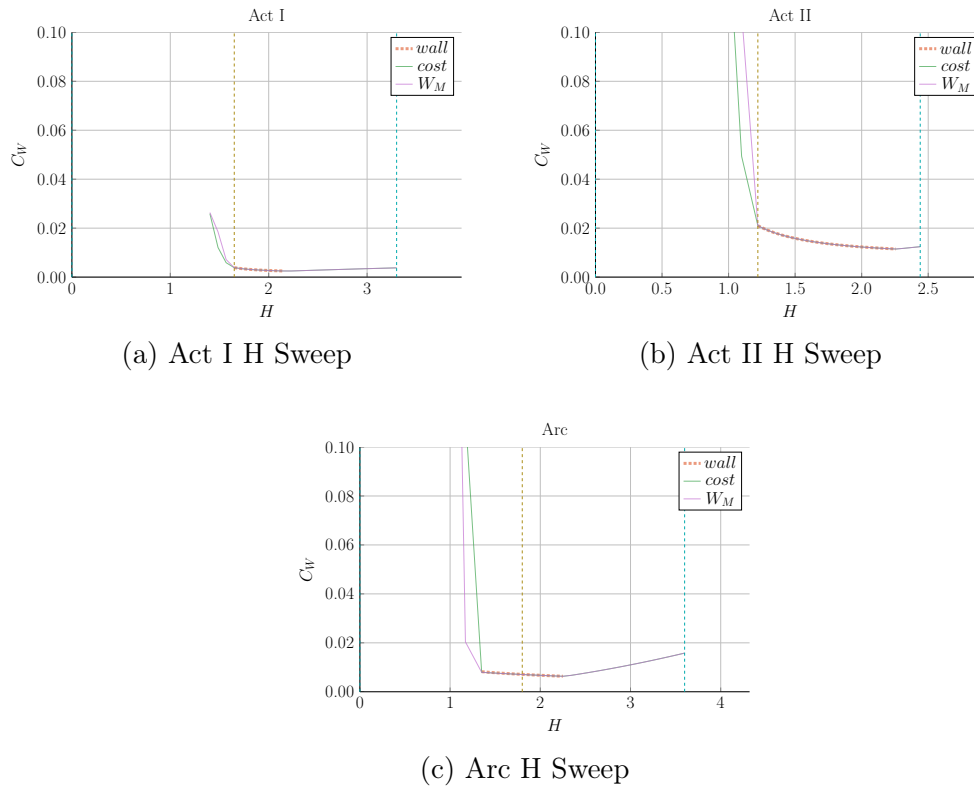


Figure 6-2: Act Studies Cost Dependence on the H Factor

2131 Act I – Advanced Physics and Engineering

2132 Act 1 is the ARIES study that assumes advanced physics and engineering design
 2133 parameters. Although this paper’s model does a good job matching the results from
 2134 their paper, it does show what optimistic design really means. As can be seen, this
 2135 design actually only surpasses the minimum possible toroidal field strength by as less
 2136 than a Tesla! Practically, this means the reactor is barely realizable.

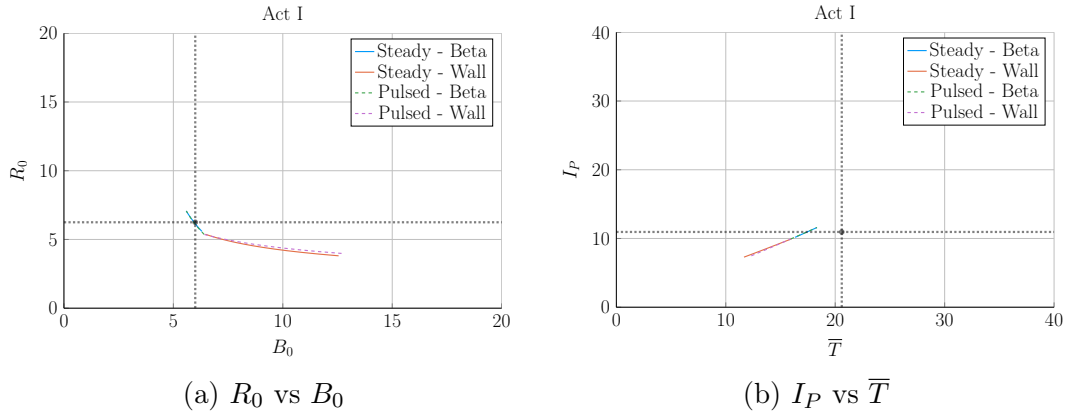


Figure 6-3: Aries Act I Model Comparison

Table 6.2: Act I Variables

(a) Input Variables

Input	Value
H	1.65
Q	42.5
N_G	1.0
ϵ	0.25
κ_{95}	2.1
δ_{95}	0.4
ν_n	0.27
ν_T	1.15
l_i	0.359
A	2.5
Z_{eff}	2.11
f_D	0.75
τ_{FT}	1.6e9
B_{CS}	12.77

(b) Output Variables

Output	Original	Fussy.jl
R_0	6.25	6.23
B_0	6.0	6.0
I_P	10.95	10.78
\bar{n}	1.3	1.3
\bar{T}	20.6	17.2
β_N	0.0427	-
q_{95}	4.5	4.0
P_W	2.45	2.00
f_{BS}	0.91	0.91
f_{CD}	0.09	0.09
f_{ID}	-	-
V	582.0	621.4
P_F	1813	1865
η_{CD}	0.188	0.185

2137 Act II – Conservative Physics and Engineering

2138 ARIES more conservative design – Act II – is much more like ARC in nature. From
 2139 the plots, it is obvious the paper’s model is basically right on top of the reactor curve
 2140 made using Fussy.jl. Much like ARC, too, it shows how the model overestimates fusion
 2141 power and underestimates bootstrap fraction due to their selection of a pedestal profile
 2142 for plasma temperature.

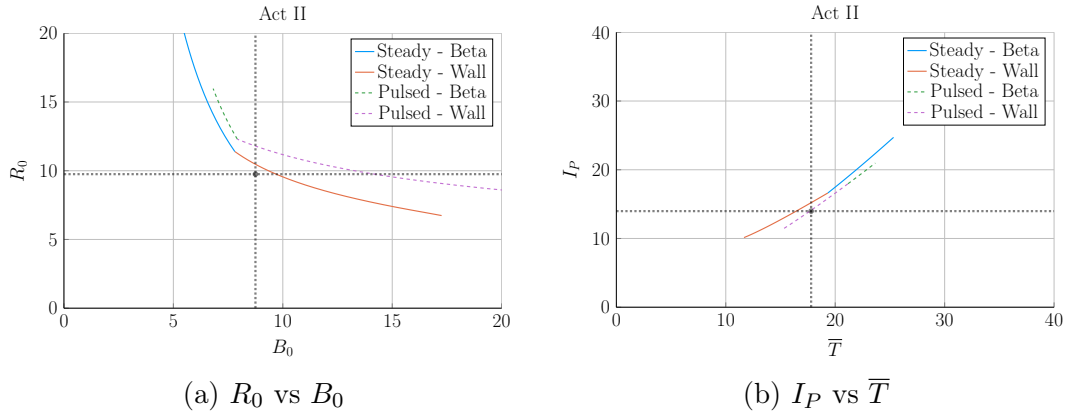


Figure 6-4: Aries Act II Model Comparison

Table 6.3: Act II Variables

(a) Input Variables

Input	Value
H	1.22
Q	25.0
N_G	1.3
ϵ	0.25
κ_{95}	1.964
δ_{95}	0.42
ν_n	0.41
ν_T	1.15
l_i	0.60275
A	2.5
Z_{eff}	2.12
f_D	0.74
τ_{FT}	1.6e9
B_{CS}	12.77

(b) Output Variables

Output	Original	Fussy.jl
R_0	9.75	10.22
B_0	8.75	9.05
I_P	13.98	14.84
\bar{n}	0.86	0.82
\bar{T}	17.8	17.4
β_N	0.026	0.023
q_{95}	8.0	6.6
P_W	1.46	-
f_{BS}	0.77	0.66
f_{CD}	0.23	0.34
f_{ID}	-	-
V	2209	2559
P_F	2637	3460
η_{CD}	0.256	0.307

2143 6.1.3 Benchmarking with the Process DEMO Designs

2144 The PROCESS team’s prospective designs for successors to ITER constitute the final
2145 set of model comparisons: the steady-state and pulsed DEMO reactors. As this paper
2146 is designed to compare these modes of operation, this study proves most fruitful. It
2147 also highlights how common model decisions can dramatically alter what reactors
2148 come out of the solvers.

2149 The first discrepancy is how the PROCESS team defines the loss term in the ELMy H-
2150 Mode scaling law. As shown in their paper, they actually subtract out a Bremsstrahlung
2151 component, while leaving the fitting coefficients the same.⁷ After modifying Fussy.jl
2152 to incorporate this definition, the steady-state reactor is easily reproducible in $R_0 -$
2153 B_0 slice of reactor space.

2154 Unlike the steady-state case, however, the modified power loss term does not fix the
2155 pulsed case, as it actually draws the reactor curves further from the design in their
2156 paper. As such, it is flux balance that is now the main culprit for discrepancies
2157 between the two models. This makes sense, as this model uses highly simplified
2158 source terms – namely neglecting anything but the central solenoid and PF coils (as
2159 well as ignoring crucial physics for these two components). Even acknowledging the
2160 differences between the two models, Fussy.jl still does remarkably well at reproducing
2161 their much more sophisticated coding framework.

2162 The final point to make is about selecting optimum points to build as the ~~dynamic~~floating
2163 variables are allowed to make curves through reactor space. Up to this point, only
2164 steady-state tokamak designs have been explored. In every single one of these, though,
2165 the paper values have been very close to the point where the beta curves and wall
2166 loading curves cross. This is because they all result in the minimum cost-per-watt.

2167 For pulsed designs, on the other hand, kink curves start to appear for low magnetic
2168 field strengths. Just as beta-wall intersections were optimum places to design for low
2169 cost-per-watt (C_W) reactors, these beta-kink intersections will prove to be the place
2170 where minimum capital cost (W_M) reactors usually occur.

2171 DEMO Steady – A Steady-State ITER Successor

2172 Hands down, this DEMO Steady reactor is the worst modeled reactor using Fussy.jl.
 2173 As mentioned previously, though, some of the discrepancy was removed by using the
 2174 PROCESS team’s modified version of heat loss. This heavily corrected the $R_0 - B_0$
 2175 curve, but had no effect on the $I_P - \bar{T}$ one. An interesting aside is that these curves
 2176 actually show how steady current is independent of ~~limitingsecondary~~ constraint (as
 2177 noted).

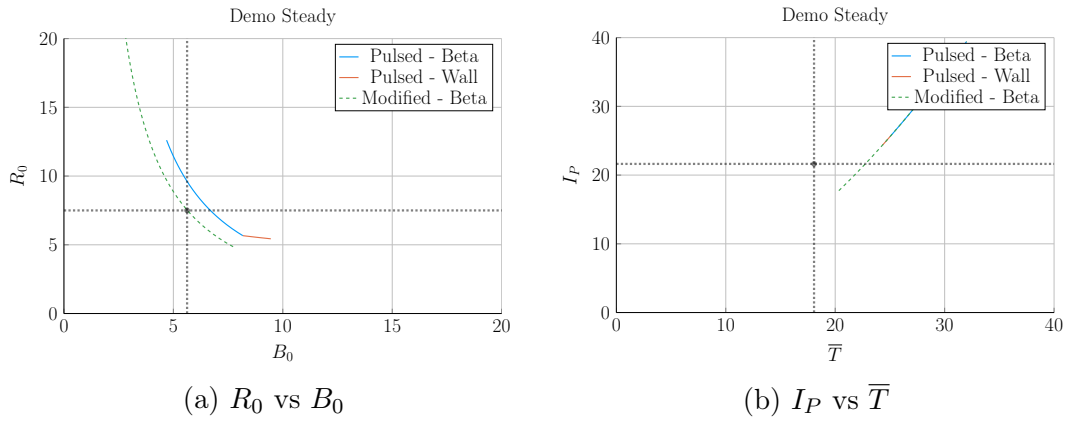


Figure 6-5: Demo Steady Model Comparison

Table 6.4: Demo Steady Variables

(a) Input Variables

Input	Value
H	1.4
Q	24.46
N_G	1.2
ϵ	0.385
κ_{95}	1.8
δ_{95}	0.333
ν_n	0.3972
ν_T	0.9187
l_i	0.9
A	2.856
Z_{eff}	4.708
f_D	0.7366
τ_{FT}	1.6e9
B_{CS}	12.85

(b) Output Variables

Output	Original	Fussy.jl
R_0	7.5	8.2
B_0	5.627	6.307
I_P	21.63	30.93
\bar{n}	0.8746	1.048
\bar{T}	18.07	27.83
β_N	0.038	-
q_{95}	4.405	3.761
P_W	1.911	4.151
f_{BS}	0.611	0.424
f_{CD}	0.389	0.576
f_{ID}	-	-
V	2217	2879
P_F	3255	8971
η_{CD}	0.4152	-

2178 DEMO Pulsed – A Pulsed ITER Successor

2179 This pulsed version of DEMO is the only reactor in our collection that is not run
 2180 in steady-state. As such, it may be the most important one. The first thing that is
 2181 abundantly clear is that this design actually has no valid wall loading portion – only a
 2182 kink and beta curve exist! Even so, the results match pretty well. It should be noted,
 2183 though, that this current drive is treated as an input and not solved self-consistently.

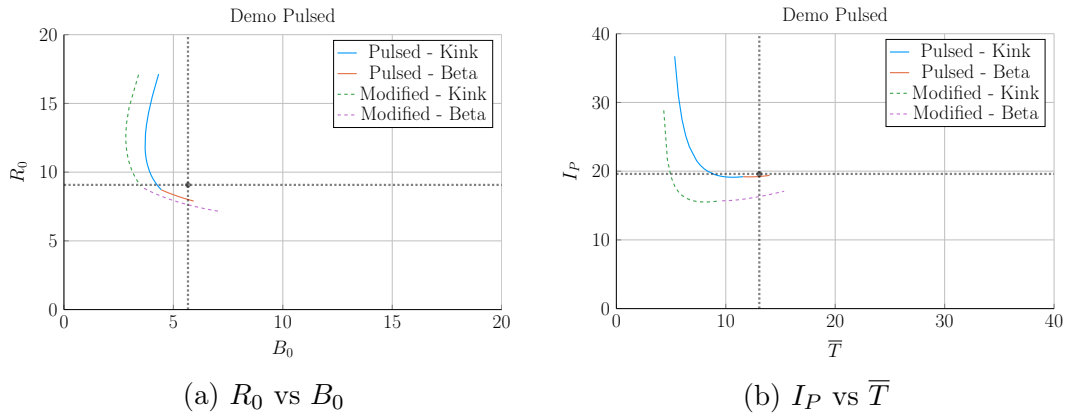


Figure 6-6: Demo Pulsed Model Comparison

Table 6.5: Demo Pulsed Variables

(a) Input Variables		(b) Output Variables		
Input	Value	Output	Original	Fussy.jl
H	1.1	R_0	9.07	8.10
Q	39.86	B_0	5.67	5.48
N_G	1.2	I_P	19.6	19.3
ϵ	0.3226	\bar{n}	0.7983	0.9795
κ_{95}	1.59	\bar{T}	13.06	13.28
δ_{95}	0.333	β_N	0.0259	-
ν_n	0.27	q_{95}	3.247	2.853
ν_T	1.094	P_W	1.05	1.47
l_i	1.155	f_{BS}	0.348	0.164
A	2.735	f_{CD}	0.096	0.106
Z_{eff}	2.584	f_{ID}	0.557	0.730
f_D	0.7753	V	2502	1751
τ_{FT}	7273	P_F	2037	2376
B_{CS}	12.77	η_{CD}	0.2721	-

6.2 Developing Prototype Reactors

Now that the model used in Fussy.jl has been tested against other fusion systems codes in the field, we will develop our own prototype reactors. Because this paper is about making a levelized comparison of pulsed and steady-state tokamaks, we will develop middle-of-the-road reactors that only differ by operating mode.

The steady-state prototype, Charybdis, is the obvious choice to start with – as the model was tested against four of these typed reactors. It was also pointed out that the model did remarkably well when recreating ARC. As the authors share many of the ARC team’s philosophies, Charybdis uses ~~static~~~~fixed~~ parameters very similar to them.

Next, although led to believe Charybdis’ pulsed twin reactor – Proteus – would be created by a simple flip of the switch, it was a slight oversimplification. The first difference is that the pulsed twin, Proteus, is assumed to be purely pulsed: $\eta_{CD} = 0$. Further, the bootstrap current is much less important than it was for steady-state tokamaks. This corresponds to a current profile peaked at the origin – i.e. a parabola.

2199 Numerically, this is done by raising l_i from around 5.5 to 6.

2200 The final difference creates the largest change in the twin reactors: the choice of
 2201 miracle. As hinted several times before, the H factor is a common way designers
 2202 artificially boost the confinement of their machines. This H value will thus be the
 2203 miracle for Charybdis, the steady-state prototype. Next, as the main conclusion of
 2204 this paper is to state the advantages of high magnetic field, a free way to boost a
 2205 central solenoid – through B_{CS} – will be employed using HTS coils.

2206 Opposite the order of how they were designed, the goal now is to lock down a value
 2207 of B_{CS} for Proteus and then use it to set the H factor for Charybdis. This selection
 2208 algorithm is depicted in Fig. 6-7. For Proteus, the point locked down was $B_{CS} = 20$ T,
 2209 which occurred at a fusion power (P_F) of around 1250 MW. As shown in the cost
 2210 curve, this was at a point where the ratio between the minimum capital cost and
 2211 the minimum cost-per-watt saturated. This choice of a 1250 MW reactor then led to
 2212 Charybdis having an H factor of 1.7.

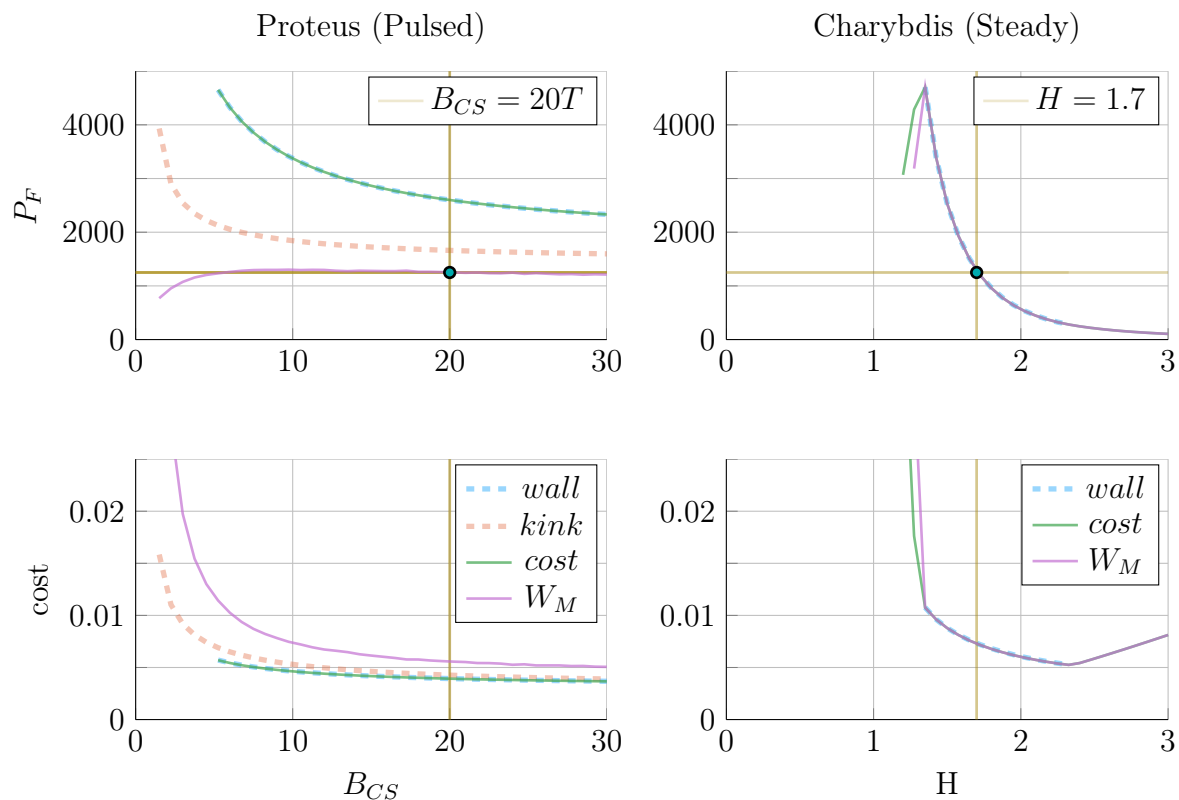


Figure 6-7: How to Build a Fusion Reactor

As is convention in fusion engineering, a good design only relies on one miracle. For steady-state reactors, we assume we can get better confinement – by increasing H . While in the pulsed case, the miracle is assuming strong magnets for the central solenoid – B_{CS} .

6.2.1 Navigating around Charybdis

The Charybdis reactor is the steady-state twin developed for this paper. As mentioned, its parameters are similar to the ARC design. This is shown in Fig. 6-8, where the two $R_0 - B_0$ curves are almost interchangeable. Before moving on, it proves useful to note that the optimum place to build on these curves is where the two portions intersect – as it minimizes costs.

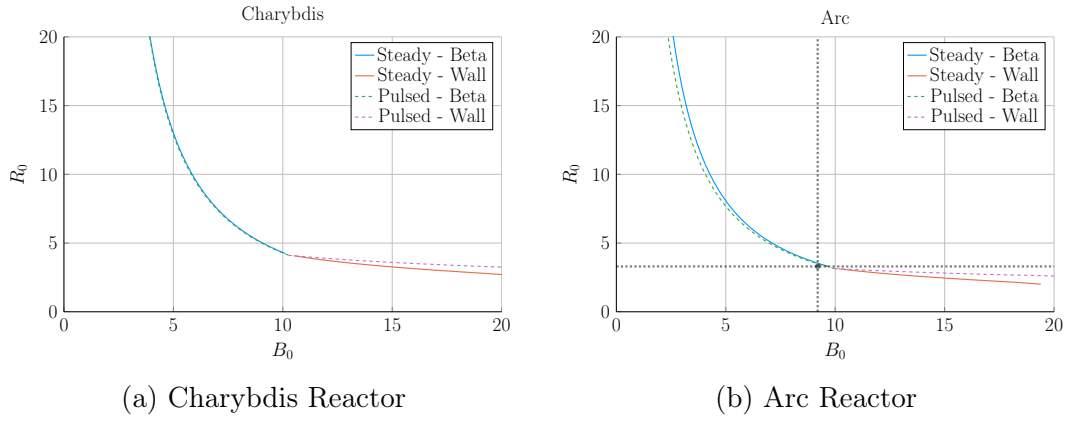


Figure 6-8: Steady State Prototype Comparison

Table 6.6: Charybdis Variables

(a) Input Variables

Input	Value
H	1.7
Q	25.0
N_G	0.9
ϵ	0.3
κ_{95}	1.8
δ_{95}	0.35
ν_n	0.4
ν_T	1.1
l_i	0.5579
A	2.5
Z_{eff}	1.75
f_D	0.9
τ_{FT}	1.6e9
B_{CS}	12.0

(b) Output Variables

Output	Value
R_0	4.13
B_0	10.28
I_P	8.98
\bar{n}	1.47
\bar{T}	15.81
β_N	0.028
q_{95}	6.089
P_W	3.003
f_{BS}	0.723
f_{CD}	0.277
f_{ID}	0.0
V	225.5
P_F	1294
η_{CD}	0.291

2219 6.2.2 Pinning down Proteus

2220 The pulsed twin reactor, Proteus, highlights the effects of a high field central solenoid.
 2221 When compared to the Pulsed Demo design, the $R_0 - B_0$ curve looks far more favor-
 2222 able – i.e. each machine built at a certain magnet strength would be more compact
 2223 (and cheaper). An interesting facet of Proteus is that it exhibits all three used limits:
 2224 kink safety factor, Troyon beta, and wall loading.

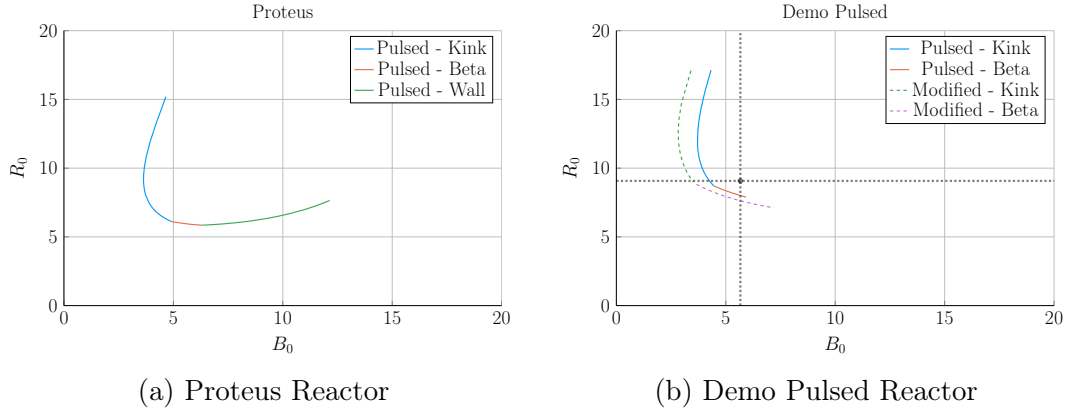


Figure 6-9: Pulsed Prototype Comparison

Table 6.7: Proteus Variables

(a) Input Variables

Input	Value
H	1.0
Q	25.0
N_G	0.9
ϵ	0.3
κ_{95}	1.8
δ_{95}	0.35
ν_n	0.4
ν_T	1.1
l_i	0.6328
A	2.5
Z_{eff}	1.75
f_D	0.9
τ_{FT}	7200
B_{CS}	20.0

(b) Output Variables

Output	Value
R_0	6.11
B_0	4.93
I_P	15.54
\bar{n}	1.16
\bar{T}	11.25
β_N	0.028
q_{95}	2.5
P_W	1.763
f_{BS}	0.2675
f_{CD}	0.0
f_{ID}	0.7325
V	732.6
P_F	1667
η_{CD}	0.0

2225 6.3 Learning from the Data

2226 Now that the model has been properly vetted and prototypes designed, we can explore
2227 how pulsed and steady-state tokamaks scale. Fitting with the Dickens theme, there
2228 will be three mostly independent results. The first result will explore how to minimize
2229 costs for a reactor by choosing optimum design points. The next will be an argument
2230 for how to properly utilize the HTS magnet technology in component design. Lastly,
2231 we will take a cursory look at the other parameters capable of lowering machine costs.

2232 6.3.1 Picking a Design Point

2233 With more than twenty design parameters, finding the most efficient reactor is a
2234 fool’s errand. Intuition building aside, finding good reactors becomes much more fea-
2235 sible when only focusing on ~~dynamic~~~~floating~~ variables – i.e. when keeping ~~static~~~~fixed~~
2236 variables constant. This method, for example, is how all the $R_0 - B_0$ curves have
2237 been produced this chapter. Once these curves are produced, it is up to the user to
2238 choose which reactor on them to build. However, the guiding metric usually involves
2239 lowering some cost, either: capital cost or cost-per-watt.

2240 Regardless of reactor type, most efficient tokamaks operate near the beta limit – where
2241 plasma pressure is greatest. Besides being a regime highly sensitive to magnetic field
2242 strength, the beta limit is a constraint that occurs on every reactor (seen by the
2243 authors). This beta limit is usually nested between the kink limit to lower B_0 values
2244 and wall loading to higher ones. Understanding these regimes is the first step towards
2245 building an intuition favoring efficient machines – see Fig. 6-10.

2246 Now that the beta limit curve has been designated as the most efficient regime to
2247 operate in (usually), the goal is to select which reactor on it is the best one to build.
2248 Starting with the easier of the two, the optimum design point for steady-state reactors
2249 is the point where wall loading first starts to dominate design. Here, engineering
2250 concerns cause the reactor to start increasing in size and cost – which is bad. This
2251 conclusion is justified by the cost curves for all five reactors in Fig. 6-11. As these

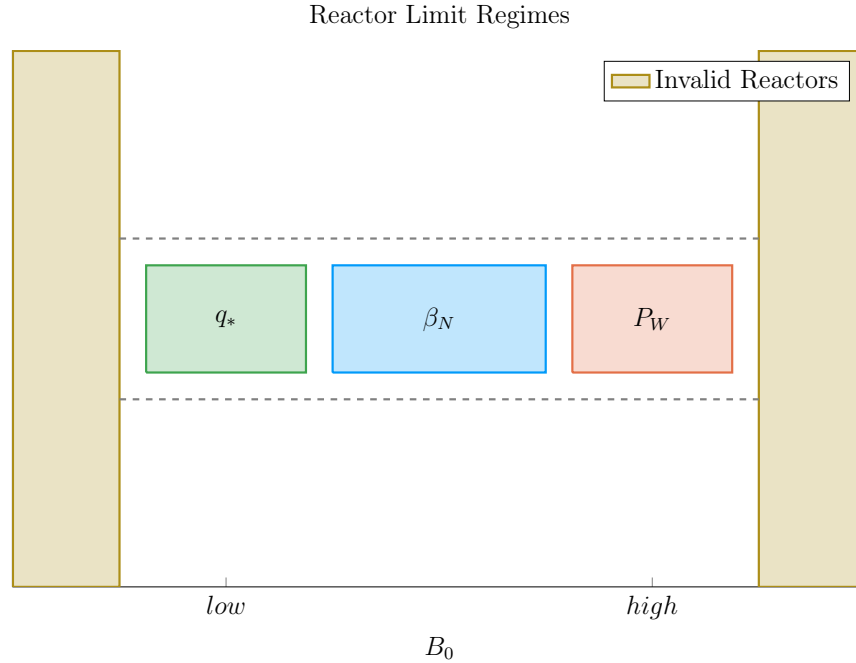


Figure 6-10: Limit Regimes as function of B_0

show, it is also where these reactor designers pinned down their tokamaks.*

The problem of selecting an optimum design is more difficult for the pulsed case. This is mainly due to the kink limit regime being actually achievable. Following the conclusion from steady-state reactors would be an oversimplification because there are actually two costs relevant to a reactor: capital cost and cost-per-watt. These beta-wall reactors are actually the points often best for minimizing cost-per-watt (i.e. your rate of return). The new beta-kink reactors, then, lead to cheap to build machines – as they minimize capital cost. These conclusions are shown in Fig. 6-12.

Summarizing the conclusions of this subsection, the beta limit is usually the best constraint to operate at. For lowering the cost-per-watt, a reactor should always be run at the highest magnetic field strength (B_0) that satisfies the beta limit. This most often occurs when wall loading takes over (for steady-state reactors) or reactors start being physically unrealizable (for pulsed ones). Building cheap to build reactors – i.e. minimizing capital cost – then actually proved to make pulsed design one of trade-offs.

*Simply stated, the optimum reactor for steady-state tokamaks is one that just barely satisfies the beta and wall loading limit simultaneously – i.e. where the two curves intersect.

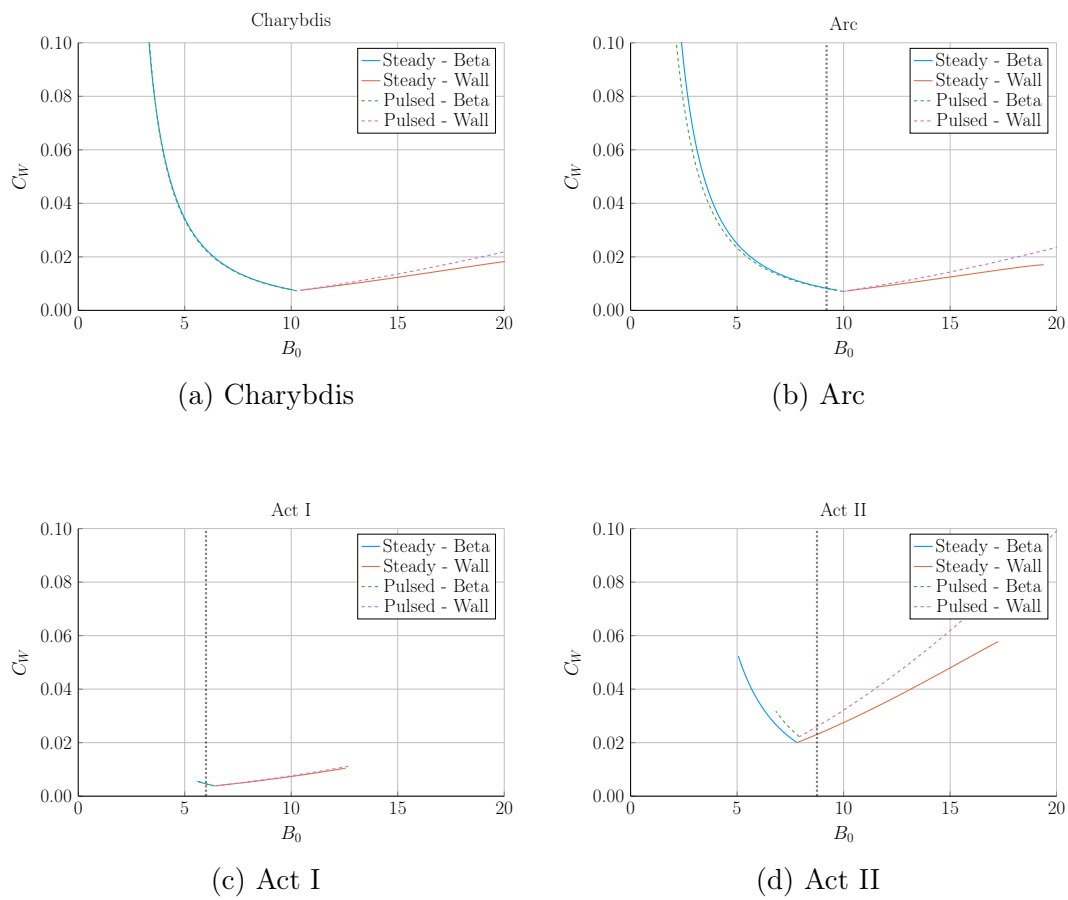
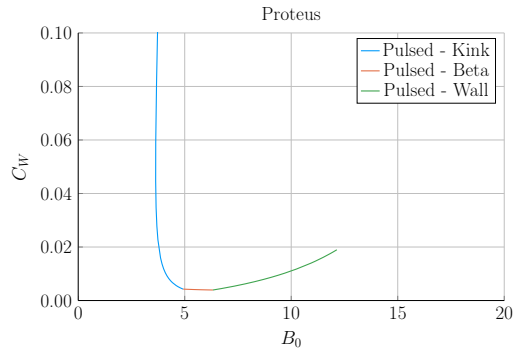
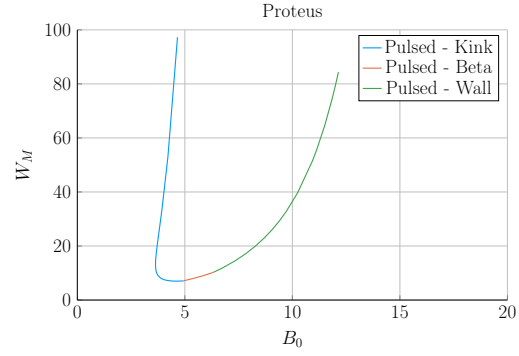


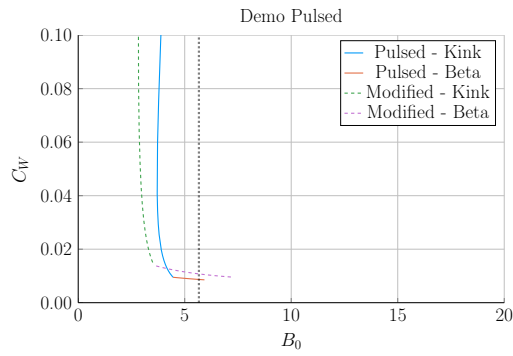
Figure 6-11: Steady State Cost Curves



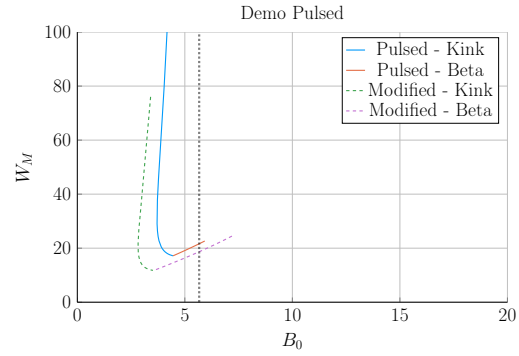
(a) Proteus Cost-per-Watt



(b) Proteus Capital Cost



(c) Demo Pulsed Cost-per-Watt



(d) Demo Pulsed Capital Cost

Figure 6-12: Pulsed Cost Curves

2266 This is because the beta-kink curve intersection produces a low capital cost reactor,
2267 but at the price of operating at a subpar cost-per-watt. Designers should therefore
2268 balance the two cost metrics.

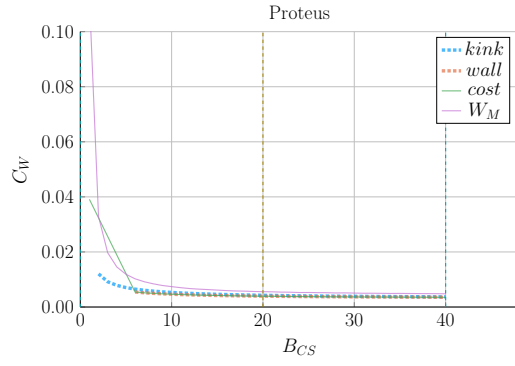
2269 6.3.2 Utilizing High Field Magnets

2270 The main conclusion for this paper is that high field magnets are the way to go to
2271 build an efficient, compact fusion reactor. In line with the MIT ARC effort, these
2272 high fields will be built with high-temperature superconducting (HTS) tape. This
2273 innovation is set to double the strength of conventional magnets. The real question
2274 is how best to use this technology.

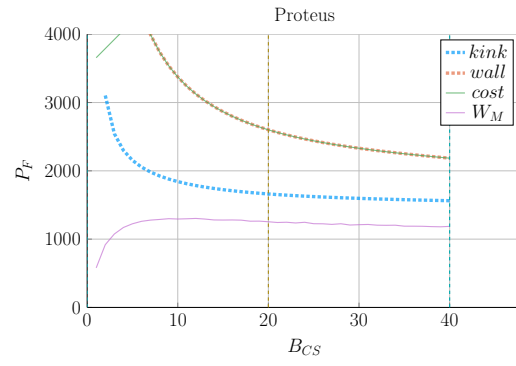
2275 At a very simple level, there are two main places strong magnets can be employed:
2276 the toroidal fields (B_0) and the central solenoid (B_{CS}). The easier mode of operation
2277 to start with is steady-state. This is because steady-state tokamaks do not rely on
2278 a central solenoid for the profitability of their machines. Further, the cost curves
2279 in Fig. 6-11 show that all these designs would benefit from toroidal fields (B_0) not
2280 achievable with conventional magnets – which can only reach around 10 T on a good
2281 day.

2282 The more interesting result is that pulsed reactors gain no real benefit from us-
2283 ing HTS toroidal field magnets. Within the modern paradigm (i.e. D-T fuel, H-
2284 Mode, etc), pulsed reactors never have to exceed the limits of ~~less expensive LTS~~
2285 ~~magnets.inexpensive, copper magnets.~~ The place HTS can really help is with the
2286 central solenoid, which governs how long a pulse can last. Further, the effect of im-
2287 proving the central solenoid saturates within the range accessible to HTS tape. Again,
2288 HTS would be more than adequate for the modern paradigm. These conclusions are
2289 shown in Figs. 6-13 and 6-14.

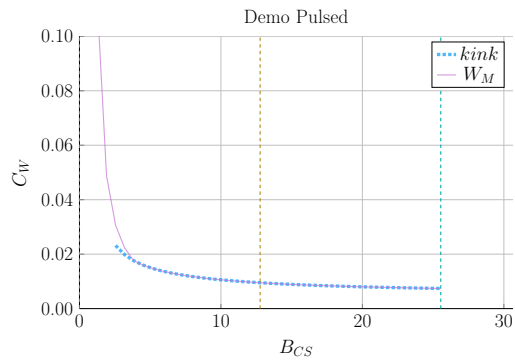
2290 Rehashing this section, HTS tape is the best way to lower the cost of fusion reactors
2291 at a commercial scale. For steady-state reactors, HTS works best in the toroidal field
2292 coils (B_0), while the tape would fare better in the central solenoid (B_{CS}) of pulsed



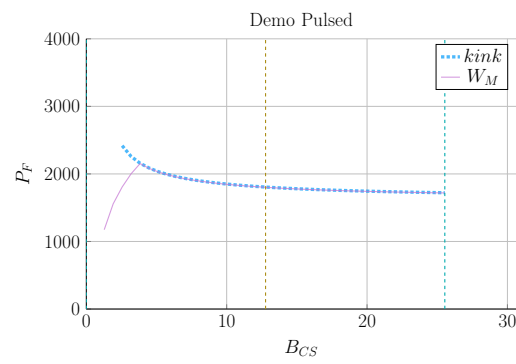
(a) Proteus Cost-per-Watt



(b) Proteus Fusion Power

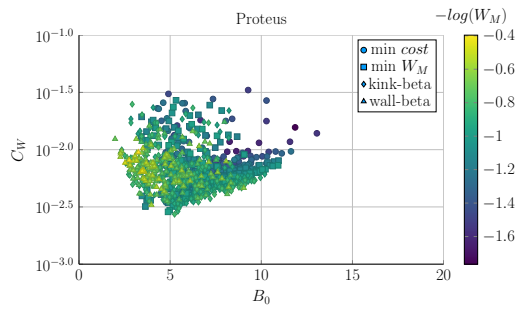


(c) Demo Pulsed Cost-per-Watt

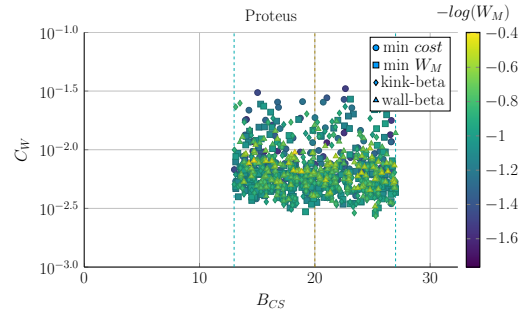


(d) Demo Pulsed Fusion Power

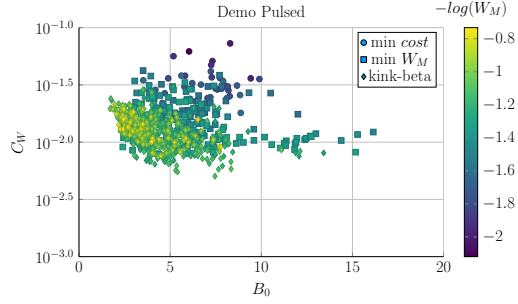
Figure 6-13: Pulsed B_{CS} Sensitivity



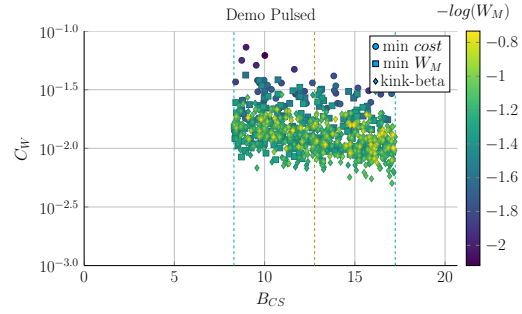
(a) Proteus B_0 Sampling



(b) Proteus B_{CS} Sampling



(c) Demo Pulsed B_0 Sampling



(d) Demo Pulsed B_{CS} Sampling

Figure 6-14: Pulsed Monte Carlo Sampling

2293 reactors. Further, both effects saturate within the range of this HTS tape, rendering
2294 more sophisticated magnetic technology unnecessary. HTS is truly the answer to
2295 affordable fusion energy.

2296 6.3.3 Looking at Design Alternatives

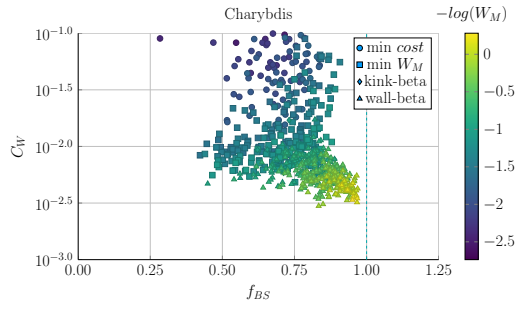
2297 Even in this relatively simple fusion model, there are more than twenty ~~static~~fixed/input
2298 variable knobs a designer can tune to improve reactor feasibility. Many have prac-
2299 tical limits, such as being physically realizable or fitting within the ELMMy H-Mode
2300 database. Thus, the goal of this subsection is to investigate some of the more inter-
2301 esting results. Although many more plots are available in the appendix.

2302 Capitalizing the Bootstrap Current

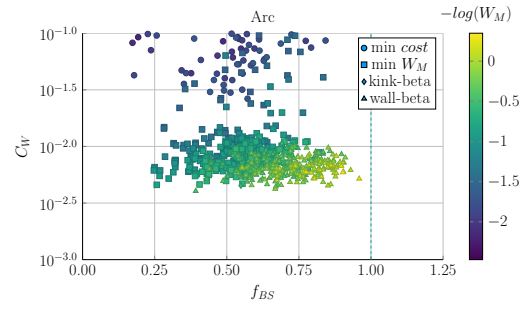
2303 Besides artificially enhancing a plasmas confinement with the H-factor, steady-state
2304 reactor designers may also heavily rely on high bootstrap currents. This is because
2305 bootstrap current is the portion of current you do not have to pay for. The research
2306 camp most focused on this miracle is General Atomic's DIII-D in San Diego. This
2307 miracle relies on tailoring current profiles to be extremely hollow.

2308 Quickly reasoning this camp's thought process are two sets of plots. The first plot
2309 (Fig. 6-15) highlights how the cheapest possible steady-state designs have bootstrap
2310 fractions approaching unity – they use almost no current drive. This makes sense as
2311 current drive is extremely cost prohibitive (i.e. why people consider pulsed tokamaks).

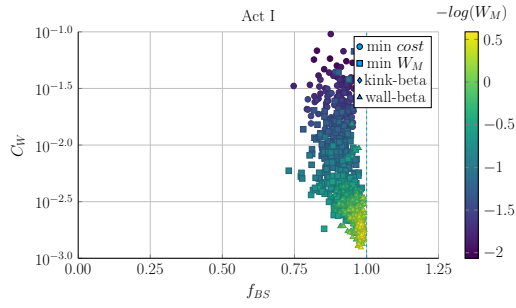
2312 The next plot is the parameter that determines a current profile's peak radius: l_i . As
2313 can be seen, the current peak approaches the outer edge of the plasma as l_i decreases.
2314 This in turn boosts the bootstrap fraction closer to one – leading to inexpensive
2315 reactors.



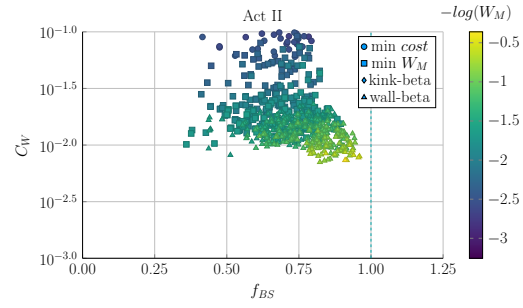
(a) Charybdis l_i Sampling



(b) Arc l_i Sampling

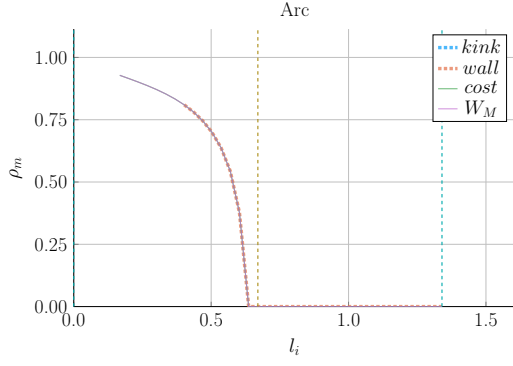


(c) Act I l_i Sampling

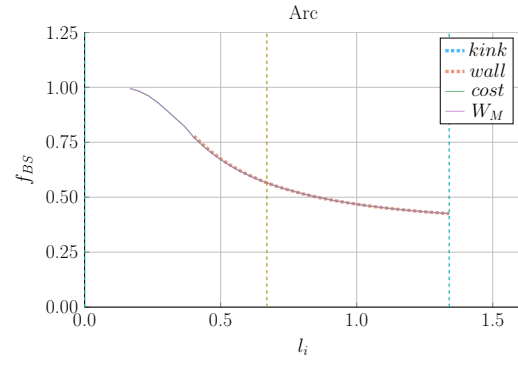


(d) Act II l_i Sampling

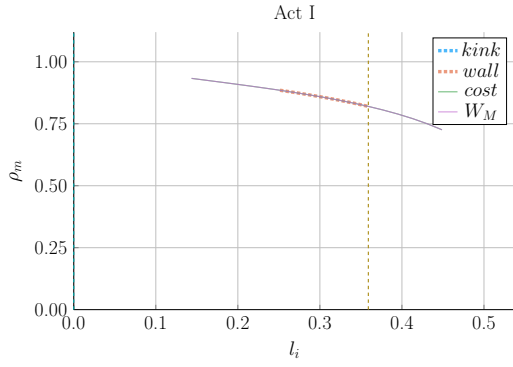
Figure 6-15: Bootstrap Current Monte Carlo Sampling



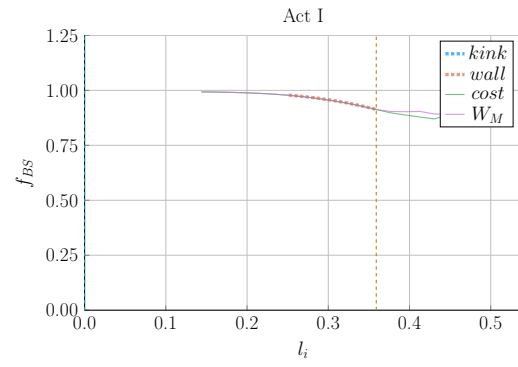
(a) Arc Peak Radius



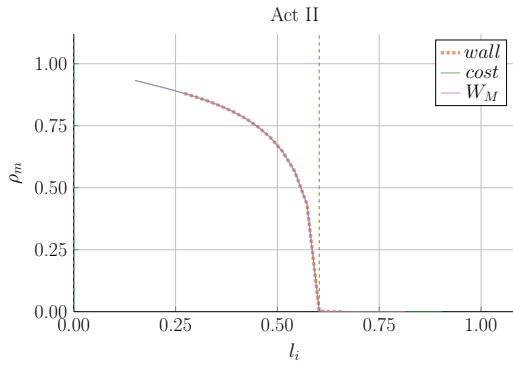
(b) Arc Bootstrap Fraction



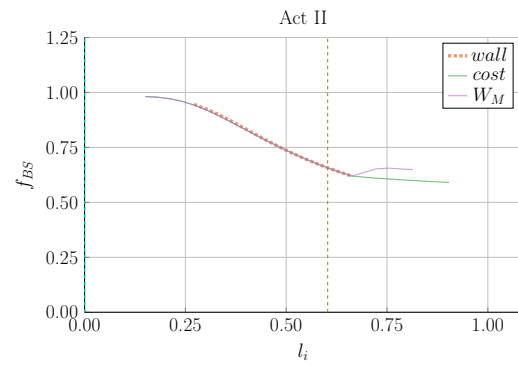
(c) Act I Peak Radius



(d) Act I Bootstrap Fraction



(e) Act II Peak Radius



(f) Act II Bootstrap Fraction

Figure 6-16: Internal Inductance Sensitivities

2316 Contextualizing the H-Factor

2317 From before, increasing the H-factor always led to more cost effective steady-state
2318 reactors. This is because the enhanced confinement allows for smaller machines.
2319 This was already heavily explored in Fig. 6-2. These plots also show that steady
2320 state reactors would not be physically possible using a default H factor of one! In
2321 other words, steady-state tokamaks require some technical advancement before they
2322 can ever be used as fusion reactors. The same cannot be said for pulsed machines.

2323 For pulsed reactors, increasing H always reduces capital cost, but may actually in-
2324 crease the cost-per-watt. The reason for this is because fusion powers are much
2325 smaller in pulsed machines. This interesting result demonstrates the unusual behav-
2326 iors of highly non-linear systems: masterclass intuition may not match model results.

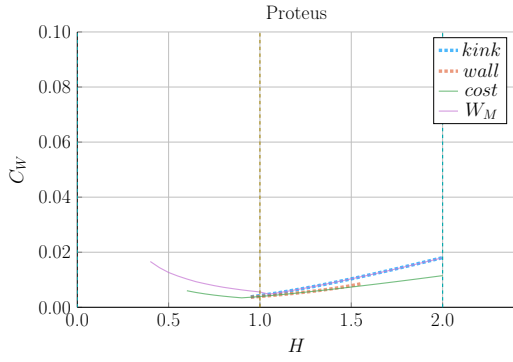
2327 Showcasing the Current Drive Efficiency

2328 The last exploration is less about building an efficient machine and more about under-
2329 standing the self-consistent current drive efficiency in steady-state tokamaks. Using
2330 the Ehst-Karney model²² coupled with Jeff's textbook³ leads to a remarkably simple
2331 and accurate solver. The model captures the physics almost spot on for the different
2332 designs.*

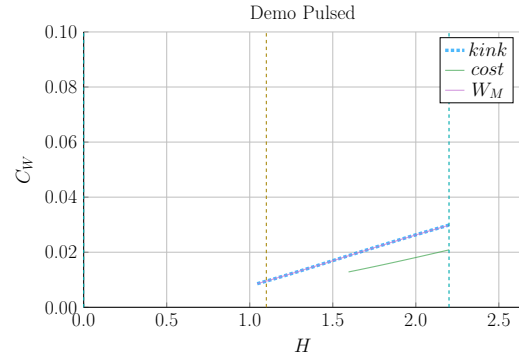
2333 In a similar fashion as the bootstrap fraction results, the variable that most captures
2334 how to directly maximize η_{CD} is the LHCD laser launch angle, θ_{wave} . When below
2335 90° it is considered outside launch, whereas up to 135° it is considered inside launch.
2336 Notably, these curves are not monotonic, there is an optimum launching angle.

2337 It should be noted that the launch angle was not found to have a major impact. This
2338 may be a due to an oversimplification of the model.

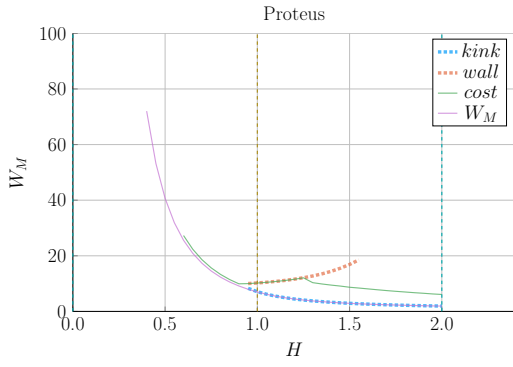
*It did, however, not converge for the DEMO steady reactor. This is probably due to lack of self-consistency for η_{CD} in their systems framework.



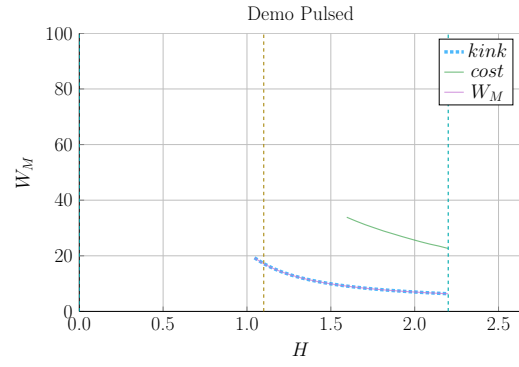
(a) Proteus Cost-per-Watt



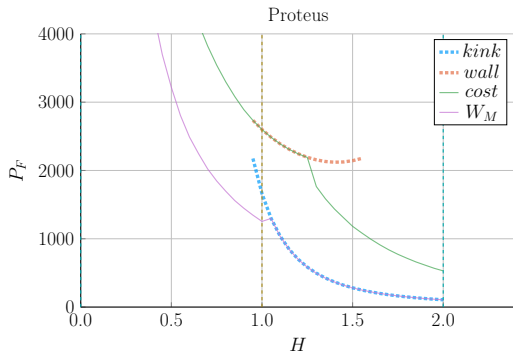
(b) Demo Pulsed Cost-per-Watt



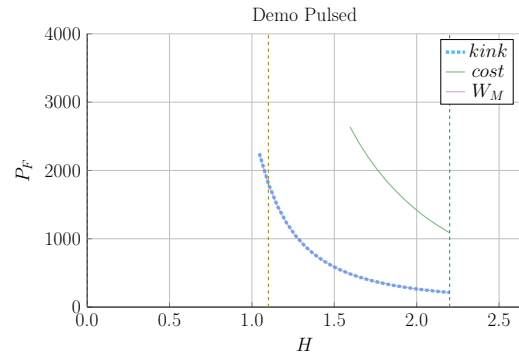
(c) Proteus Capital Cost



(d) Demo Pulsed Capital Cost

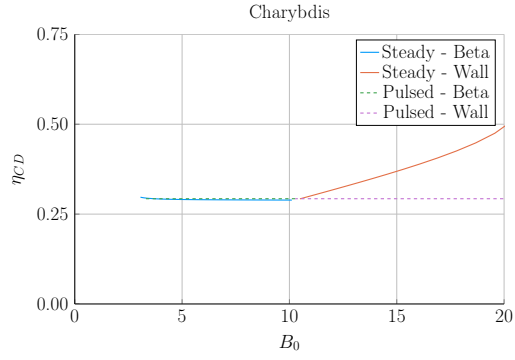


(e) Proteus Fusion Power

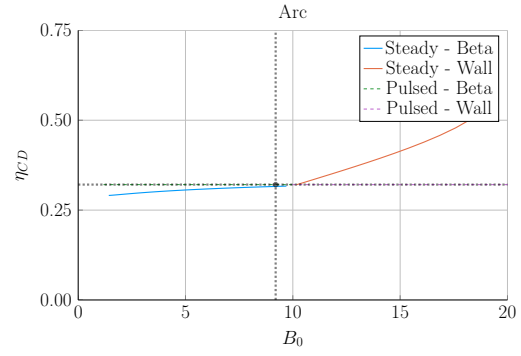


(f) Demo Pulsed Fusion Power

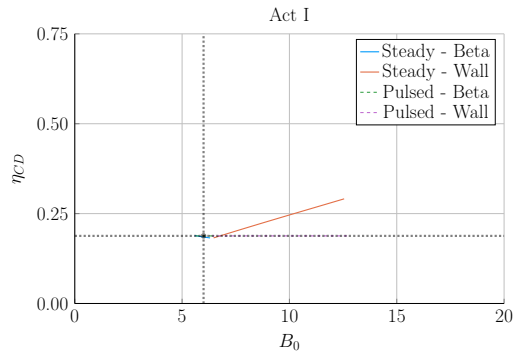
Figure 6-17: Pulsed H Sensitivities



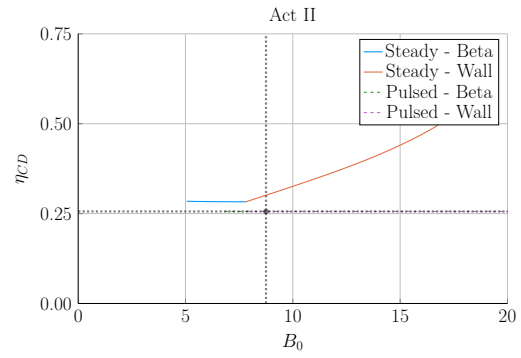
(a) Charybdis



(b) Arc

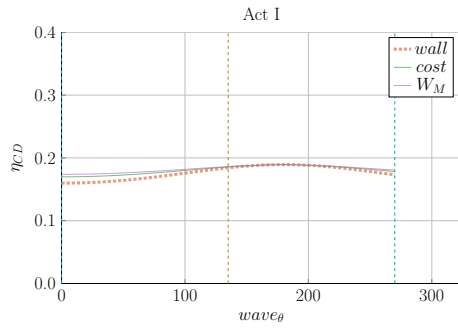


(c) Act I

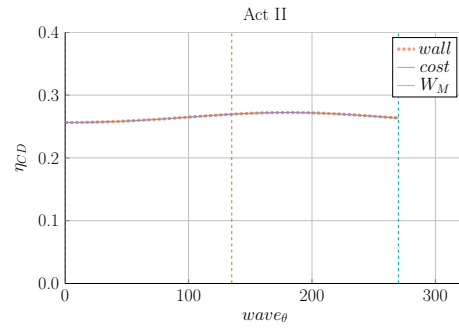


(d) Act II

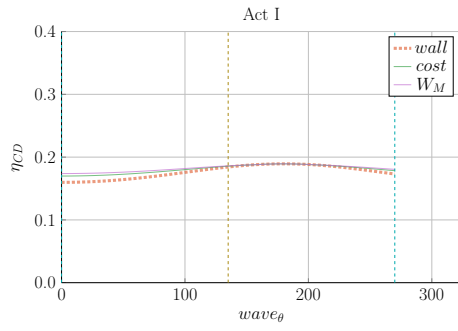
Figure 6-18: Steady State Current Drive Efficiency



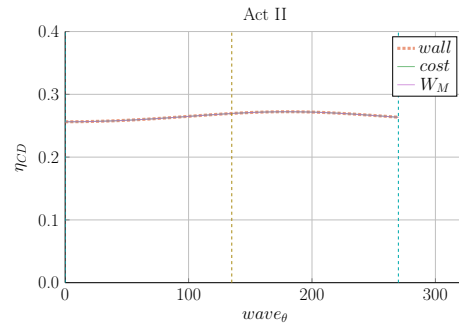
(a) Charybdis



(b) Arc



(c) Act I



(d) Act II

Figure 6-19: Current Drive Efficiency vs Launch Angle

2339 Chapter 7

2340 Planning Future Work

2341 This model may run and produce interesting results, but there is always more to do.

2342 This chapter explores three potential fusion reactors that could help guide real world
2343 designs. It then goes into a laundry list of possible model improvements.

2344 The three reactors covered are: a stellarator (Ladon), a steady-state/pulsed hybrid
2345 (Janus), and a tokamak capable of reaching H, L, and I modes (Daedalus).

2346 7.1 Incorporating Stellarator Technology – Ladon

2347 A stellarator is, at a basic level, a tokamak helically twisted along the length of its
2348 major circle. For a long time they were dismissed because of the difficulty involved in
2349 building spiraled magnets. Recent technological improvements, though, have eased
2350 this situation – as seen with the Wendelstein 7-X device in Germany. The problem
2351 now is engrained in the missing scaling laws stemming from a lack of machines and,
2352 more fundamentally, data points.

2353 Optimistically, expanding this model would just involve developing a new confinement
2354 time scaling law and replacing the Greenwald density limit. The reason the Greenwald
2355 density limit is no longer important is because stability is much easier to maintain in
2356 a stellarator. Most likely, the density limit will now be governed by Bremsstrahlung

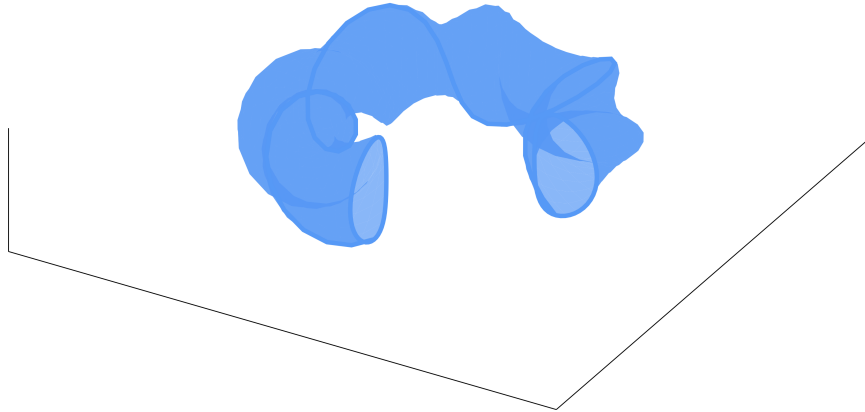


Figure 7-1: Cut-Away of Stellarator Reactor

2357 radiation. If this were the case, each equation would need to be redivided using it.
 2358 Ladon would be the reactor built using this enhancement.

2359 7.2 Making a Hybrid Reactor – Janus

2360 The next interesting reactor would be a hybrid tokamak incorporating pulsed and
 2361 steady-state operation, codenamed: Janus. Fundamentally, this would mean current
 2362 would come from both LHCD (steady-state) and inductive (pulsed) sources. This was
 2363 actually used in Demo Pulsed, but the current drive was not handled self-consistently.
 2364 Coupling these two current sources could reduce reliance on bootstrap current and
 2365 lead to much more compact machines.

2366 The arguments against this are mainly technical: why build two difficult auxiliary
 2367 systems when one is needed – especially when they probably work against each other.
 2368 Although rational, the argument implicitly assumes a current is achievable through
 2369 only one source (i.e. either through LHCD or from a central solenoid). Using two
 2370 may allow for stronger plasma currents.

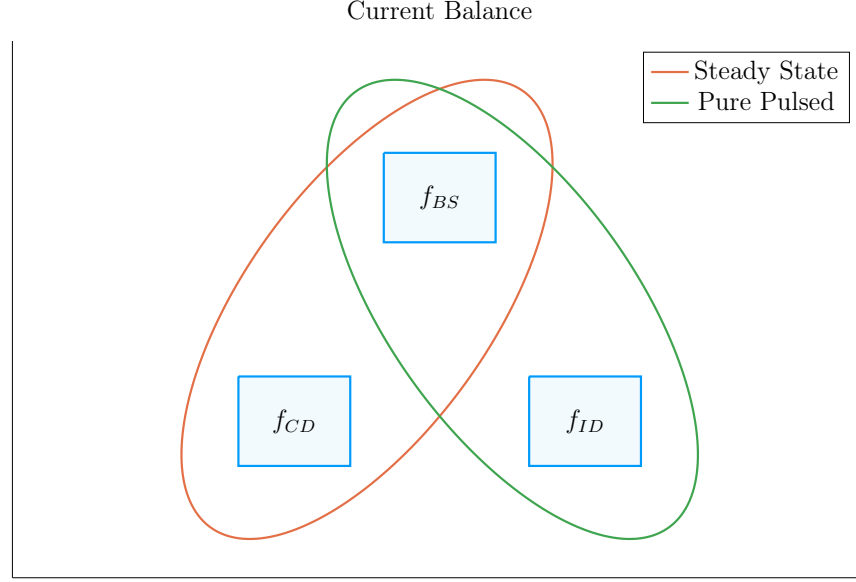


Figure 7-2: Current Balance in a Tokamak

In a tokamak, there needs to be a certain amount of current – and that current has to come from somewhere. All good reactors have an adequate bootstrap current. What provides the remaining current is what distinguishes steady state from pulsed operation.

2371 7.3 Bridging Confinement Scalings – Daedalus

2372 The final potential reactor – Daedalus – is designed to collect as many scaling laws
 2373 as possible. As a baseline, it should be able to run in H-Mode, L-Mode, and I-Mode.
 2374 Because L-Mode is available on any machine, the first step is building under H-Mode.
 2375 The goal then is to find reactors that can also reach I-Mode – thus improving the
 2376 scaling law’s fit and making the actual reactor more cost effective.

2377 Presented below are the three confinement scaling laws, as well as the generalized
 2378 formula. As should be noted, the I-Mode scaling currently lacks a true radial de-
 2379 pendence – as it has only been found on two machines. This is one reason Daedalus
 2380 would be so valuable.

$$\tau_E^G = K_\tau H \frac{I_P^{\alpha_I} R_0^{\alpha_R} a^{\alpha_a} \kappa^{\alpha_\kappa} \bar{n}^{\alpha_n} B_0^{\alpha_B} A^{\alpha_A}}{P_{src}^{\alpha_P}} \quad (3.26)$$

$$\tau_E^H = 0.145 H \frac{I_P^{0.93} R_0^{1.39} a^{0.58} \kappa^{0.78} \bar{n}^{0.41} B_0^{0.15} A^{0.19}}{P_{src}^{0.69}} \quad (3.28)$$

$$\tau_E^L = 0.048 H \frac{I_P^{0.85} R_0^{1.2} a^{0.3} \kappa^{0.5} \bar{n}^{0.1} B_0^{0.2} A^{0.5}}{P_{src}^{0.5}} \quad (7.1)$$

$$\tau_E^I = \frac{0.014 H}{0.68^{\lambda_R} \cdot 0.22^{\lambda_a}} \cdot \frac{I_P^{0.69} R_0^{\lambda_R} a^{\lambda_a} \kappa^{0.0} \bar{n}^{0.17} B_0^{0.77} A^{0.0}}{P_{src}^{0.29}} \quad (7.2)$$

$$\lambda_R + \lambda_a = 2.2 \quad (7.3)$$

A final point to make is reemphasizing that the I-Mode scaling law is not battle-tested. It is the target of ongoing research at the MIT PSFC.

7.4 Addressing Model Shortcomings

Before moving on to the final conclusions, we will give a quick recap of the more audacious simplifications used within this fusion systems framework. These include: approximating temperature profiles as simple parabolas, neglecting all radiation except Bremsstrahlung, and handling flux sources at too basic a level.

7.4.1 Integrating Pedestal Temperature Profiles

The most dubious simplification in the code at this point is modeling temperature profiles as parabolas. Although these parabolas work for densities and L-Mode plasma temperatures, the same cannot be said about H-Mode temperatures. This is because they have a distinct pedestal region on the outer edge of the plasma.

The usage of pedestal temperatures – discussed in the appendix – improves two aspects of the model: the fusion power and the bootstrap current. These were shown in the results to be over-calculated and underestimated, respectively. Pedestals, having a lower core temperature, would decrease the total fusion power. As well, they would boost bootstrap current due to the quick drop near the plasma’s edge (i.e. they have

2401 a large derivative there).

2402 These improvements could easily be added to the code, because temperature was
2403 addressed as a difficult parameter to handle from the beginning.

2404 **7.4.2 Expanding the Radiation Loss Term**

2405 The next area that would be improved by more sophisticated theory would be the
2406 radiation loss term. From before, it was pointed out that the Bremsstrahlung ra-
2407 diation was the dominant term within the plasma core and, therefore, provided a
2408 first-order approximation. Drawing the radiation losses closer to real world values
2409 would involve adding line radiation and synchrotron radiation. The former of which
2410 would be needed as high-Z impurities become more important.

2411 **7.4.3 Taking Flux Sources Seriously**

2412 The final oversimplification in the model deals with the flux sources involved in a
2413 pulsed reactor – existing at almost every level. First, the derivation of flux balance
2414 started with a simple transformer between a solenoid primary and a plasma secondary.
2415 Even this initial step is probably too simple.

2416 After we developed an equation for flux balance, we compared it to ones in the
2417 literature (i.e. PROCESS) to build confidence in the model. To draw this equation
2418 closer to theirs, we then added a PF coil contribution a posteriori. This implicitly
2419 ignored coupling between most of the components. Thus leading to another source
2420 of error for the model. Moreover, this formula for PF coil contribution was much
2421 simpler than ones found in other fusion systems codes.

2422 Even though this model may be extremely simple, it does remarkably well at matching
2423 more sophisticated codes – and does so at a much faster pace. These suggestions were
2424 all just ways to draw results closer to real world values.

2425 Chapter 8

2426 Concluding Reactor Discussion

2427 The goal of this document was to develop a simple fusion systems model that can
2428 work for both pulsed and steady-state tokamaks. The main conclusion was that the
2429 best way to build a more efficient, compact reactor is to invest in strong magnets –
2430 as MIT is doing with high-temperature superconducting (HTS) tape. Further it was
2431 shown that to best utilize materials, the tape should be incorporated into the toroidal
2432 field coils for steady-state machines and in the central solenoid for pulsed ones.

2433 Although some skepticism should be allotted to these conclusions, it was shown that
2434 this simple algebraic solver matched sophisticated multiyear research studies with
2435 speed and ease. This model may not provide an engineer's rigor in measuring cost,
2436 but the same can be said for any code or theory. The fusion system is as nonlinear
2437 a problem as they come, but we still managed to build a framework that can hone
2438 even a well-trained physicist's intuition.

2439 The final point to make is that this model actually predicts that HTS technology can
2440 provide the optimum magnetic field strength for a reactor. Once HTS doubles the
2441 maximum achievable teslas, the law of diminishing returns heavily kicks in. This of
2442 course assumes H-Mode D-T plasmas at the Greenwald density limit.

Appendix A

Presenting ~~Static~~Fixed Variables

Table A.1: List of ~~Static~~Fixed Variables

Name	Value
is_pulsed	is reactor pulsed or steady-state
H	h factor for ELMy H-mode scaling
Q	Physics Gain (P_F/P_H)
ϵ	inverse aspect ratio
κ_{95}	elongation at 95 flux surface
δ_{95}	triangularity at 95 flux surface
ν_n	parabolic density peaking factor
ν_T	parabolic temperature peaking factor
Z_{eff}	effective charge
f_D	dilution factor
A	average mass number (in amus)
l_i	internal inductance (interchangeable with ρ_m)
ρ_m	normalized radius of current peak (interchangeable with l_i)
N_G	Greenwald density fraction
η_T	thermal efficiency of the reactor
η_{RF}	efficiency of the RF antenna
τ_{FT}	time of flattop of reactor pulse
B_{CS}	strength of magnetic field in central solenoid
$(\beta_N)_{max}$	max allowed normalized beta normal
$(q_{*95})_{max}$	min allowed safety factor
$(P_W)_{max}$	maximum allowed wall loading power per surface area

2445 Appendix B

2446 Simulating with Fussy.jl

2447 Fussy.jl is a 0-D fusion systems code written using the Julia language. The reason for
2448 choosing Julia over say Matlab and Python was due to metaprogramming concerns
2449 and its tight-knit computational community, respectively. Incorporating the model
2450 used throughout this paper, the code is quick to run and matches more sophisticated
2451 frameworks with high fidelity.

2452 This chapter will be broken down into three steps. The first is getting a user up
2453 and running with the code. Once the user gets to this point, hopefully they will
2454 wonder how the code is structured. This will be the second step. The final step
2455 will be explaining the various functions callable on reactor objects – the atomic data
2456 structure for Fussy.jl.

2457 B.1 Getting the Code to Work

2458 The hardest step of any codebase is getting it up and running. These instructions
2459 should get a user to a point where they are a few internet searches away from a
2460 working copy of Fussy.jl. As an aide, you can view an interactive collection of Fussy.jl
2461 Jupyter notebooks at the following website:

2462 www.fusion.codes

2463 Although `fusion.codes` is a nice tool for viewing this document’s results, it is a little
2464 slow for producing new data – and it also lacks a method for storing it. Therefore,
2465 an advanced user should first download a copy of Julia from:

2466 julialang.org/downloads

2467 Currently the `Fussy.jl` codebase is written using `v0.6`, but should be `v1.0` compatible
2468 by 2019. Using Julia nomenclature, `Fussy.jl` is a Julia package. It can be cloned using
2469 Julia conventions from the following Github repository:

2470 <https://github.com/djseagal/Fussy.jl.git>

2471 Once the `Fussy.jl` package has been cloned into your Julia package library, you should
2472 be able to access it through the Julia REPL or a Jupyter notebook. You can now
2473 reproduce every plot in this text. A quick test to see if your code works is:

2474

```
2475     using Fussy
2476     cur_reactor = Reactor(15)
2477
2478     @assert cur_reactor.T_bar == 15
```

2479 B.2 Sorting out the Codebase

2480 Assuming the user got to this section, the code works and now you want to know
2481 what you can do with it. The place to start is in the `src` folder, again viewable online
2482 at:

2483 git.io/tokamak

2484 Within the `src` folder are several subfolders as well as a few files (e.g. `Fussy.jl` and
2485 `defaults.jl`). In an attempt to not bore the reader, we will be painting with thick
2486 brushstrokes. Further, the `methods` subfolder will be the topic of the next section –
2487 as most involve calls on a reactor object.

2488 **B.2.1 Typing out Structures**

2489 The place to start in any modeling framework is its data structures. These type
2490 definitions allow the building of nested hierarchies of constructed objects. The most
2491 atomic of these is the Reactor struct, but several other ones allow for solving broader
2492 scoped questions (i.e. Scans, Sensitivities, and Samplings.)

2493 **The Reactor Structure**

2494 Reactors are the most atomic data structure in this fusion systems model. They
2495 store all the fields needed to represent a reactor as it exists in reactor space. This
2496 obviously includes its temperature, current, and radius, but also includes derived
2497 quantities, such as the cost-per-watt and bootstrap fraction. They can be initialized,
2498 solved, updated, and honed. Most other data structures are just wrappers to hold
2499 these reactors – they are described next.

2500 **The Scan Structure**

2501 A Scan object is a collection of reactors made from scanning a list of temperatures.
2502 For example, a scan of five temperatures from 5 keV to 25 keV would result in several
2503 arrays of five reactors. Most often, one of these lists would correspond to beta reactors,
2504 one to kink reactors, and one to wall loading reactors. There may then be fewer than
2505 five reactors in a list if some of the reactors are invalid or fundamentally unsolvable.
2506 This is the data structure that produces the various comparison plots in the results.

2507 **The Sensitivity Structure**

2508 Sensitivity studies are how computationalists test the effect of changing a variable
2509 over multiple values – i.e. do a 20% sensitivity around the H factor. Like Scans,
2510 Sensitivities store various lists of reactors, each corresponding to an interesting data
2511 point. These include limit reactors where the beta limit and kink limit are just

2512 satisfied or when the beta limit and wall loading are just satisfied. Additionally, they
2513 include the minimum capital cost reactors and the minimum cost-per-watt ones.

2514 **The Sampling Structure**

2515 The Sampling struct was created to do simple Monte Carlo runs over a reactor's
2516 ~~static~~~~fixed~~ values. While sensitivities only allow one variable to change at a time,
2517 samplings randomly assign a list of variables to some neighborhood of possible values.
2518 These are how the scatter plots are made. Succinctly, where sensitivity studies show
2519 local changes to variables, Monte Carlo samplings show global trends in reactor design.

2520 **The Equation Structure**

2521 In order to store the various equations from Table 5.1 is the Equation Struct. It stores
2522 the γ exponents for: R_0 , B_0 , and I_P . – as well as the function representing $G(\bar{T})$.
2523 Repeated these are the unknowns in:

$$R_0^{\gamma_R} \cdot B_0^{\gamma_B} \cdot I_P^{\gamma_I} = G(\bar{T}) \quad (5.3)$$

2524 Concretely, there are 16 objects that use this struct – one for each equation (e.g. for
2525 fusion power, the beta limit, and temperature assignment).

2526 **The Equation Set Structure**

2527 The step up from the Equation struct are the Equation Sets. These collections of
2528 three equations allow R_0 , B_0 , and maybe I_P to be substituted out of the current
2529 balance root-solving equation. This is where Eqs. (5.4) to (5.10) come into play.

2530 B.2.2 Referencing Input Decks and Solutions

2531 With more than twenty ~~static~~~~fixed~~ variables in the model, the range of tokamak
2532 reactors is basically infinite. To help users build a net of designs to explore reactor
2533 space are seven input decks. These are the ones given in the results: Arc, Act I
2534 /II, Demo Steady/Pulsed, Proteus and Charybdis. Coupled with the non-prototype
2535 reactors are solution reactors that store various quantities from the original papers
2536 (e.g. P_F , f_{BS} , R_0). These are how the comparison tables were constructed.

2537 B.2.3 Acknowledging Utility Functions

2538 For the uninitiated, utility functions are grab bag functions that do not really belong
2539 in a codebase – but do anyway. This sentiment does not mean they are worthless,
2540 just not fusion related at all. In Fussy.jl, the most notable are a normalized integral
2541 calculator, a filter that includes numeric tolerances, and a robust root solver.

2542 Although since incorporated into the official Roots.jl package, `find_roots` allows
2543 finding an arbitrary number of roots within a bounded range. This was needed
2544 because many roots can be found at various levels of the reactor solving problem –
2545 i.e. for I_P , \bar{T} , η_{CD} , etc.

2546 B.2.4 Mentioning Base Level Files

2547 In addition to subdirectories within the `src` folder are three files: Fussy.jl, abstracts.jl,
2548 and defaults.jl. Fussy.jl is the package’s main file that actually stores the Fussy
2549 module. While, abstracts.jl stores various abstract structures that help clean up
2550 other files.

2551 Finally, defaults.jl stores various default values that are important to the codebase.
2552 For example, this is where the various scaling law exponents are stored. It is also
2553 where the bounding values for the different root solving problems live. These include
2554 minimum and maximum values for: I_P , \bar{T} , η_{CD} .

2555 Now that a majority of the files have been discussed, we can turn to the reactor
2556 methods. These constitute most of the interesting functionality within the codebase.

2557 B.3 Delving into Reactor Methods

2558 The reactor is the most atomic data structure in this model. It therefore makes
2559 sense that it has many instance methods. These include all the coefficients, fluxes,
2560 powers, etc. It also includes methods that solve a reactor, perform a match on some
2561 field's value, or converge η_{CD} to self-consistency. The various subdirectories within
2562 the `src/methods/reactors` folder will now be discussed.

2563 Calculations

2564 The calculation subdirectory of reactor methods are used to set various important
2565 values in the solver. For ~~dynamicfloating~~ variables, these include: \bar{n} , R_0 , B_0 , and
2566 I_P . This folder also includes the calculation of the Bosch-Hale reactivity and the
2567 Ehst-Karney current drive efficiency.

2568 Coefficients and Composites

2569 The coefficients and composites directories correspond to the model's ~~staticfixed~~ and
2570 ~~dynamicfloating~~ coefficients, respectively. For clarity, ~~staticfixed~~ coefficients, includ-
2571 ing K_n and K_{CD} , were labeled with a K. Whereas, ~~dynamicfloating~~ coefficients then
2572 started with G's – i.e. G_{PB} and G_V .

2573 Fluxes and Powers

2574 Within flux balance and power balance were around a dozen terms or sub-terms.
2575 Although not directly used in the conservation equations, sub-terms are used to com-
2576 pare the model to ones from the literature. For clarity, fluxes include: Φ_{CS} , Φ_{PF} ,
2577 Φ_{RU} , Φ_{FT} , Φ_{res} , and Φ_{ind} . The powers, then, include: P_F , P_{BR} , P_κ , P_{src} , P_W , etc.

2578 Profiles

2579 The next collection of reactor methods are the various profiles. Most obviously, these
2580 include radial plasma profiles for density, temperature, and current. However, this
2581 folder also includes the magnetic field strength as a function of radius – as was used
2582 within current drive efficiency calculations.

2583 Geometries

2584 Additionally, there are many geometric relations. These include the various tokamak
2585 thicknesses: a, b, c, d – as well as the radius and height of the central solenoid. This
2586 group also includes the volume, perimeter, surface area, and cross-sectional area. It
2587 also includes the many subscripted fields. For example, the elongation (i.e. κ_{95})
2588 includes the following alternative definitions: κ_X , κ_P , and κ_T

2589 Formulas

2590 The final set of reactor methods are formulas that do not really fit anywhere else.
2591 If a method is not related to geometry, power, calculations, etc, it ends up here.
2592 For example, this group includes: β_N , f_{BS} , C_W , and τ_E . Total, there are around 25
2593 formulas – as of the writing of this document.

2594 B.4 Demonstrating Code Usage

2595 Now that the Fussy.jl package has been described in detail, the final step is showing a
2596 simple example that can recreate a figure from the results chapter. This will closely
2597 match the Jupyter notebook available at:

2598 www.git.io/fussy_sensitivity

2599 Our goal will be to make a cost curve for the ARC reactor as a function of H – a so
2600 called sensitivity study plot.

2601 B.4.1 Initializing the Workspace

2602 The first step for any Fussy.jl Jupyter notebook is loading the required packages – i.e.
2603 the Fussy.jl and Plots.jl packages. This can be done using the following commands:*

```
2604     addprocs(6)
2605
2606     @everywhere using Fussy
2607     using Plots
```

2608 The Plots.jl package may take a minute to load – similar to Matlab’s initial boot
2609 time. If the kernel raises an error about Plots.jl not being installed, use the following
2610 lines:

```
2611     import Pkg
2612     Pkg.add("Plots")
```

2613 B.4.2 Running a Study

2614 Now that the necessary packages have been loaded, we can move on to actually
2615 running the sensitivity study. We will split this command into two steps to make it
2616 more explicit.

2617 The first step will be making several variables that store: boolean flags, numbers, and
2618 symbols – which are like strings, but prefaced with a colon (:) instead of surrounded
2619 by double quotes (").

```
2620     cur_param = :H
2621     cur_deck = :arc
2622     is_pulsed = false
2623     is_consistent = true
2624     cur_sensitivity = 1.0
```

*The `addprocs` and `@everywhere` commands are to parallelize the code. This is because `addprocs(6)` activates 6 worker processes and `@everywhere Fussy.jl` adds Fussy.jl to the main kernel and worker processes.

```
2625     cur_num_points = 41
```

2626 These six variables almost completely describe a sensitivity study. The first two
2627 saw we are using the Arc reactor deck and running a sensitivity over the H-factor
2628 parameter. Next, the two boolean values refer to the reactor (1) being treated as
2629 pulsed or steady-state and (2) whether to handle η_{CD} self-consistently.* Ergo, what
2630 these two flags do is make sure ARC is being handled as a steady-state reactor with
2631 a self-consistent η_{CD} . The last two variables are then ways to change the sensitivity
2632 of the study (with 1.0 \rightarrow 100%) and the number of reactors it will produce (i.e. 41).
2633 Now all six of these variables can be piped into a call to the **Study** struct to start
2634 running the sensitivity study:

```
2635     cur_study = Study(  
2636         cur_param,  
2637         deck = cur_deck,  
2638         is_pulsed = is_pulsed,  
2639         is_consistent = is_consistent,  
2640         sensitivity = cur_sensitivity,  
2641         num_points = cur_num_points  
2642     )
```

2643 Note here that the equal signs inside the parentheses are called keyword arguments,
2644 which are common to most modern programming languages. After executing the
2645 command, the code will need to run for a few minutes.

2646 B.4.3 Extracting Results

2647 At this point, a user should have a completed sensitivity study they wish to plot.
2648 To make the plot useful, the study data structure first has to be unpacked and its
2649 contents cleaned. This is the goal of this subsection.

2650 First and foremost, a study has four families of reactors within it: beta-wall (i.e.

*Note that, currently, a pulsed reactor cannot be self-consistent in η_{CD} – it therefore causes an error.

2651 "wall"), beta-kink (i.e. "kink"), minimum capital cost (i.e. "W_M"), and minimum
2652 cost-per-watt (i.e. "cost"). Therefore, we will extract these reactor lists into a new
2653 dictionary data structure:

```
2654     cur_dict = Dict()  
2655  
2656     cur_dict["Beta-Wall"] = cur_study.wall_reactors  
2657     cur_dict["Beta-Kink"] = cur_study.kink_reactors  
2658  
2659     cur_dict["Min Cost per Watt"] = cur_study.cost_reactors  
2660     cur_dict["Min Capital Cost"] = cur_study.W_M_reactors
```

2661 Next, we will want to filter out all the invalid reactors that constitute non-physically
2662 realizable ones. These would likely be reactors that could fit in your hand or take up
2663 a whole city block.

```
2664     for (cur_key, cur_value) in cur_dict  
2665         cur_dict[cur_key] = filter(  
2666             cur_reactor -> cur_reactor.is_valid,  
2667             deepcopy(cur_value)  
2668         )  
2669     end
```

2670 B.4.4 Plotting Curves

2671 Our goal is now to turn our unpacked, clean reactor lists into plots – i.e. measuring
2672 costs-per-watt as a function of H. For simplicity, this will lack a lot of the features
2673 shown in the Jupyter notebook from the beginning of the section. Additionally, we
2674 will be doing it in an iterative process made possible by the Plots.jl framework.

2675 The first step is simply making a plot object

```
2676     cur_plot = plot()
```

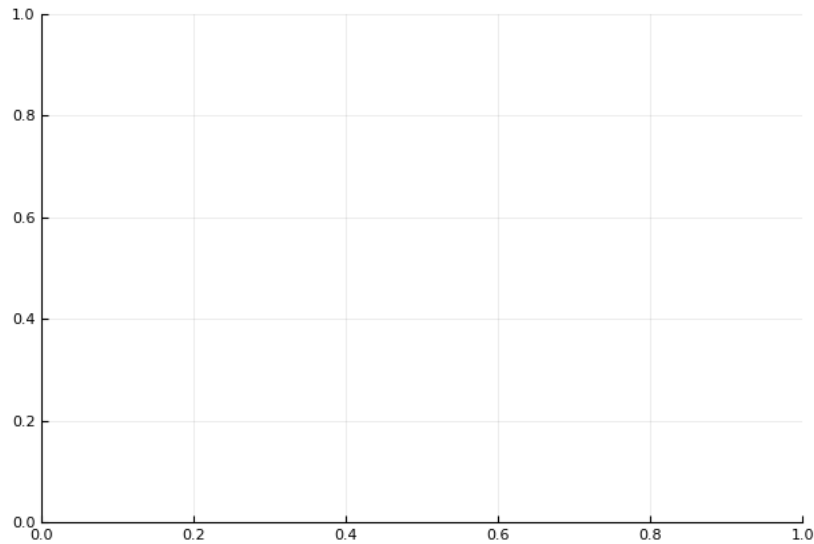


Figure B-1: A Blank Plot

A simple 2-D plot with no labels or data.

2677 After execution, this should produce the plank 2-D plot shown in Fig. B-1.

2678 Next we will add a simple title and labels for the axes:

```
2679     title!("Arc")
2680
2681     xlabel!("H")
2682     ylabel!("Cost")
```

2683 The exclamation marks ensure this title and the labels are added to the `cur_plot`.

2684 Upon execution, you should see a plot with this information (Fig. B-2).

2685 Now we will loop over the dictionary of reactors and add them one at a time.

```
2686     for (cur_key, cur_value) in cur_dict
2687         cur_x = map(cur_reactor -> cur_reactor.H, cur_value)
2688         cur_y = map(cur_reactor -> cur_reactor.cost, cur_value)
2689         plot!(cur_x, cur_y, label=cur_key)
2690     end
2691     plot!()
```

2692 This results in the not very useful plot shown in Fig. B-3. Note that each label is

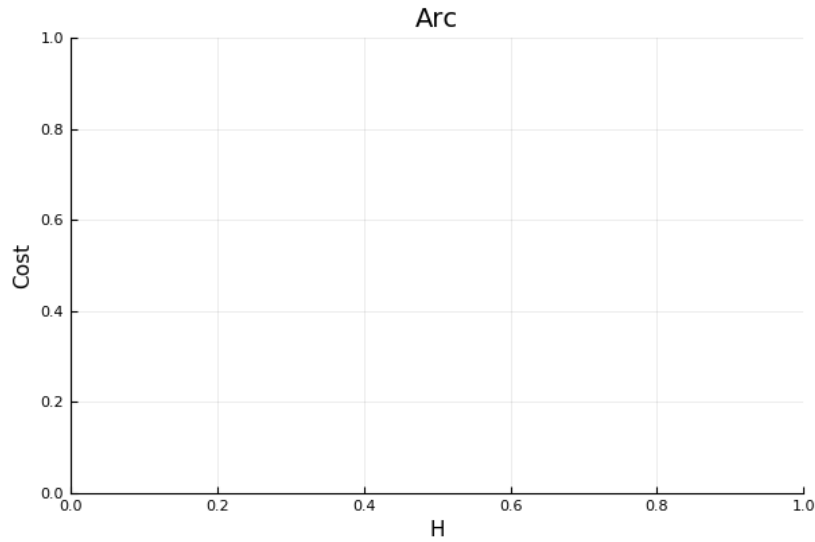


Figure B-2: An Empty Plot

A simple 2-D plot with labels, but no data.

2693 exactly the key assigned to it in `cur_dict`.

2694 The final step is adding proper limits to make what is going on obvious to the reader:

2695 `ylims!(0, 0.03)`

2696 The addition of which can be seen in Fig. B-4.

2697 This completes the example. At this point, you should now be able to use every
2698 feature of `Fussy.jl`. Good luck!

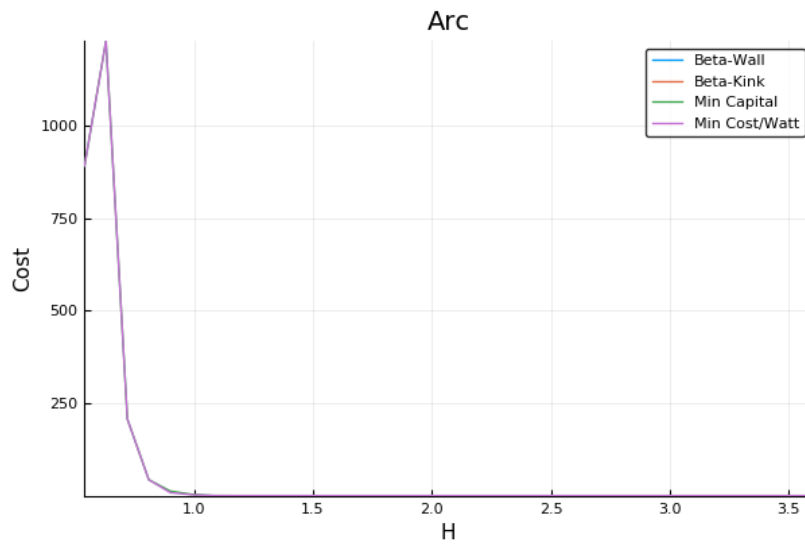


Figure B-3: An Unscaled Plot

A simple 2-D plot with Bad Limits.

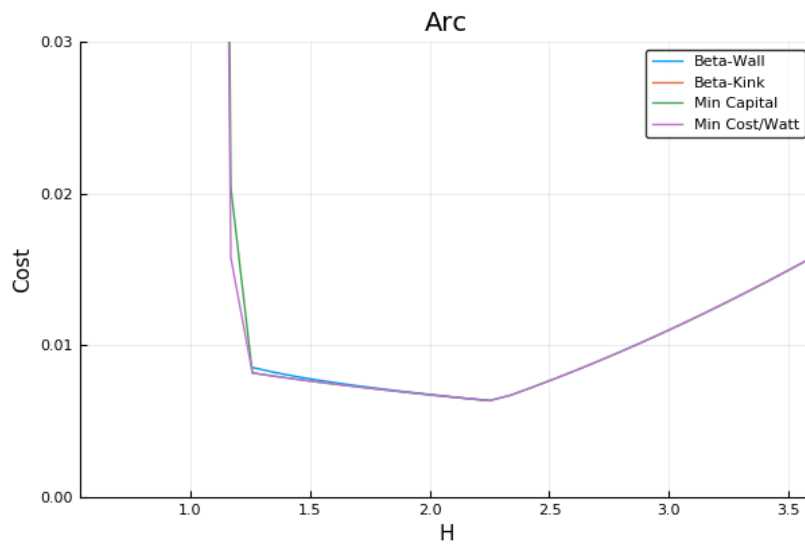


Figure B-4: A Scaled Plot

An example plot showing cost as a function of the H factor.

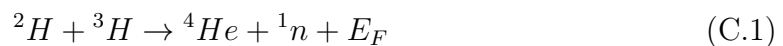
2699 Appendix C

2700 Discussing Fusion Power

2701 C.1 Fusion Power – P_F

2702 This requires a more first-principles approach than those used up until now. As such,
2703 a quick background is given to motivate the parameters it adds – i.e. the dilution
2704 factor (f_D) and the Bosch-Hale fusion reactivity (σv).

2705 The natural place to start when talking about fusion is the binding-energy per nucleon
2706 plot (see Fig. C-1). As can be seen, the function reaches a maximum value around the
2707 element Iron (A=56). What this means at a basic level is: elements lighter than iron
2708 can *fuse* into a heavier one (i.e. hydrogens into helium), whereas heavier elements
2709 can *fission* into lighter ones (e.g. uranium into krypton and barium). This is what
2710 differentiates fission (uranium-fueled) reactors from fusion (hydrogen-fueled) ones.
2711 For fusion reactors, the most common reaction in a first-generation tokamak will be:



2712

$$E_F = 17.6 \text{ MeV} \tag{C.2}$$

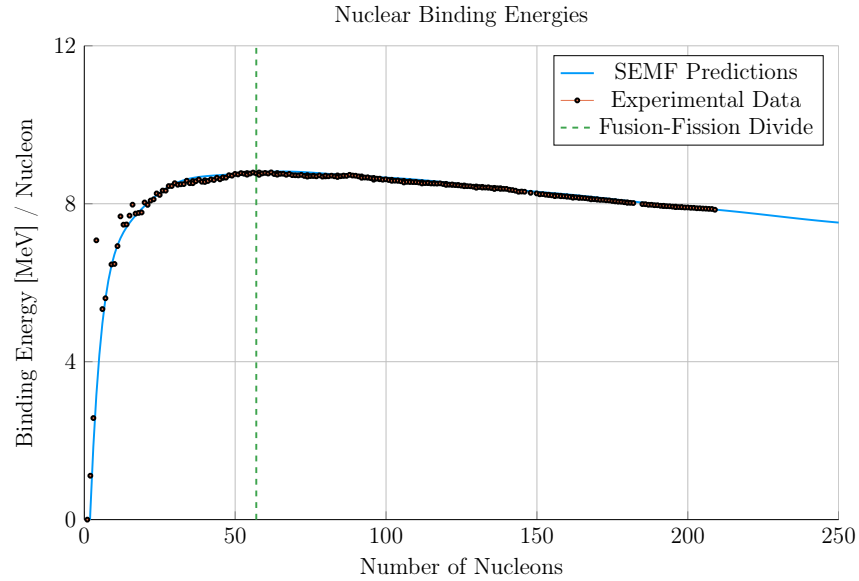


Figure C-1: Comparing Nuclear Fusion and Fission

The binding energy per nucleon is what differentiates nuclear fusion from fission. Nuclei heavier than Iron fission (e.g. Uranium), while light ones – such as Hydrogen – fuse.

2713 What this reaction describes is two isotopes of hydrogen – i.e. deuterium and tritium
 2714 – fusing into a heavier element, helium, while simultaneously ejecting a neutron. The
 2715 entire energy of the fusion reaction (E_F) is then divvied up 80-20 between the neutron
 2716 and helium, respectively. Quantitatively, the helium (hereafter referred to as an alpha
 2717 particle) receives 3.5 MeV.

2718 The final point to make before returning to the fusion power derivation is the main
 2719 difference between the two fusion products: helium (i.e. the alpha particle) and the
 2720 neutron. First, neutrons lack a charge – they are neutral. This means they cannot
 2721 be confined with magnetic fields. As such, they simply move in straight lines until
 2722 they collide with other particles. As the structure of a tokamak is mainly metal, the
 2723 neutron is much more likely to collide there than the gaseous plasma, which is orders
 2724 of magnitude less dense. Conversely, alpha particles are charged – when stripped of
 2725 their electrons – and can therefore be kept within the plasma using magnets. What
 2726 this means practically is that of the 17.6 MeV that comes from every fusion reaction,
 2727 only 3.5 MeV remains inside the plasma (within the helium particle species).

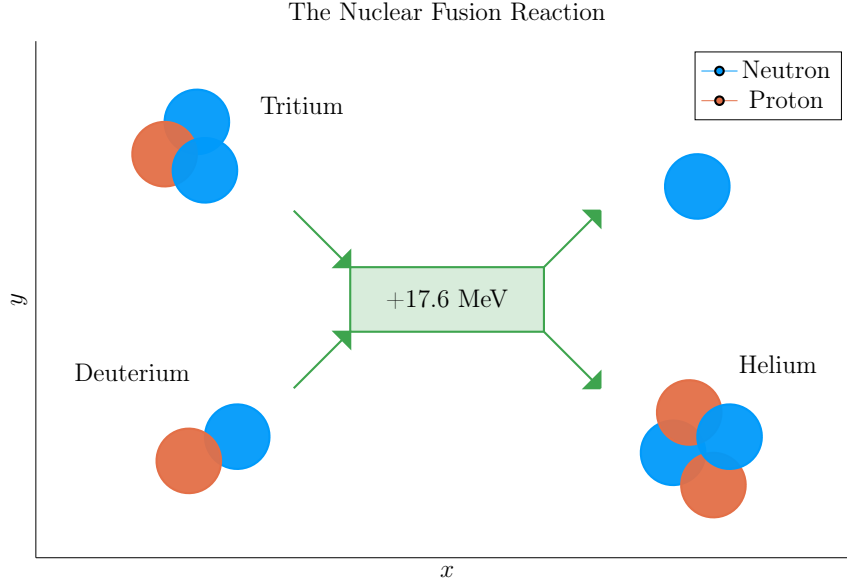


Figure C-2: The D-T Fusion Reaction

In a first generation tokamak reactor, the main source of energy will come from two hydrogen isotopes fusing into a helium particle – and ejecting a 14.1 MeV neutron.

As mentioned before, this fusion power is divided up 80-20 between the neutron and alpha particle. These relations will be used shortly. For now, they can be described mathematically as:

$$P_{\alpha} = 0.2 \cdot P_F \quad (\text{C.3})$$

$$P_n = 0.8 \cdot P_F \quad (\text{C.4})$$

C.2 Reactivity – $\langle \sigma v \rangle$

When discussing reactivity, the place to start is talking about fusion power,

$$P_F = \int E_F n_D n_T \langle \sigma v \rangle d\mathbf{r} \quad (\text{C.5})$$

For the tokamak geometry given, volume integrals can be reduced to 0-D forms.

2736 An arbitrary $F(\rho)$ has that:

$$F_V = 4 \pi^2 R_0 a^2 \kappa g \int_0^1 F(\rho) \rho d\rho \quad (\text{C.6})$$

2737 Given that $E_F = 17.6$ MeV and,

$$n_D = n_T = f_D \frac{n_e}{2} = \frac{f_D}{2} \cdot (\bar{n} (1 + \nu_n) (1 - \rho^2)^{\nu_n}) \quad (\text{C.7})$$

2738 Fusion power can be expressed as,

$$P_F = K_F \cdot (\bar{n}^2 R_0^3) \cdot (\sigma v) \quad [MW] \quad (\text{C.8})$$

2739

$$(\sigma v) = 10^{21} (1 + \nu_n)^2 \int_0^1 (1 - \rho^2)^{2\nu_n} \langle \sigma v \rangle \rho d\rho \quad (\text{C.9})$$

2740

$$K_F = 278.3 (f_D^2 \epsilon^2 \kappa g) \quad (\text{C.10})$$

2741 The Bosch-Hale parametrization of the volumetric reaction rates is then given by,^{30,31}

$$\langle \sigma v \rangle = C_1 \cdot \theta \cdot \exp(-3\xi) \cdot \sqrt{\frac{\xi}{m_\mu c^2 T^3}} \quad [\text{m}^3/\text{s}] \quad (\text{C.11})$$

2742

$$\theta = T \cdot \left(1 - \frac{T(C_2 + T(C_4 + TC_6))}{1 + T(C_3 + T(C_5 + TC_7))} \right)^{-1} \quad (\text{C.12})$$

2743

$$\xi = \left(\frac{B_G^2}{4\theta} \right)^{1/3} \quad (\text{C.13})$$

2744 Where approximate DT volumetric reaction rate ($10 \lesssim T [\text{keV}] \lesssim 20$)

$$\langle \sigma v \rangle_{\text{DT}} = 1.1 \times 10^{-24} \cdot T^2 \quad [\text{m}^3/\text{s}] \quad (\text{C.14})$$

2745 In our model, each appearance of T is set to the profile defined earlier.

Bosch-Hale parametrization coefficients for volumetric reaction rates

	${}^2\text{H}(\text{d},\text{n}){}^3\text{He}$	${}^2\text{H}(\text{d},\text{p}){}^3\text{H}$	${}^3\text{H}(\text{d},\text{n}){}^4\text{He}$	${}^3\text{He}(\text{d},\text{p}){}^4\text{He}$
B_G [keV $^{1/2}$]	31.3970	31.3970	34.3827	68.7508
$m_\mu c^2$ [keV]	937 814	937 814	1 124 656	1 124 572
C_1	5.43360×10^{-12}	5.65718×10^{-12}	1.17302×10^{-9}	5.51036×10^{-10}
C_2	5.85778×10^{-3}	3.41267×10^{-3}	1.51361×10^{-2}	6.41918×10^{-3}
C_3	7.68222×10^{-3}	1.99167×10^{-3}	7.51886×10^{-2}	-2.02896×10^{-3}
C_4	0.0	0.0	4.60643×10^{-3}	-1.91080×10^{-5}
C_5	-2.96400×10^{-6}	1.05060×10^{-5}	1.35000×10^{-2}	1.35776×10^{-4}
C_6	0.0	0.0	-1.06750×10^{-4}	0.0
C_7	0.0	0.0	1.36600×10^{-5}	0.0
Valid range (keV)	$0.2 < T_i < 100$	$0.2 < T_i < 100$	$0.2 < T_i < 100$	$0.5 < T_i < 190$

 Tabulated Bosch-Hale reaction rates [m 3 s $^{-1}$]

T (keV)	${}^2\text{H}(\text{d},\text{n}){}^3\text{He}$	${}^2\text{H}(\text{d},\text{p}){}^3\text{H}$	${}^3\text{H}(\text{d},\text{n}){}^4\text{He}$	${}^3\text{He}(\text{d},\text{p}){}^4\text{He}$
1.0	9.933×10^{-29}	1.017×10^{-28}	6.857×10^{-27}	3.057×10^{-32}
1.5	8.284×10^{-28}	8.431×10^{-28}	6.923×10^{-26}	1.317×10^{-30}
2.0	3.110×10^{-27}	3.150×10^{-27}	2.977×10^{-25}	1.399×10^{-29}
3.0	1.602×10^{-26}	1.608×10^{-26}	1.867×10^{-24}	2.676×10^{-28}
4.0	4.447×10^{-26}	4.428×10^{-26}	5.974×10^{-24}	1.710×10^{-27}
5.0	9.128×10^{-26}	9.024×10^{-26}	1.366×10^{-23}	6.377×10^{-27}
8.0	3.457×10^{-25}	3.354×10^{-25}	6.222×10^{-23}	7.504×10^{-26}
10.0	6.023×10^{-25}	5.781×10^{-25}	1.136×10^{-22}	2.126×10^{-25}
12.0	9.175×10^{-25}	8.723×10^{-25}	1.747×10^{-22}	4.715×10^{-25}
15.0	1.481×10^{-24}	1.390×10^{-24}	2.740×10^{-22}	1.175×10^{-24}
20.0	2.603×10^{-24}	2.399×10^{-24}	4.330×10^{-22}	3.482×10^{-24}

2746

Appendix D

2747

Selecting Plasma Profiles

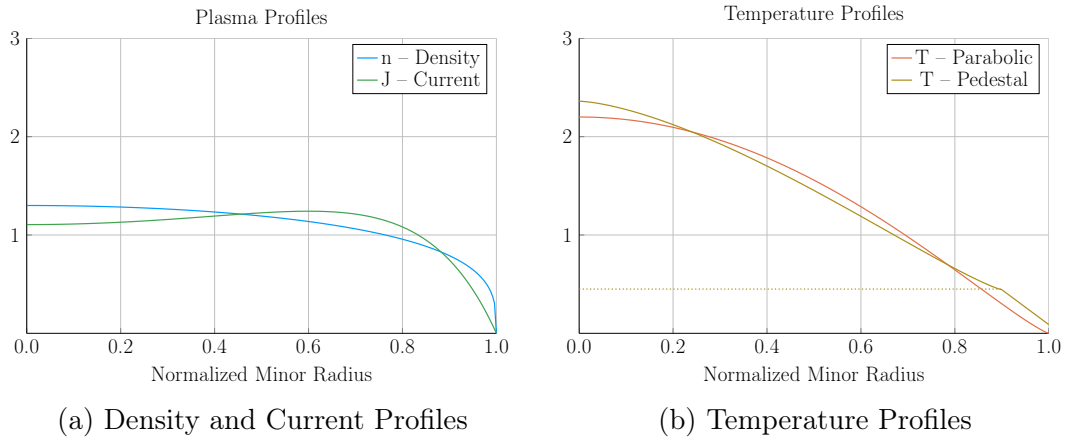


Figure D-1: Radial Plasma Profiles

The three most fundamental properties of a fusion plasma are its temperature, density, and current. These profiles allow the model to reduce from three dimensions to half of one.

2748

D.1 Density – n

2749

The Density is important to us. We use it in the Greenwald density limit, so it should

2750

be clean in both line-averaged and volume-averaged forms. Because of its flat profile,

2751

a parabola is a good approximation for H-mode pulses:

$$n(\rho) = \bar{n} \cdot (1 + \nu_n) \cdot (1 - \rho^2)^{\nu_n} \quad (\text{D.1})$$

2752 The line average density is related to \bar{n} through:

$$\hat{n} = \bar{n} \cdot \left(\frac{\pi^{1/2}}{2} \right) \cdot \frac{\Gamma(\nu_n + 2)}{\Gamma(\nu_n + 3/2)} \quad (\text{D.2})$$

2753 The convenience of this function comes from how the volumetric average comes out.

2754 To relate this to the volume integral, we use:

$$\bar{x} = \frac{1}{V} \int x(\rho) dV \quad (\text{D.3})$$

2755 For a normalized radial profile that does not depend on angle,

$$V = \int_0^1 \rho d\rho = 1/2 \quad (\text{D.4})$$

2756 Then, when $x = n$,

$$\bar{n} = 2 \int_0^1 n(\rho) \rho d\rho = \bar{n} \quad (\text{D.5})$$

2757 Additionally, the Greenwald Density limit that we will use throughout,

$$\hat{n} = N_G \cdot \left(\frac{I_M}{\pi a^2} \right) \quad (\text{D.6})$$

2758 can now be written in the following form:

$$\bar{n} = K_n \cdot \left(\frac{I_M}{R_0^2} \right) \quad (\text{D.7})$$

2759

$$K_n = \frac{2 N_G}{\epsilon^2 \pi^{3/2}} \cdot \left(\frac{\Gamma(\nu_n + 3/2)}{\Gamma(\nu_n + 2)} \right) \quad (\text{D.8})$$

2760 D.2 Temperature – T

2761 The Temperature is the swept variable in our model framework. Therefore, it's the
 2762 one we can allow people to be the most cavalier with. Additionally, as temperature
 2763 profiles are highly peaked, their pedestal region is sometimes wrongfully neglected
 2764 with a parabola.

$$T(\rho) = \bar{T} \cdot (1 + \nu_T) \cdot (1 - \rho^2)^{\nu_T} \quad (\text{D.9})$$

2765 Therefore, our model sometimes treats the system as if it had a pedestal region. This
 2766 is mainly for the bootstrap current and fusion power, which were previously known
 2767 to misalign and overshoot, respectively.

$$T(\rho) = \begin{cases} T_{para} , & x \in [0, \rho_{ped}] \\ T_{line} , & x \in (\rho_{ped}, 1] \end{cases} \quad (\text{D.10})$$

2768 Where the piecewise functions are given by,

$$T_{para} = T_{ped} + (T_0 - T_{ped}) \cdot \left(1 - \left(\frac{\rho}{\rho_{ped}} \right)^{\lambda_T} \right)^{\nu_T} \quad (\text{D.11})$$

2769

$$T_{line} = T_{sep} + (T_{ped} - T_{sep}) \cdot \left(\frac{1 - \rho}{1 - \rho_{ped}} \right) \quad (\text{D.12})$$

2770 This temperature profile is related to the volume-averaged temperature through,

$$\bar{T} \cdot V = \int_0^{\rho_{ped}} T_{para}(\rho) \rho d\rho + \int_{\rho_{ped}}^1 T_{line}(\rho) \rho d\rho \quad (\text{D.13})$$

2771 Starting with the second integral,

$$\int_{\rho_{ped}}^1 T_{line}(\rho) \rho d\rho = \frac{1}{3} \cdot (1 - \rho_{ped}) \cdot ((T_{sep} + T_{ped}/2) + \rho_{ped} \cdot (T_{ped} + T_{sep}/2)) \quad (D.14)$$

The first integral can be handled by breaking it into to,

$$\begin{aligned} \int_0^{\rho_{ped}} T_{para}(\rho) \rho d\rho &= T_{ped} \cdot \int_0^{\rho_{ped}} \rho d\rho + \\ &\quad (T_0 - T_{ped}) \cdot \int_0^{\rho_{ped}} \left(1 - \left(\frac{\rho}{\rho_{ped}}\right)^{\lambda_T}\right)^{\nu_T} \cdot \rho d\rho \end{aligned} \quad (D.15)$$

2772 The first sub-integral is then,

$$T_{ped} \cdot \int_0^{\rho_{ped}} \rho d\rho = \frac{T_{ped} \rho_{ped}^2}{2} \quad (D.16)$$

2773 Utilizing the following transformation,

$$u = \frac{\rho}{\rho_{ped}} \quad (D.17)$$

$$2774 \quad d\rho = \rho_{ped} du \quad (D.18)$$

$$2775 \quad u(\rho = \rho_{ped}) = 1 \quad (D.19)$$

2776 The second sub-integral becomes (assuming independence from T_0 and T_{ped}),

$$(T_0 - T_{ped}) \cdot \rho_{ped}^2 \cdot \int_0^1 (1 - u^{\lambda_T})^{\nu_T} \cdot u du \quad (D.20)$$

2777 Where:

$$\int_0^1 (1 - u^{\lambda_T})^{\nu_T} \cdot u du = \frac{\Gamma(1 + \nu_T) \Gamma\left(\frac{2}{\lambda_T}\right)}{\lambda_T \cdot \Gamma\left(1 + \nu_T + \frac{2}{\lambda_T}\right)} \quad (D.21)$$

2778 We are now in a position to solve for T_0 in terms of \bar{T} :

$$T_0 = T_{ped} + \frac{\bar{T} - K_{TU}}{K_{TD}} \quad (D.22)$$

$$K_{TU} = T_{ped} \rho_{ped}^2 + \frac{(1 - \rho_{ped})}{3} \cdot ((2T_{sep} + T_{ped}) + \rho_{ped} \cdot (2T_{ped} + T_{sep})) \quad (D.23)$$

$$K_{TD} = \rho_{ped}^2 \cdot \left(\frac{2}{\lambda_T} \right) \cdot \frac{\Gamma(1 + \nu_T) \Gamma\left(\frac{2}{\lambda_T}\right)}{\Gamma\left(1 + \nu_T + \frac{2}{\lambda_T}\right)} \quad (D.24)$$

2781 Which although not pretty, can be plugged into the original equation.

2782 D.3 Pressure – p

2783 The first point to make is that we are not using the same temperature profile for
2784 the pressure as for the temperature. This is because it would lead to hypergeometric
2785 functions that are not worth the headache.

2786 As most of the pressure is at the center, we use simple parabolic profile. This leads
2787 to:

$$\bar{p} = 0.1581 (1 + f_D) \frac{(1 + \nu_n)(1 + \nu_T)}{1 + \nu_n + \nu_T} \bar{n} \bar{T} \quad [atm] \quad (D.25)$$

2788 D.4 Bootstrap Current – f_{BS}

2789 We start with,

$$f_{BS} = \frac{I_{BS}}{I_P} = \frac{2\pi a^2 \kappa}{I_P} \int_0^1 J_B \rho d\rho \quad (D.26)$$

2790 Expanding the previous equation using the following relations,

$$J_B = -4.85 \cdot R_0 \epsilon^{1/2} \cdot \left(\frac{\rho^{1/2} n T}{d\psi/d\rho} \right) \cdot \left(\frac{dn/d\rho}{n} + 0.54 \cdot \frac{dT/d\rho}{T} \right) \quad (D.27)$$

2791

$$\frac{d\psi}{d\rho} = \frac{\mu_0 R_0 I_P}{\pi} \cdot \left(\frac{\kappa}{1 + \kappa^2} \right) \cdot b_p(\rho) \quad (D.28)$$

2792 Yields:

$$f_{BS} = -K_{BS} \int_0^1 (1 - \rho^2)^{\nu_n} \cdot \left(\frac{\rho^{3/2}}{b_p(\rho)} \right) \cdot \left(\frac{T}{n} \cdot \frac{dn}{d\rho} + 0.54 \cdot \frac{dT}{d\rho} \right) d\rho \quad (D.29)$$

2793

$$K_{BS} = K_n \cdot \left(\frac{2\pi^2 \cdot 4.85 \cdot \epsilon^{5/2}}{\mu_0} \right) \cdot (1 + \nu_n) \cdot (1 + \kappa^2) \quad (D.30)$$

2794 Here, b_p comes from:

$$b_p(\rho) = \frac{-e^{\gamma\rho^2}(\gamma\rho^2 - 1 - \gamma) - 1 - \gamma}{\rho(e^\gamma - 1 - \gamma)} \quad (D.31)$$

2795 And the value of γ comes from the the normalized internal inductance:

$$l_i = \frac{4\kappa}{1 + \kappa^2} \int_0^1 b_p^2 \frac{d\rho}{\rho} \quad (D.32)$$

2796 With our profiles,

$$-\left(\frac{T}{n} \cdot \frac{dn}{d\rho} \right) = 2\nu_n \cdot \left(\frac{T \cdot \rho}{1 - \rho^2} \right) \quad (D.33)$$

2797 While treating temperature differently results in,

$$-\left(\frac{dT}{d\rho} \right)_{para} = \left(\frac{T_0 - T_{ped}}{\rho_{ped}^{\lambda_T}} \right) \cdot (\nu_T \lambda_T) \cdot \rho^{\lambda_T - 1} \cdot \left(1 - \left(\frac{\rho}{\rho_{ped}} \right)^{\lambda_T} \right)^{\nu_T - 1} \quad (D.34)$$

2798

$$-\left(\frac{dT}{d\rho} \right)_{line} = \left(\frac{T_{ped} - T_{sep}}{1 - \rho_{ped}} \right) \quad (D.35)$$

2799 Where we will be using the new symbol definition,

$$\partial T = - \left(\frac{dT}{d\rho} \right) \quad (D.36)$$

Which ultimately allows us to write,

$$f_{BS} = K_{BS} \int_0^1 H_{BS} d\rho \quad (D.37)$$

$$H_{BS} = (1 - \rho^2)^{\nu_n - 1} \cdot \left(\frac{\rho^{3/2}}{b_p(\rho)} \right) \cdot \left(2\nu_n \cdot \rho \cdot T + 0.54 \cdot (1 - \rho^2) \cdot \partial T \right) \quad (D.38)$$

2800 Where the values of T are determined through,

$$T_{para} = T_{ped} + (T_0 - T_{ped}) \cdot \left(1 - \left(\frac{\rho}{\rho_{ped}} \right)^{\lambda_T} \right)^{\nu_T} \quad (D.39)$$

2801

$$T_{line} = T_{sep} + (T_{ped} - T_{sep}) \cdot \left(\frac{1 - \rho}{1 - \rho_{ped}} \right) \quad (D.40)$$

2802 And the values of ∂T are:

$$\partial T_{para} = \left(\frac{T_0 - T_{ped}}{\rho_{ped}^{\lambda_T}} \right) \cdot (\nu_T \lambda_T) \cdot \rho^{\lambda_T - 1} \cdot \left(1 - \left(\frac{\rho}{\rho_{ped}} \right)^{\lambda_T} \right)^{\nu_T - 1} \quad (D.41)$$

2803

$$\partial T_{line} = \left(\frac{T_{ped} - T_{sep}}{1 - \rho_{ped}} \right) \quad (D.42)$$

2804 D.5 Volume Averaged Powers

2805 The first thing to consider in a fusion reactor is power balance.

2806 It is what separates a profitable device from a toaster. It's given by:

$$P_\alpha + P_H = P_\kappa + P_B \quad (D.43)$$

2807

$$P_\alpha = \frac{P_F}{5} \quad (\text{D.44})$$

2808

$$P_H = \frac{P_F}{Q} \quad (\text{D.45})$$

2809

$$P_\kappa = \frac{3}{2\tau_E} \int p \, d\mathbf{r} \quad [3D] \quad (\text{D.46})$$

2810

$$P_B = 5.35e3 \, Z_{eff} \int n_{\bar{n}}^2 \sqrt{T} \, d\mathbf{r} \quad [3D] \quad (\text{D.47})$$

2811 As mentioned before, P_F is handled by (σv) and therefore the lefthand-side uses the
 2812 pedestal temperature profiles. However, for the same reasons as discussed earlier, the
 2813 righthand-side (P_κ and P_B) need to use the parabolic temperature profiles.

2814 Using the parabolic profiles (for n and T) gives for the Bremsstrahlung radiation,

$$P_B = K_B \cdot \left(R_0^3 \bar{n}^2 \sqrt{\bar{T}} \right) \quad [MW] \quad (\text{D.48})$$

2815

$$K_B = 0.1056 \cdot Z_{eff} \cdot (\epsilon^2 \kappa g) \cdot \frac{(1 + \nu_n)^2 (1 + \nu_T)^{1/2}}{1 + 2\nu_n + 0.5\nu_T} \quad (\text{D.49})$$

2816 And a similar exercise for the thermal conduction losses results in:

$$P_\kappa = K_\kappa \cdot \left(\frac{R_0^3 \bar{n} \bar{T}}{\tau_E} \right) \quad [MW] \quad (\text{D.50})$$

2817

$$K_\kappa = 0.4744 \cdot (1 + f_D) \cdot (\epsilon^2 \kappa g) \cdot \frac{(1 + \nu_n)(1 + \nu_T)}{1 + \nu_n + \nu_T} \quad (\text{D.51})$$

2818 Appendix E

2819 Determining Plasma Flux Surfaces

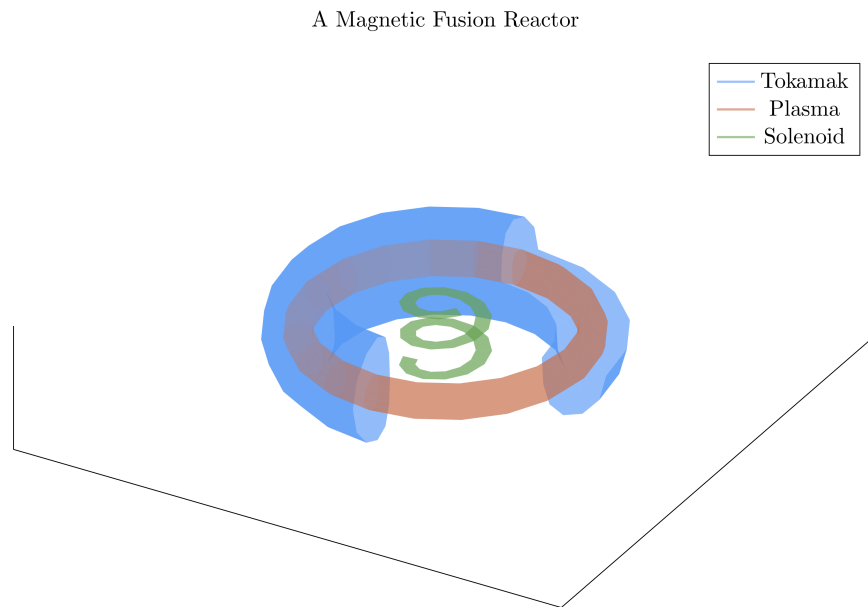


Figure E-1: Cut-Away of Tokamak Reactor

The three main components of a magnetic fusion reactor are: the tokamak structure, the plasma fuel, and the spring-like solenoid at the center.

2820 E.1 Flux Surface Coordinates

2821 We begin with the shape of the outer plasma surface (i.e. the 95% flux surface)
2822 written in terms of normalized coordinates x and y as follows – with α being an

2823 angle-like coordinate:

$$R = R_0 + ax(\alpha) \quad (\text{E.1})$$

2824

$$Z = ay(\alpha) \quad (\text{E.2})$$

2825

$$0 \leq \alpha \leq 2\pi \quad (\text{E.3})$$

2826 The surface representation can now be written as:

$$x(\alpha) = c_0 + c_1 \cos(\alpha) + c_2 \cos(2\alpha) + c_3 \cos(3\alpha) \quad (\text{E.4})$$

2827

$$y(\alpha) = \kappa \sin(\alpha) \quad (\text{E.5})$$

2828 The constraints determining c_j – for $j = 1, 2, 3$ – are chosen as:

$$x(0) = 1 \quad (\text{E.6})$$

2829

$$x(\pi) = -1 \quad (\text{E.7})$$

2830

$$x\left(\frac{\pi}{2}\right) = -\delta \quad (\text{E.8})$$

2831

$$x_{\alpha\alpha}(\pi) = 0.3 \cdot (1 - \delta^2) \quad (\text{E.9})$$

2832 The last constraint, which is related to the surface curvature at $\alpha = \pi$, is chosen to
 2833 make sure that the surface is always convex. A trial and error empirical fit resulted
 2834 in the choice $x_{\alpha\alpha}(\pi) = 0.3 \cdot (1 - \delta^2)$. The constraint relations are easily evaluated and
 2835 then solved, leading to values for the c_j ,

$$c_0 = -\frac{\delta}{2} \quad (\text{E.10})$$

2836

$$c_1 = g \quad (\text{E.11})$$

2837

$$c_2 = \frac{\delta}{2} \quad (\text{E.12})$$

2838

$$c_3 = 1 - g \quad (\text{E.13})$$

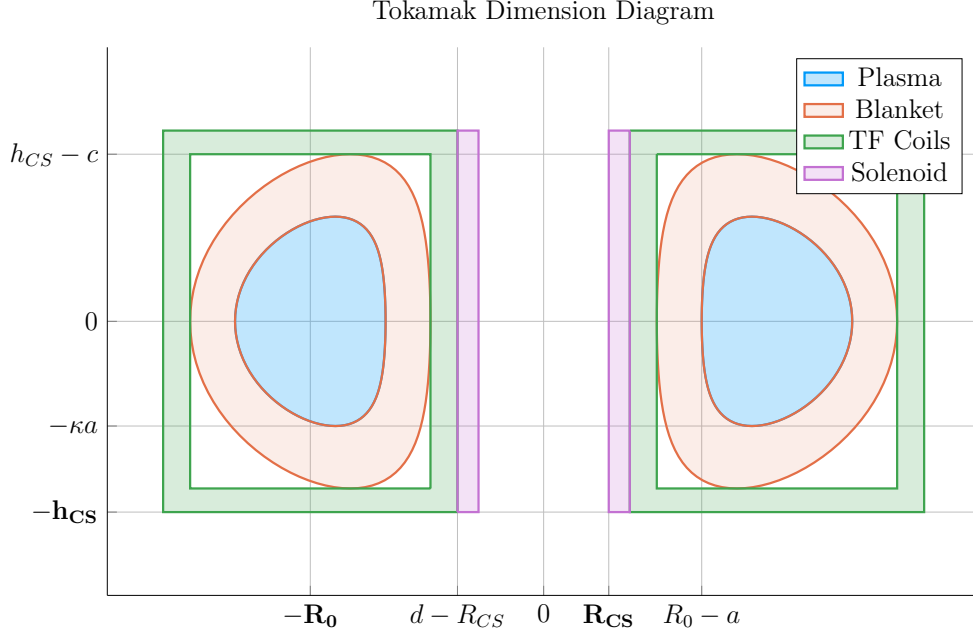


Figure E-2: Dimensions of Tokamak Cross-Section

Here, g is a shaping parameter approximately equal to one:

$$g = \frac{9 - 2\delta - 0.3 \cdot (1 - \delta^2)}{8} \quad (\text{E.14})$$

E.2 Cross-sectional Area and Volume

The plasma cross-sectional area and volume can be evaluated by straightforward calculations,

$$\begin{aligned} A &= \int \int dR dZ = a^2 \int \int dx dy = a^2 \int_0^{2\pi} x \frac{dy}{d\alpha} d\alpha \\ &= \pi a^2 \kappa g \end{aligned} \quad (\text{E.15})$$

$$\begin{aligned} V &= \int \int \int R dR dZ d\Phi = 2\pi a^2 \int \int R dx dy \\ &= 2\pi a^2 R_0 \int_0^{2\pi} \left(x + \epsilon \frac{x^2}{2} \right) \frac{dy}{d\alpha} d\alpha \approx 2\pi a^2 R_0 \int_0^{2\pi} x \frac{dy}{d\alpha} d\alpha \\ &= 2\pi^2 R_0 a^2 \kappa g \end{aligned} \quad (\text{E.16})$$

2844 The second form of the volume integral makes use of the small inverse aspect ratio
 2845 expansion, $\epsilon \ll 1$, which is a good approximation and used throughout the analysis.

2846 E.3 Surface and Volume Integrals

2847 Eqs. (E.4) and (E.5) are simple formulas describing the shape of the outer plasma
 2848 surface. We next modify the model so that it gives a plausible description of the
 2849 interior flux surfaces as well. The idea is to introduce a normalized flux label, which
 2850 is radial-like in behavior. This label is denoted by ρ and $\rho \in [0, 1]$ with $\rho = 1$ being
 2851 the outer plasma surface (i.e. the 95% surface) and $\rho = 0$ being the magnetic axis.
 2852 Additional trial and error results in the following representation for the flux surfaces,

$$x(\rho, \alpha) = \sigma(1 - \rho^2) + c_0\rho^4 + c_1\rho \cos(\alpha) + c_2\rho^2 \cos(2\alpha) + c_3\rho^3 \cos(3\alpha) \quad (\text{E.17})$$

2853

$$y(\rho, \alpha) = \kappa\rho \sin(\alpha) \quad (\text{E.18})$$

2854 with σ being the shift of the magnetic axis. Usually, $\sigma \sim 0.1$ for a high field tokamak.
 2855 Lastly, we note that in the course of the work it will be necessary to integrate functions
 2856 of ρ over the volume and cross-sectional area of the plasma. Specifically we will need
 2857 to evaluate:

$$Q_V = \int \int \int Q(\rho) R dR dZ d\Phi \approx 2\pi R_0 a^2 \int \int Q(\rho) dx dy \quad (\text{E.19})$$

2858

$$Q_A = \int \int Q(\rho) dR dZ = a^2 \int \int Q(\rho) dx dy \quad (\text{E.20})$$

2859 Here, $Q(\rho)$ is an arbitrary function of ρ such as pressure or temperature. In the large
 2860 aspect ratio limit, both integrals require the evaluation of the same quantity:

$$K = \int \int Q(\rho) dx dy \quad (\text{E.21})$$

2861 To evaluate this integral, we need to convert from x, y coordinates to ρ, α coordinates.

2862 Using the Jacobian of the transformation leads to

$$K = \int \int Q(\rho)(x_\rho y_\alpha - x_\alpha y_\rho) d\rho d\alpha \quad (\text{E.22})$$

2863 Here,

$$\begin{aligned} x_\rho y_\alpha - x_\alpha y_\rho = & \kappa \sin(\alpha) \cdot (c_1 \rho \sin(\alpha) + 2c_2 \rho^2 \sin(2\alpha) + 3c_3 \rho^3 \sin(3\alpha)) \\ & + \kappa \rho \cos(\alpha) \cdot \left[\right. \\ & \quad - 2\rho\sigma + 4\rho^3 c_0 + c_1 \cos(\alpha) \\ & \quad + 2c_2 \rho \cos(2\alpha) + 3c_3 \rho^2 \cos(3\alpha) \\ & \left. \right] \end{aligned} \quad (\text{E.23})$$

2864 Since Q is only a function of ρ , the α integral can be carried out analytically. The
2865 only term that survives the averaging are the ones containing c_1 . A simple integration
2866 over α then yields the desired results:

$$Q_V = 4\pi^2 R_0 a^2 \kappa g \int_0^1 Q(\rho) \rho d\rho \quad (\text{E.24})$$

2867

$$Q_S = 2\pi a^2 \kappa g \int_0^1 Q(\rho) \rho d\rho \quad (\text{E.25})$$

2868

2869 Appendix F

2870 Expanding on the Bootstrap Current

2871 The bootstrap current fraction – f_{BS} – is an important parameter that enters in
2872 the design of tokamak reactors. It must be calculated with reasonable accuracy to
2873 determine how much external current drive is required. The value of f_{BS} thus has
2874 a strong impact on the overall fusion energy gain. Obtaining reasonable accuracy
2875 requires a moderate amount of analysis, which is presented in a following section.
2876 The results are summarized below.

2877 F.1 Summarized Results

2878 The analysis is based on an expression for the bootstrap current valid for arbitrary
2879 cross section assuming (1) equal temperature electrons and ions $T_e = T_i = T$, (2) large
2880 aspect ratio $\epsilon \ll 1$, and (3) negligible collisionality $\nu_* \rightarrow 0$. Under these assumptions
2881 the bootstrap current $\mathbf{J}_{BS} \approx J_{BS} \mathbf{e}_\phi$ has the form

$$J_{BS} = -3.32 f_T R_0 n T \left(\frac{1}{n} \frac{dn}{d\psi} + 0.054 \frac{1}{T} \frac{dT}{d\psi} \right) \quad (\text{F.1})$$

2882 Here, $f_T \approx 1.46(r/R_0)^{1/2}$ is an approximate expression for the trapped particle frac-
2883 tion and ψ is the poloidal flux.

2884 The analysis next section shows that Eq. (F.1) leads to an expression for the bootstrap
 2885 fraction, assuming for simplicity elliptical flux surfaces, that can be written as:

$$f_{BS} = \frac{I_{BS}}{I} = \frac{2\pi a^2 \kappa}{I} \int_0^1 J_{BS} \rho d\rho = \frac{K_{BS}}{K_n} \frac{\bar{n} \bar{T} R_0^2}{I_P^2} \quad (\text{F.2})$$

$$K_{BS} = 4.879 \cdot K_n \cdot \left(\frac{1 + \kappa^2}{2} \right) \cdot \epsilon^{5/2} \cdot H_{BS} \quad (\text{F.3})$$

$$H_{BS} = (1 + \nu_n)(1 + \nu_T)(\nu_n + 0.054\nu_T) \int_0^1 \frac{\rho^{5/2} (1 - \rho^2)^{\nu_n + \nu_T - 1}}{b_p} d\rho \quad (\text{F.4})$$

$$b_p(\rho) = \frac{-e^{\gamma \rho^2} (\gamma \rho^2 - 1 - \gamma) - 1 - \gamma}{\rho (e^\gamma - 1 - \gamma)} \quad (\text{F.5})$$

$$\bar{J}_\phi(\rho) = -\frac{I}{\pi a^2 \kappa} \left[\frac{\gamma^2 (1 - \rho^2) e^{\gamma \rho^2}}{e^\gamma - 1 - \gamma} \right] \quad (\text{F.6})$$

2890 In this expression b_p is a normalized form of the poloidal magnetic field derived from
 2891 a prescribed model for the *total* flux surface averaged current density profile $\bar{J}_\phi(\rho)$.
 2892 The $\bar{J}_\phi(\rho)$ profile, in analogy with the density and temperature profiles, is not self-
 2893 consistent but is chosen to have a plausible experimental shape characterized by the
 2894 parameter γ . The profile can have either an on-axis ($\gamma < 1$) or off-axis peak ($\gamma > 1$).
 2895 The normalized internal inductance l_i and radial location of the current peak ρ_m are
 2896 related to the value of γ by:

$$\frac{4\kappa}{1 + \kappa^2} \int_0^1 b_p^2 \frac{d\rho}{\rho} \quad (\text{F.7})$$

$$\rho_m = \begin{cases} \left(\frac{\gamma}{\gamma - 1} \right)^{1/2}, & \gamma > 1 \\ 0, & \gamma < 1 \end{cases} \quad (\text{F.8})$$

2898 F.2 Detailed Analysis

2899 The starting point for the analysis is the general expression for the bootstrap current
 2900 in a tokamak with arbitrary cross section.³² This expression can be simplified by

2901 assuming (1) equal temperature electrons and ions $T_e = T_i = T$, (2) large aspect ratio
 2902 $\epsilon \ll 1$, and (3) negligible collisionality $\nu_* \rightarrow 0$. The bootstrap current $\mathbf{J}_{BS} \approx J_{BS} \mathbf{e}_\phi$
 2903 reduces to

$$J_{BS} = -3.32 f_T R_0 n T \left(\frac{1}{n} \frac{dn}{d\psi} + 0.054 \frac{1}{T} \frac{dT}{d\psi} \right) \quad (\text{F.9})$$

2904 Several values of the trapped particle fraction f_T have been given in the literature.³³
 2905 For simplicity we use a form valid for large aspect ratio. This is a slightly optimistic
 2906 value but saves a large amount of detailed calculation. It can be written as,

$$f_T \approx 1.46 (r/R_0)^{1/2} = 1.46 \epsilon^{1/2} \rho^{1/2} \quad (\text{F.10})$$

2907 Here, as in the main text, ρ is a radial-like flux surface label that varies between
 2908 $0 \leq \rho \leq 1$. In other words $\psi = \psi(\rho)$. Under these assumptions the bootstrap current
 2909 reduces to:

$$J_{BS} = -4.85 R_0 \epsilon^{1/2} \left(\frac{\rho^{1/2} n T}{d\psi/d\rho} \right) \left(\frac{1}{n} \frac{dn}{d\rho} + 0.054 \frac{1}{T} \frac{dT}{d\rho} \right) \quad (\text{F.11})$$

2910 Since we have specified profiles for $n(\rho)$ and $T(\rho)$ all that remains in order to be able
 2911 to evaluate $J_{BS}(\rho)$ is to determine $\psi' = d\psi/d\rho$. Keep in mind that at this point, in
 2912 spite of the approximations that have been made, the expression for $J_{BS}(\rho)$ is still
 2913 valid for arbitrary cross section.

2914 The analysis that follows shows how to calculate ψ' for an arbitrary cross section
 2915 including finite aspect ratio. As an example an explicit expression for large aspect
 2916 ratio, finite elongation ellipse is obtained. Consider the Grad-Shafranov equation for
 2917 the flux: $\Delta^* \psi = -\mu_0 R J_\psi$. We integrate this equation over the volume of an arbitrary
 2918 flux surface making use of Gauss' theorem, which leads to:

$$\int_S \frac{\mathbf{n} \cdot \nabla \psi}{R^2} dS = -\mu_0 \int_V \frac{J_\phi}{R} d\mathbf{r} \quad (\text{F.12})$$

2919 Next, assume that the coordinates of the flux surface can be expressed in terms of ρ
 2920 and an angular-like parameter α with $0 \leq \alpha \leq 2\pi$. In other words, the flux surface

coordinates can be written as $R = R(\rho, \alpha) = R_0 + ax(\rho, \alpha)$ and $Z = Z(\rho, \alpha) = ay(\rho, \alpha)$. The functions $R(\rho, \alpha)$ and $Z(\rho, \alpha)$ are assumed to be known. The term on the left hand side can be evaluated by noting that

$$dl = dlt \quad (\text{F.13})$$

$$dl = (R_\alpha^2 + Z_\alpha^2)^{1/2} d\alpha \quad (\text{F.14})$$

$$\mathbf{t} = \frac{R_\alpha \mathbf{e}_R + Z_\alpha \mathbf{e}_Z}{(R_\alpha^2 + Z_\alpha^2)^{1/2}} \quad (\text{F.15})$$

$$\mathbf{n} = \mathbf{e}_\phi \times \mathbf{t} = \frac{Z_\alpha \mathbf{e}_R - R_\alpha \mathbf{e}_Z}{(R_\alpha^2 + Z_\alpha^2)^{1/2}} \quad (\text{F.16})$$

$$dS = R d\phi dl = 2\pi R (R_\alpha^2 + Z_\alpha^2)^{1/2} d\alpha \quad (\text{F.17})$$

It then follows that

$$\mathbf{n} \cdot \nabla \psi = \frac{1}{(R_\alpha^2 + Z_\alpha^2)^{1/2}} \left(Z_\alpha \frac{\partial \psi}{\partial R} - R_\alpha \frac{\partial \psi}{\partial Z} \right) = \frac{1}{(R_\alpha^2 + Z_\alpha^2)^{1/2}} \frac{d\psi}{d\rho} Z_\alpha \rho_R - R_\alpha \rho_Z \quad (\text{F.18})$$

We can rewrite the last term by noting that

$$\begin{aligned} dR = R_\rho d\rho + R_\alpha d\alpha &\rightarrow d\rho = (Z_\alpha dR - R_\alpha dZ) / (R_\rho Z_\alpha - R_\alpha Z_\rho) \\ dZ = Z_\rho d\rho + Z_\alpha d\alpha &\rightarrow d\alpha = (-Z_\rho dR + R_\rho dZ) / (R_\rho Z_\alpha - R_\alpha Z_\rho) \end{aligned} \quad (\text{F.19})$$

from which follows

$$\begin{aligned} \rho_R &= \frac{Z_\alpha}{(R_\rho Z_\alpha - R_\alpha Z_\rho)} \\ \rho_Z &= -\frac{R_\alpha}{(R_\rho Z_\alpha - R_\alpha Z_\rho)} \end{aligned} \quad (\text{F.20})$$

the normal gradient reduces to

$$\mathbf{n} \cdot \nabla \psi = \frac{R_\alpha^2 + Z_\alpha^2}{(R_\rho Z_\alpha - R_\alpha Z_\rho)} \frac{d\psi}{d\rho} \quad (\text{F.21})$$

2932 Using this relation we see that the left hand side of Eq. (F.12) can now be written as:

$$\int_S \frac{\mathbf{n} \cdot \nabla \psi}{R^2} dS = 2\pi \frac{d\psi}{d\rho} \int_0^{2\pi} \frac{R_\alpha^2 + Z_\alpha^2}{(R_\rho Z_\alpha - R_\alpha Z_\rho)} \frac{d\alpha}{R} \quad (\text{F.22})$$

2933 Consider now the right hand side of Eq. (F.12). The critical assumption is that the
 2934 current density is approximated by its flux surface averaged value, $J_\phi(\rho, \alpha) \approx \bar{J}_\phi(\rho)$.
 2935 This is obviously not self-consistent with the Grad-Shafranov equation. Even so, it
 2936 should suffice for present purposes where we only need to evaluate global volume
 2937 integrals. Also, in the same spirit as prescribing $n(\rho)$ and $T(\rho)$ we assume that $\bar{J}_\phi(\rho)$
 2938 is also prescribed. Under these assumptions the right hand side of Eq. (F.12) simplifies
 2939 to:

$$\begin{aligned} -\mu_0 \int_V \frac{J_\phi}{R} d\mathbf{r} &= -2\pi\mu_0 \int_A J_\phi dA \\ &= -2\pi\mu_0 \int_0^\rho d\rho \int_0^{2\pi} J_\phi (R_\rho Z_\alpha - R_\alpha Z_\rho) d\alpha \\ &\approx -2\pi\mu_0 \int_0^\rho d\rho \left[\bar{J}_\phi \int_0^{2\pi} (R_\rho Z_\alpha - R_\alpha Z_\rho) d\alpha \right] \end{aligned} \quad (\text{F.23})$$

2940 Combining the results in Eqs. (F.22) and (F.23) leads to the required general expres-
 2941 sion for $d\psi/d\rho$,

$$\frac{d\psi}{d\rho} \int_0^{2\pi} \frac{R_\alpha^2 + Z_\alpha^2}{(R_\rho Z_\alpha - R_\alpha Z_\rho)} \frac{d\alpha}{R} = -\mu_0 \int_0^\rho d\rho \left[\bar{J}_\phi \int_0^{2\pi} (R_\rho Z_\alpha - R_\alpha Z_\rho) d\alpha \right] \quad (\text{F.24})$$

2942 Next, to help specify a plausible choice for \bar{J}_ϕ it is useful to define the kink safety
 2943 factor and the actual local safety factor. The kink safety factor is defined by

$$q_* = \frac{2\pi a^2 B_0}{\mu_0 R_0 I} \left(\frac{1 + \kappa^2}{2} \right) \quad (\text{F.25})$$

2944 where

$$I = \int J_o dA = \int_0^1 d\rho \left[\bar{J}_o \int_0^{2\pi} (R_\rho Z_\alpha - R_\alpha Z_\rho) d\alpha \right] \quad (\text{F.26})$$

2945 This leads to

$$\frac{1}{q_*} = \frac{\mu_0 R_0}{2\pi a^2 B_0} \left(\frac{2}{1 + \kappa^2} \right) \int_0^1 d\rho \left[\bar{J}_\phi \int_0^{2\pi} (R_\rho Z_\alpha - R_\alpha Z_\rho) d\alpha \right] \quad (\text{F.27})$$

2946 Similarly, the local safety factor can be expressed as

$$q(\rho) = \frac{F(\rho)}{2\pi} \int \frac{dl}{RB_p} \quad (\text{F.28})$$

2947 Here, $F(\rho) = RB_o$. Substituting $RB_p = \mathbf{n} \cdot \nabla \psi$ then yields

$$q(\rho) = \frac{F(\rho)}{2\pi \psi'} \int_0^{2\pi} \frac{1}{R} (R_\rho Z_\alpha - R_\alpha Z_\rho) d\alpha \quad (\text{F.29})$$

2948 with $\psi' = d\psi/d\rho$.

2949 For present purposes we can obtain relatively simple analytic expressions for all the
 2950 quantities of interest by assuming the flux surfaces are concentric ellipses, character-
 2951 ized by $R = R_0 + a\rho \cos \alpha$ and $Z = \kappa a\rho \sin \alpha$. We assume low β so that $F(\rho) \approx R_0 B_0$.
 2952 This model accounts for elongation but neglects the effects of triangularity and finite
 2953 aspect ratio. The derivatives in Eqs. (F.24), (F.27) and (F.29) can now be easily
 2954 evaluated. Also, after some trial and error we chose $\bar{J}_\phi(\rho)$ to be a plausible profile
 2955 which is peaked off-axis at $\rho = \rho_m$.

$$\bar{J}_\phi(\rho) = -\frac{I}{\pi a^2 \kappa} \left[\frac{\gamma^2 (1 - \rho^2) e^{\gamma \rho^2}}{e^\gamma - 1 - \gamma} \right] \quad (\text{F.30})$$

2956 Here, $\gamma = 1/(1 - \rho_m^2)$.

2957 These profiles are substituted into Eq. (F.24) after which each of the integrals can be
 2958 evaluated analytically. A straightforward calculation yields:

$$\begin{aligned}
\rho \frac{d\psi}{d\rho} &= -2\mu_0 R_0 a^2 \left(\frac{\kappa^2}{1+\kappa^2} \right) \int_0^\rho \bar{J}_\phi \rho d\rho \\
&= \frac{\mu_0 R_0 I}{\pi} \left(\frac{\kappa}{1+\kappa^2} \right) \frac{(1+\gamma-\gamma\rho^2) e^{\gamma\rho^2} - 1 - \gamma}{e^\gamma - 1 - \gamma}
\end{aligned} \tag{F.31}$$

2959 The safety factors are given by

$$\begin{aligned}
\frac{1}{q_*} &= \frac{\psi'(1)}{\kappa a^2 B_0} \\
\frac{q(\rho)}{q_*} &= \frac{\rho\psi'(1)}{\psi'(\rho)}
\end{aligned} \tag{F.32}$$

2960 Eq. (F.31) is now substituted into the expression for the bootstrap current given by
2961 Eq. (F.11). The resulting expression can then be integrated over the plasma cross
2962 section to yield the bootstrap fraction. A straightforward calculation leads to:

$$f_{BS} = \frac{I_{BS}}{I} = \frac{2\pi a^2 \kappa}{I} \int_0^1 J_{BS} \rho d\rho = \frac{K_{BS}}{K_n} \frac{\bar{n} \bar{T} R_0^2}{I_P^2} \tag{F.33}$$

2963

$$K_{BS} = 4.879 \cdot K_n \cdot \left(\frac{1+\kappa^2}{2} \right) \cdot \epsilon^{5/2} \cdot H_{BS} \tag{F.34}$$

2964

$$H_{BS} = (1+\nu_n)(1+\nu_T)(\nu_n+0.054\nu_T) \int_0^1 \frac{\rho^{5/2} (1-\rho^2)^{\nu_n+\nu_T-1}}{b_p} d\rho \tag{F.35}$$

2965

$$b_p(\rho) = \frac{-e^{\gamma\rho^2}(\gamma\rho^2-1-\gamma)-1-\gamma}{\rho(e^\gamma-1-\gamma)} \tag{F.36}$$

2966 This is the desired result.

Bibliography

- [1] P J Knight and M D Kovari. A User Guide to the PROCESS Fusion Reactor Systems Code, 2016.
- [2] Martin Greenwald. Density limits in toroidal plasmas, 2002.
- [3] Jeffrey P Freidberg. *Plasma Physics and Fusion Energy*, volume 1. 2007.
- [4] C E Kessel, M S Tillack, F Najmabadi, F M Poli, K Ghantous, N Gorelenkov, X R Wang, D Navaei, H H Toudeshki, C Koehly, L El-Guebaly, J P Blanchard, C J Martin, L Mynsburge, P Humrickhouse, M E Rensink, T D Rognlien, M Yoda, S I Abdel-Khalik, M D Hageman, B H Mills, J D Rader, D L Sadowski, P B Snyder, H. St. John, A D Turnbull, L M Waganer, S Malang, and A F Rowcliffe. The ARIES advanced and conservative tokamak power plant study. *Fusion Science and Technology*, 67(1):1–21, 2015.
- [5] Meszaros et al. Demo I Input File.
- [6] Ian H Hutchinson. Principles of plasma diagnostics. *Plasma Physics and Controlled Fusion*, 44(12):2603, 2002.
- [7] M Kovari, R Kemp, H Lux, P Knight, J Morris, and D J Ward. " PROCESS " : A systems code for fusion power plants—Part 1: Physics. *Fusion Engineering and Design*, 89(12):3054–3069, 2014.
- [8] B Labombard, E Marmar, J Irby, T Rognlien, and M Umansky. ADX: a high field, high power density, advanced divertor and RF tokamak Nuclear Fusion. Technical report, 2017.
- [9] W Biel, M Beckers, R Kemp, R Wenninger, and H Zohm. Systems code studies on the optimization of design parameters for a pulsed DEMO tokamak reactor, 2016.
- [10] Stephen O Dean. Fusion Power by Magnetic Confinement Program Plan. Technical Report 4, 1998.
- [11] DOE. FY 1987 Congressional Budget Request. Technical report.
- [12] DOE. FY 2019 Congressional Budget Request. Technical report.

- [13] Marsha Freeman. The True History of The U.S. Fusion Program. Technical report, 2009.
- [14] D. G. Whytea, A E Hubbard, J W Hughes, B Lipschultz, J E Rice, E S Marmar, M Greenwald, I Cziegler, A Dominguez, T Golfopoulos, N Howard, L. Lin, R. M. McDermottb, M Porkolab, M L Reinke, J Terry, N Tsujii, S Wolfe, S Wukitch, and Y Lin. I-mode: An H-mode energy confinement regime with L-mode particle transport in Alcator C-Mod. *Nuclear Fusion*, 50(10), 2010.
- [15] J. W. Connor, T Fukuda, X Garbet, C Gormezano, V Mukhovatov, M Wakatani, M. Greenwald, A. G. Peeters, F. Ryter, A. C.C. Sips, R. C. Wolf, E. J. Doyle, P. Gohil, C. M. Greenfield, J. E. Kinsey, E. Barbato, G. Bracco, Yu Baranov, A. Becoulet, P. Buratti, L. G. Ericsson, B. Esposito, T. Hellsten, F. Imbeaux, P. Maget, V. V. Parail, T Fukuda, T. Fujita, S. Ide, Y. Kamada, Y. Sakamoto, H. Shirai, T. Suzuki, T. Takizuka, G. M.D. Hogewij, Yu Esipchuk, N. Ivanov, N. Kirneva, K. Razumova, T. S. Hahm, E. J. Synakowski, T. Aniel, X Garbet, G. T. Hoang, X. Litaudon, J. Weiland, B. Unterberg, A. Fukuyama, K. Toi, S. Lebedev, V. Vershkov, and J. E. Rice. A review of internal transport barrier physics for steady-state operation of tokamaks, apr 2004.
- [16] K C Shaing, A Y Aydemir, W A Houlberg, and M C Zarnstorff. Theory of Enhanced Reversed Shear Mode in Tokamaks. *Physical Review Letters*, 80(24):5353–5356, 1998.
- [17] David J. Griffiths. *Introduction to electrodynamics*.
- [18] D C McDonald, J G Cordey, K Thomsen, C Angioni, H Weisen, O J W F Kardaun, M Maslov, A Zabolotsky, C Fuchs, L Garzotti, C Giroud, B Kurzan, P Mantica, A G Peeters, and J Stober. Scaling of density peaking in H-mode plasmas based on a combined database of AUG and JET observations. *Nucl. Fusion*, 47:1326–1335, 2018.
- [19] T Onjun, G Bateman, A H Kritz, and G Hammett. Models for the pedestal temperature at the edge of H-mode tokamak plasmas. *Physics of Plasmas*, 9(10), 2002.
- [20] G Saibene, L D Horton, R Sartori, and A E Hubbard. Physics and scaling of the H-mode pedestal The influence of isotope mass, edge magnetic shear and input power on high density ELMy H modes in JET Physics and scaling of the H-mode pedestal. *Control. Fusion*, 42:15–35, 2000.
- [21] J Jacquinet,) Jet, S Putvinski,) Jct, G Bosia, Jct), A Fukuyama, U) Okayama, R Hemsworth, Cea Cadarache), S Konovalov, Rrc Kurchatov), W M Nevins, Llnl), F Perkins, K A Rasumova, Rrc-) Kurchatov, F Romanelli, Enea-) Frascati, K Tobita, Jaeri), K Ushigusa, J W Van, U Dam, V Texas), Rrc Vdovin, S Kurchatov), R Zweben, Erm Koch, Kms-) Brussels, J.-G Wégrowe, Cea-) Cadarache, V V Alikaev, B Beaumont, A Bécoulet, S Bern-Abei, Pppl), V P

- 3034 Bhatnagar, Ec Brussels), S Brémond, and M D Carter. Chapter 6: Plasma
3035 auxiliary heating and current drive. *ITER Physics Basis Editors Nucl. Fusion*,
3036 39, 1999.
- 3037 [22] D A Ehst and C F F Karney. Approximate formula for radiofrequency current
3038 drive efficiency with magnetic trapping, 1991.
- 3039 [23] Tobias Hartmann, Thomas Hamacher, Hon-Prof rer nat Hartmut Zohm, and
3040 Hon-Prof rer nat Sibylle Günter. Development of a Modular Systems Code to
3041 Analyse the Implications of Physics Assumptions on the Design of a Demonstra-
3042 tion Fusion Power Plant.
- 3043 [24] N A Uckan. ITER Physics Design Guidelines at High Aspect Ratio. pages 1–4,
3044 2009.
- 3045 [25] J P Freidberg, F J Mangiarotti, and J Minervini. Designing a tokamak fusion
3046 reactor - How does plasma physics fit in? *Physics of Plasmas*, 22(7):070901,
3047 2015.
- 3048 [26] B. N. Sorbom, J. Ball, T. R. Palmer, F. J. Mangiarotti, J. M. Sierchio, P. Bonoli,
3049 C. Kasten, D. A. Sutherland, H. S. Barnard, C. B. Haakonsen, J. Goh, C. Sung,
3050 and D. G. Whyte. ARC: A compact, high-field, fusion nuclear science facility
3051 and demonstration power plant with demountable magnets. *Fusion Engineering*
3052 *and Design*, 100:378–405, nov 2015.
- 3053 [27] S P Hirshman and G H Neilson. External inductance of an axisymmetric plasma.
3054 *Physics of Fluids*, 29(3):790–793, 1986.
- 3055 [28] D P Schissel and B B Mcharg. Data Analysis Infrastructure at the Diii-D Na-
3056 tional Fusion Facility. (October), 2000.
- 3057 [29] Jeff P Freidberg, Antoin Cerfon, and Jungpyo Lee. Tokamak elongation: how
3058 much is too much? I Theory. *arXiv.org*, pages 1–34, 2015.
- 3059 [30] H Bosch and G M Hale. Improved formulas for fusion cross-sections and thermal
3060 reactivities. 611.
- 3061 [31] Zachary S Hartwig and Yuri A Podpaly. Magnetic Fusion Energy Formulary.
3062 Technical report, 2014.
- 3063 [32] John Wesson and David J Campbell. *Tokamaks*, volume 149. Oxford University
3064 Press, 2011.
- 3065 [33] C. E. Kessel. Bootstrap current in a tokamak. *Nuclear Fusion*, 34(9):1221–1238,
3066 1994.